

**Low-grade metamorphism and fission  
track analysis in the Main Cordillera of  
the Andes - Central Chile, 35° South**

Inauguraldissertation  
zur  
Erlangung der Würde eines Doktors der Philosophie  
vorgelegt der  
Philosophisch-Naturwissenschaftlichen Fakultät  
der Universität Basel

von  
Katherine Waite  
aus London (Vereinigtes Königreich)

Basel 2005

Genehmigt von der Philosophisch-Naturwissenschaftlichen Fakultät auf Antrag  
von

PD Dr. Bernhard Fügenschuh

Prof.Dr. Stefan M. Schmid

PD Dr. Susanne Th. Schmidt and Dr. Diane Seward

Basel, den .....2006 \_\_\_\_\_(Dekan)



# Summary

In the Rio Tinguiririca valley in the Main Cordillera of the Andes of central Chile, 35° south, parts of a stratigraphic section ranging from the late Jurassic to the Quaternary are exposed. Fission track analysis was carried out on samples from all the stratigraphic units exposed in the area in order to gain information on the low-grade metamorphic history of the Central Andes and to test older models for the metamorphic and tectonic evolution of the area. The sequence exposed in the Rio Tinguiririca valley is characterised by several distinctive features not found in other localities in the Central Andes; the deposits of the middle Cretaceous (Aptian – Albian) Colimapu Formation and of the middle to late Miocene Farellones Formation are completely missing in the study area. Instead, a volcanic tuff layer, the White Tuff, and a unit consisting of fan deposits and alluvial plane deposits, the Brownish–Red Clastic Unit, unconformably overlie the Late Jurassic deposits of the Baños del Flaco Formation. The fission track data give some indications on the style and timing of metamorphic events in the study area, enable more accurate constraint of the age of the Brownish–Red Clastic Unit and allow some statements on the tectonic evolution of the study area from the Late Jurassic to present. Burial metamorphism has been proposed by various authors as the main mechanism to produce large suites of rocks altered at low grades in the Central Andes. The results of this study indicate that, on the contrary, hydrothermal alteration connected to magmatic and/or volcanic activity was the main cause of alteration of the rocks and that burial metamorphism played at most a very minor role. Pulses of hydrothermal activity appear to have occurred from Cretaceous to almost recent times and led to alteration of the rocks at slightly varying metamorphic conditions at different times in different parts of the study area. A new model is proposed for the tectonic evolution of the study area. Fission track analysis of detrital zircons from the Brownish–Red Clastic Unit shows that the

---

unit must have been deposited during the latest Cretaceous (Maastrichtian) and that it is certainly younger than the White Tuff. Thermal modelling shows that considerable exhumation of the lower part of the Rio Damas Formation occurred during the Late Cretaceous to Early Tertiary. This exhumation is thought to be connected to tilting and erosion of the Mesozoic units in the area prior to the formation of an extensional basin in the Late Eocene. Data from the Eocene to Miocene Coya Machali Formation imply that sedimentation within the Tertiary basin continued somewhat longer than hitherto supposed.

# Acknowledgements

This study was originally initiated by the late Professor Martin Frey who, sadly, did not live to see this project completed.

I would like to thank Stefan Schmid for taking over the formal supervision of the project and thus enabling me to complete the work started under the supervision of Martin Frey. Stefan Schmid provided valuable support on many issues.

Bernhard Fügenschuh and Susanne Schmidt took over the main supervision of the project, reviewed the manuscript and, together with Stefan Schmid, accompanied me on my first trip to Chile. All my supervisors helped and encouraged me during the whole of the project.

Bernhard Fügenschuh provided valuable support on fission track sample preparation and analysis. He helped to interpret the data and encouraged the development of new ideas and models. He also carefully reviewed the manuscript and gave constructive feedback. Susanne Schmidt was my main contact person for all questions concerning low grade metamorphism, even after she left Basel and moved to Geneva. I am indebted to her for many fruitful discussions and ideas concerning the metamorphic evolution of the study area and also for critical reviews of the manuscript.

I would especially like to thank Diane Seward from the ETH in Zürich for her review of the manuscript and her acceptance of the role of second reviewer at very short notice.

Christian de Capitani and Willem Stern gave me access to the geochemical laboratories at the institute in Basel and supervised the electron microprobe measurements and X-ray diffraction analyses.

Lukas Keller and Carlos Venegas accompanied me on my trips to the field in Chile and assisted with mapping and sampling. My thanks to both of them for good and productive fieldwork.

---

The fission track group in Basel, Bernhard Fügenschuh, Heike Gröger, Horst Dresmann and Zoltan Timar–Geng provided valuable feedback and discussion of my data.

I am especially grateful to my brother, Richy Waite, and to Heike Gröger for reviews of various parts of the manuscript.

Matthias Tischler provided competent and efficient help in interpreting the paleostress data and important moral support during the last months of the project.

I would like to thank Mauricio Belmar for discussions in the field and at home, especially on metamorphism in the study area, and for administrative help during all my trips to Chile.

I am indebted to the technical personnel at the Institute in Basel: to Willy Tschudin for preparation of thin sections, Thomas Fischer, Hansruedi Rüegg, Heinz Hürlimann and Claude Schneider for help with various technical issues, Koni Leu for prompt and efficient computer support and Susanne Tobler, Joelle Glanzmann, Verena Scheuring and Bernadette Oberlein for administrative support.

Finally, I would like to thank my colleagues at the institute in Basel, my family and friends for contributing in so many ways to the successful completion of this thesis.

# Contents

<b>1</b>	<b>Introduction</b>	<b>1</b>
1.1	Structure of the thesis . . . . .	2
1.2	Study area . . . . .	4
1.2.1	Tectonic overview . . . . .	6
1.2.2	Stratigraphic units in the Tinguiririca valley . . . . .	7
1.3	Key issues . . . . .	13
1.3.1	Age and style of metamorphism . . . . .	13
1.3.2	Stratigraphy . . . . .	13
1.3.3	Tectonic history of the area . . . . .	15
1.4	Methods: fission track analysis . . . . .	16
1.4.1	Fission track analysis . . . . .	16
1.4.2	Method . . . . .	18
1.4.3	Microscope analysis . . . . .	18
1.4.4	Age calculation . . . . .	19
1.4.5	Zeta-calibration . . . . .	20
1.5	Metamorphism in the study area . . . . .	20
1.5.1	Previous work . . . . .	21
1.5.2	Secondary minerals found in the present study . . . . .	22
1.5.3	Metamorphic conditions in the study area . . . . .	28
1.5.4	Pattern of metamorphism . . . . .	30
<b>2</b>	<b>Fission track analysis and low-grade metamorphism in the Rio Tinguiririca valley in the central Chilean Andes</b>	<b>35</b>
2.1	Abstract . . . . .	35
2.2	Introduction . . . . .	36
2.2.1	Geological setting . . . . .	37

---

2.2.2	Distribution of metamorphic minerals and facies assemblages	42
2.3	Results from fission track analysis	45
2.3.1	Zircon fission track data	46
2.3.2	Apatite ages	55
2.4	Discussion	63
2.4.1	Constraints on the thermal history of the units derived from the fission track data	63
2.4.2	Type of metamorphism: Burial or no burial?	66
2.5	Conclusions	69
<b>3</b>	<b>Constraining the age of the Brownish–Red Clastic Unit: new ev- idence from fission track dating</b>	<b>71</b>
3.1	Introduction	71
3.1.1	Geological setting	71
3.2	Discussion	76
3.3	Conclusions	79
<b>4</b>	<b>New insights into the tectonic development of the Rio Tinguiririca valley area, in the main Cordillera of the Andes, 35° south, from fission track dating</b>	<b>83</b>
4.1	Abstract	83
4.2	Introduction	84
4.2.1	Geological setting	84
4.3	Previous work	89
4.4	Results	91
4.4.1	Zircon fission track data	92
4.4.2	Apatite ages	101
4.4.3	Paleostress analysis	109
4.5	Discussion	112
4.5.1	Age of the White Tuff	112
4.5.2	Age of the BRCU	113
4.5.3	Tilting of the Mesozoic units	114
4.5.4	Deposition of the Coya Machali Formation and inversion of the extensional basin	115
4.5.5	Extensional phase after basin inversion	116

---

4.5.6	Late heating near Termas del Flaco . . . . .	116
4.6	Model for the evolution of the study area from the mid Jurassic to the present . . . . .	116
4.6.1	Mid to late Jurassic . . . . .	120
4.6.2	Early to mid Cretaceous . . . . .	120
4.6.3	Late Cretaceous . . . . .	121
4.6.4	Late Cretaceous to early Tertiary . . . . .	121
4.6.5	Eocene to early Miocene . . . . .	121
4.6.6	Quaternary . . . . .	122
4.7	Conclusions . . . . .	122
<b>5</b>	<b>Conclusions</b>	<b>125</b>
5.1	Metamorphism . . . . .	125
5.2	Stratigraphy . . . . .	126
5.3	Tectonic evolution of the area . . . . .	127
	<b>Bibliography</b>	<b>131</b>
	<b>Appendix</b>	<b>137</b>
<b>A</b>	<b>Map and schematic crossection</b>	<b>137</b>





# List of Figures

1.1	Overview of the geology of central Chile and Argentina . . . . .	5
1.2	Geological map of the study area and photo of the various outcropping units . . . . .	11
1.3	Schematic stratigraphic columns of units found in the study area and at other localities in the Central Andes . . . . .	12
1.4	Zeolite analyses from the Coya Machali Formation . . . . .	23
1.5	Detailed sampling and analysis of minerals from an intrusion in the Coya Machali Formation . . . . .	24
1.6	Microprobe analyses of phyllosilicates . . . . .	26
1.7	Microprobe analyses of chlorites . . . . .	27
1.8	Metamorphic zones in the study area . . . . .	30
1.9	Photomicrograph of a cracked amygdale . . . . .	31
1.10	Metamorphic index minerals found in the study area . . . . .	33
2.1	Location of the study area . . . . .	38
2.2	Geological map of the study area . . . . .	39
2.3	Schematic stratigraphic columns of units found in the study area and at other localities in the Central Andes . . . . .	40
2.4	Metamorphic zones in the study area . . . . .	43
2.5	Photomicrograph of a cracked amygdale . . . . .	45
2.6	Zircon fission track data . . . . .	48
2.7	Radial plots of samples from the Rio Damas Fm. . . . .	49
2.8	ZFT single grain ages of 9 samples from the Rio Damas Formation .	50
2.9	Radial plots of samples from the Baños del Flaco Fm. . . . .	50
2.10	ZFT single grain ages of 2 samples from the Baños del Flaco Fm. .	51
2.11	Radial plot of the ZFT sample from the White Tuff. . . . .	51

---

2.12	ZFT single grain ages of a sample from the White Tuff . . . . .	51
2.13	Radial plots of samples from the BRCU . . . . .	52
2.14	Bar chart showing all ZFT single grain ages measured in the 6 sam- ples from the BRCU. . . . .	53
2.15	Radial plots of 8 ZFT samples from the Coya Machali Fm. . . . .	54
2.16	ZFT single grain ages from the Coya Machali Fm. . . . .	55
2.17	Radial plot of a ZFT sample from the Quaternary volcanics. . . . .	55
2.18	Apatite fission track data . . . . .	56
2.19	Radial plots of AFT samples from the Rio Damas Fm. . . . .	59
2.20	Thermal modelling of a sample from the lower Rio Damas Formation	60
2.21	Radial plot of an AFT sample from the Baños del Flaco Fm. . . . .	61
2.22	Radial plot of an AFT sample from the Coya Machali Fm. . . . .	61
2.23	Thermal modelling of a sample from the Coya Machali Fm. . . . .	62
2.24	Zones of thermal overprint . . . . .	68
3.1	Schematic stratigraphic columns of units found in the study area and at other localities in the Central Andes . . . . .	72
3.2	Radial plots of samples from the BRCU . . . . .	77
3.3	Radial plot of the sample from the White Tuff . . . . .	78
3.4	ZFT single grain ages from the BRCU . . . . .	78
3.5	ZFT single grain ages of a sample from the White Tuff . . . . .	79
3.6	Relative positions of the units in the Rio Tinguiririca valley . . . . .	80
3.7	Stratigraphic column in the Rio Tinguiririca valley . . . . .	81
4.1	Location of the study area . . . . .	85
4.2	Geological map of the study area . . . . .	86
4.3	Schematic stratigraphic columns of units found in the study area and at other localities in the Central Andes . . . . .	87
4.4	Zircon fission track data . . . . .	94
4.5	Radial plots of samples from the Rio Damas Fm. . . . .	95
4.6	ZFT single grain ages of 9 samples from the Rio Damas Formation .	96
4.7	Radial plots of samples from the Baños del Flaco Fm. . . . .	96
4.8	ZFT single grain ages of 2 samples from the Baños del Flaco Fm. .	97
4.9	Radial plot of the sample from the White Tuff . . . . .	97
4.10	ZFT single grain ages of a sample from the White Tuff . . . . .	97

---

4.11	Radial plots of samples from the BRCU . . . . .	98
4.12	ZFT single grain ages from the BRCU . . . . .	99
4.13	Radial plots of 8 ZFT samples from the Coya Machali Fm. . . . .	100
4.14	ZFT single grain ages from the Coya Machali Fm. . . . .	101
4.15	Radial plot of a ZFT sample from the Quaternary volcanics. . . . .	101
4.16	Apatite fission track data . . . . .	102
4.17	Radial plots of AFT samples from the Rio Damas Fm. . . . .	105
4.18	Thermal modelling of a sample from the lower Rio Damas Formation	106
4.19	Radial plot of an AFT sample from the Baños del Flaco Fm. . . . .	107
4.20	Radial plot of an AFT sample from the Coya Machli Fm. . . . .	107
4.21	Thermal modelling of a sample from the Coya Machali Fm. . . . .	108
4.22	Paleostress axes plotted for 11 outcrops in the study area . . . . .	112
4.23	Zones of thermal overprint . . . . .	117
4.24	Tectonic model part 1 . . . . .	118
4.25	Tectonic model part 2 . . . . .	119

---

# Chapter 1

## Introduction

The Andes have long been a focus of metamorphic petrologists on account of the widespread occurrence of large suites of low-grade metamorphic rocks, especially in the central part of the orogen. Metamorphic grade ranges from diagenetic to lower greenschist facies conditions and the rocks are often more or less undeformed. Various studies (Levi (1970); Offler et al. (1980); Levi et al. (1982); Aguirre et al. (1987, 1989); Levi et al. (1982); Vergara et al. (1993, 1994)) have attributed the alteration at low temperatures and pressures to burial metamorphism in subsiding basins, ocean floor metamorphism, hydrothermal activity or contact metamorphism. Belmar (2000) studied the low-grade metamorphism in the Rio Tinguiririca valley in the Andes of central Chile at about 35° south. He found an increase in metamorphic grade from West to East in the study area, that is from stratigraphically young to old rocks. No breaks in metamorphic grade occur over major stratigraphic unconformities or fault zones in the area. Belmar (2000) proposed a long-lasting burial event that affected the whole stratigraphic sequence and led to alteration in the rocks ranging from diagenetic to prehnite–pumpellyite facies conditions. However, the pattern of metamorphism is often disturbed by local effects such as contact metamorphism near intrusions and the rocks are thought to have a polymetamorphic history with several periods of alteration at subgreenschist facies conditions.

The aim of the present study is to refine the model of Belmar (2000) and gain information on the age and style of metamorphic events in the same area. Fission track analysis of zircon and apatite was chosen as the ideal method to complement the results of the study on low-grade metamorphism because the fission track

method provides information on low-temperature thermal evolution of samples between about 300 °C (upper temperature limit of the zircon partial annealing zone, Tagami and Shimada (1996); Tagami et al. (1996, 1998); Timar-Geng et al. (2004)) and 60 °C (lower temperature limit of the apatite partial annealing zone, Green et al. (1986, 1989); Laslett et al. (1987); Duddy et al. (1988)). A burial event, as proposed by Belmar (2000), with associated alteration at sub-greenschist facies conditions would cause annealing of fission tracks in apatites and maybe also in zircon and a characteristic pattern of ages would be expected. Modelling of temperature-time paths of individual samples should give information on exhumation and maybe allow determination of exhumation rates. Additionally, fission track analysis could possibly provide better constraint on the tectonic evolution of the study area.

## 1.1 Structure of the thesis

In this thesis, results of a study are presented that was originally initiated with the aim of dating the low-grade metamorphism in an area in the Chilean Andes and, if possible, of modelling the low temperature history of the area. The project is a follow-up of the project of M. Belmar (2000), who studied the low-grade metamorphism in the same area. The thesis is structured as follows:

**Chapter 1: Introduction** An overview of the geological setting is given and the stratigraphic units found in the study area are described. Key issues are presented based on earlier studies. A short overview is given of the concepts and methods of fission track dating, which was the main analytical method used in this study. Metamorphism in the study area is discussed based on earlier results of the study of Belmar (2000) and own results are presented. The findings of this study are in agreement with those of Belmar (2000). Results of both studies on low-grade metamorphism (the present study and Belmar (2000)) will be published as one of two papers on low-grade metamorphism and fission track dating in the study area.

**Chapter 2: Fission track dating and low grade metamorphism in the Termas del Flaco area** Results from fission track analysis are presented and

their implications for timing and style of metamorphism in the area are discussed. The contents of this chapter form the base of the second paper on low-grade metamorphism and fission track dating. For this reason, another short overview of the geological setting of the area is given.

### **Chapter 3: Constraining the age of the Brownish-Red Clastic Unit**

The implications of the fission track data on the stratigraphic position and age of the hitherto undated Brownish-Red Clastic Unit are presented and discussed. These data will be integrated into a comprehensive paper on the Brownish-Red Clastic Unit that will be mainly based on work by Prof. R. Charrier, Universidad de Chile, Santiago, Chile, and others.

### **Chapter 4: New insights into the tectonic development of the Rio Tinguiririca valley area, in the main Cordillera of the Andes, 35 South, from fission track dating**

In this chapter, a geological overview and the results from fission track dating are again presented and the implications for the tectonic evolution of the area are discussed. The data allow constraints of several events in the tectonic evolution of the area as well as giving information on the style and timing of metamorphism as discussed in chapter 2 and on the stratigraphic positions and ages of some of the units as discussed in chapter 3. Finally, a model for the Late Jurassic to present evolution of the study area is proposed based on earlier studies by other authors (Charrier et al. (1996, 2002)) and the results of the present study.

**Chapter 5: Conclusions** The main conclusions from chapters 2, 3 and 4 are summarised.

**Appendix:** The Appendix contains microprobe analyses of secondary minerals from samples in the study area, X-ray diffraction analyses, paleostress data (fault-slip sets) measured in the study area and details of zeta calibration for fission track dating. A geological map of the study area and a schematic cross-section are also enclosed.

## 1.2 Study area

The study area is located in the main Cordillera of the Andes of central Chile at about  $35^\circ$  south. Here, the Tinguiririca river valley cuts rocks ranging in age from the late Jurassic to early Miocene (see Fig. 1.1). A suite of Quaternary volcanic deposits lies unconformably on top of the older units. Field work consisted of mapping and sampling an east-west transect that runs from the border between Chile and Argentina in the east to the confluence of the Tinguiririca and Azufre rivers in the west. The village of Termas del Flaco lies in the study area and is known for the Termas (= hot springs) where water of about  $50^\circ\text{C}$  reaches the surface. The river valley runs more or less northwest-southeast and therefore roughly perpendicular to the strike of the units and major structures in the area. Figure 1.1 shows the setting of the study area, which lies east of the town of San Fernando in the VI. Region of Chile.



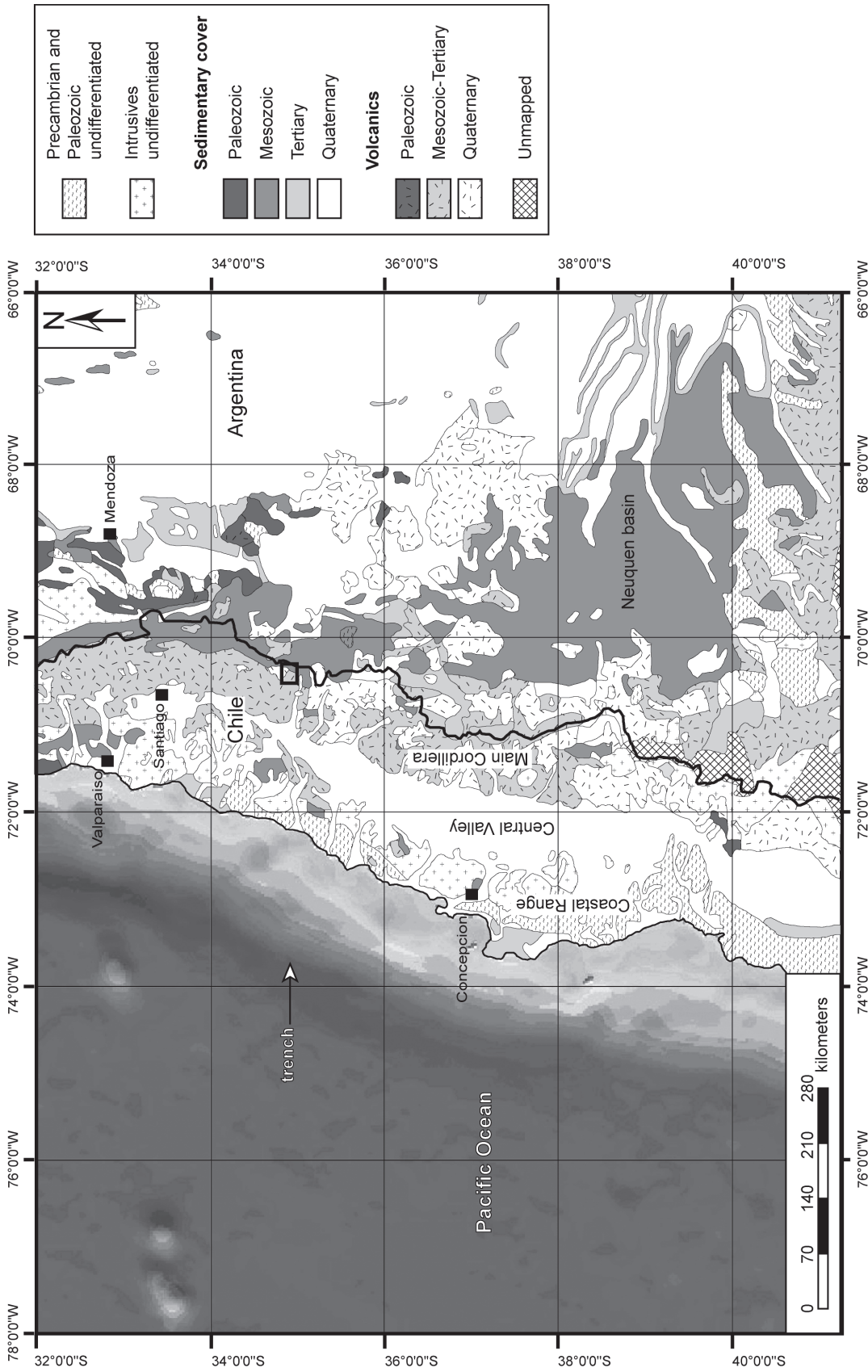


**Figure 1.1:** Overview of the geology of central Chile and Argentina overlaid on a digital elevation map. The study area is marked by the black box and lies at the transition between the deposits of the Neuquen backarc basin in the east and the Mesozoic to Tertiary volcanic deposits in the Main Cordillera of the Andes.

### 1.2.1 Tectonic overview

Figure 1.1 shows the setting of the study area in the Andes of central Chile. For an overview of the development of the Andes of Chile see Mpodozis and Ramos (1989). Along the west coast of South America, subduction of oceanic crust has been occurring since the Palaeozoic. In the Early Palaeozoic several terranes (i.e. the Precordillera terrane and Chilenia) were accreted to the western margin of the continent. In the late Palaeozoic (Gondwana tectonic cycle) an active magmatic arc formed to the east of the subduction zone in the area of the present-day Coastal Cordillera in Chile. In the Jurassic a series of backarc basins formed behind the magmatic arc. The Mesozoic development differs from north to south along the Andes and five segments with distinctive characteristics can be recognised. The study area is at the transition between segments B and C *sensu* Mpodozis and Ramos (1989). The northern segment (B *sensu* Mpodozis and Ramos (1989)) is characterised by the following features: A sedimentary platform (the Aconcagua platform) developed in the backarc during the Jurassic. In the Early Cretaceous an aborted marginal basin developed West of the platform and thick sequences of basalts and andesites were erupted. In the middle Cretaceous a change in the tectonic regime occurred and a compressional period in the backarc area led to the formation of a fold and thrust belt (Aconcagua fold and thrust belt). The magmatic arc migrated to the West during the Late Cretaceous and Early Tertiary. The southern segment (C *sensu* Mpodozis and Ramos (1989)) has the following characteristics: A large backarc basin (the Neuquen basin) developed in the Early Jurassic and was active until the Early Cretaceous. Conditions in the basin varied and three phases of sedimentation in the Neuquen basin have been described; one in the Early Jurassic one in the middle to Late Jurassic and one in the Tithonian to Neocomian. In this segment, there was also a change from extensional to compressional tectonics in the middle Cretaceous and a fold and thrust belt formed in the Neuquen basin. The magmatic arc remained more or less stationary in this part of the Andes from the Jurassic up to the Quaternary. Volcanic and intrusive rocks of Mesozoic age are concentrated in the arc and backarc area and there is a scarcity of such rocks in the coastal range.

The Andean orogenic cycle began in the Tertiary and three major compressional phases have so far been distinguished: the Incaic phase starting about 42 Ma ago, the Quechua phase that started about 10 Ma ago and the Diaguitic phase,

which began 2 Ma ago (Ramos (1988)). In the late Eocene a period of extension within the arc led to the development of another large basin or series of interconnected basins in the Central Andes West of the Neuquen backarc basin. They were filled with lavas, volcanoclastic material and fluvial and lacustrine sediments (the Coya Machali or Abanico Formation, see Charrier et al. (2002)) and were later inverted during a compressive phase in the middle Miocene. The deposits were folded and thrust before another period of sedimentation occurred in the late Miocene (Farellones Formation).

Figure 1.2 shows a geological map of the study area near the village of Termas del Flaco in the Rio Tinguiririca valley. The study area lies at the north-western edge of the Neuquen basin, on the contact between the deposits of the Neuquen basin and those of the Tertiary intra-arc basin and its development corresponds mainly to segment C *sensu* Mpodozis and Ramos (1989) (see figure 1.1). Mesozoic deposits in the area belong to the middle to Late and latest Jurassic cycles of sedimentation in the Neuquen basin. These deposits are tilted to the west probably due to a major thrust fault located further to the east but are otherwise internally more or less undeformed. Formation of a fold and thrust belt in the middle Cretaceous was concentrated further to the west in Argentina. The Mesozoic units outcropping in the study area were deposited along the western edge of the Neuquen backarc basin and are unconformably overlain by sedimentary rocks deposited in a Tertiary intra-arc basin that formed to the west of the Neuquen basin. A major stratigraphic unconformity exists between the Mesozoic and Cenozoic deposits in the study area. Tertiary deposits belong to the infill of the extensional intra-arc basin that opened in the Eocene. These deposits were deformed during basin inversion in the Early Miocene (end of the Incaic phase, Ramos (1988)) and are folded and thrust. To the north of the study area a thick sequence of Miocene lavas and pyroclastics was deposited but these deposits are not present neither in the study area nor south of it (see Charrier et al. (2002)).

## 1.2.2 Stratigraphic units in the Tinguiririca valley

### Rio Damas Formation

The Rio Damas Formation consists of a 3700 m thick sequence of continental sediments and volcanic deposits (figures 1.3, 1.2). It is the oldest unit exposed in

the study area. To the east in Argentina, where the base of the unit is exposed, it conformably overlies the marine deposits of the Nacientes del Teno Formation (Charrier et al. (1996)). It is dated as Kimmeridgian based on the well constrained ages of the bracketing marine units (Nacientes del Teno Formation, Oxfordian, and Baños del Flaco Formation, Tithonian) but no biostratigraphically significant fossils have been found in the deposits to allow direct dating. The Rio Damas Formation is the equivalent of the Tordillo Formation in Argentina.

### **Baños del Flaco Formation (= Lo Valdes Formation)**

The Baños del Flaco Formation consists of marine limestones and sandstones with abundant fossils. It conformably overlies the Rio Damas Formation and is dated as Tithonian in the study area based on several stratigraphically significant ammonite species found in the unit. In the study area, the Baños del Flaco Formation is only about 400 m thick and the upper part has been eroded. In other localities in the Central Andes, the formation has a thickness of up to 2000 m and deposition is known to have continued up to the Neocomian. The deposits represent a transgressive regressive cycle from platform to deep shelf sediments and back to platform.

In the study area the middle Cretaceous Colimapu Formation is missing. In other localities to the north and south, the Colimapu Formation conformably overlies the deposits of the Baños del Flaco Formation and consist of a 2000 to 3000 m thick sequence of continental sandstones and volcanic deposits (Charrier et al. (1996)) It is unknown whether the Colimapu Formation was deposited in the study area and later eroded or if it was never deposited.

### **White Tuff**

A white volcanic tuff layer lies unconformably on the eroded surface of the Baños del Flaco Formation on the south side of the Rio Tinguiririca valley. The layer is 3 – 4 m thick. This tuff has been dated at  $104 \pm 0.5$  Ma with Ar–Ar dating (Wyss et al. (1994); Charrier et al. (1996)) and therefore is neither part of the Baños del Flaco Formation nor of the overlying Coya Machali Formation. No other volcanic deposits of similar age have been found in the area and the exact tectonostratigraphic meaning of the White Tuff is still a matter of debate.

### **Brownish–Red Clastic Unit (BRCU)**

The BRCU is about 250 m thick and consists of a series of fan deposits and alluvial plane deposits that lie unconformably but with no angular unconformity on top of the eroded surface of the Baños del Flaco Formation. The BRCU has so far only been found in the Tinguiririca valley and wedges out both to the North and South. Non–avian dinosaur bones found near the top of the unit constrain it to the Cretaceous (Charrier et al. (1996)). The BRCU was formerly mapped as the middle Cretaceous Colimapu Formation but Charrier et al. (1996) defined it as a separate member that is probably younger than the Colimapu Formation. However, no fossils have been found that allow precise dating of the unit and, so far, no reliable radiometric age data exist. The exact age of the BRCU remains a matter of debate. The White Tuff is exposed to the South of where the BRCU wedges out but there is no direct contact between these two units. Therefore, their stratigraphic relations are not clear.

### **Coya Machali Formation (=Abanico Formation)**

The Coya Machali Formation is about 1600 m thick in the study area (Charrier et al. (1996)) and consists of continental sediments and abundant volcanic deposits. It unconformably overlies the BRCU, the White Tuff and the Baños del Flaco Formation with a slight angular unconformity. Previously, the Coya Machali Formation was mapped as the Cretaceous Colimapu Formation until the finding of mammal fossils (Wyss et al. (1990)) near the base of the unit showed it to be Tertiary (Charrier et al. (1996)). Since then, K–Ar and Ar–Ar age dating have confirmed a late Eocene to early Oligocene onset of deposition of the unit in this and other areas (see Charrier et al. (2002)) and sedimentation probably continued until the Early Miocene.

### **Quaternary volcanic rocks**

All the Mesozoic and Tertiary units are unconformably overlain by a layer of Quaternary basalts and tuffs attributed to the Tinguiririca Volcanic Group. The Tinguiririca volcanics have been dated at about 1 Ma (Arcos et al. (1988); Charrier et al. (1996)). These deposits lie almost horizontally on top of the west–dipping Mesozoic and Cenozoic units.

Intrusive bodies, sills and dykes of various sizes and compositions are found all over the area and within all stratigraphic units. Most of these are Tertiary in age.

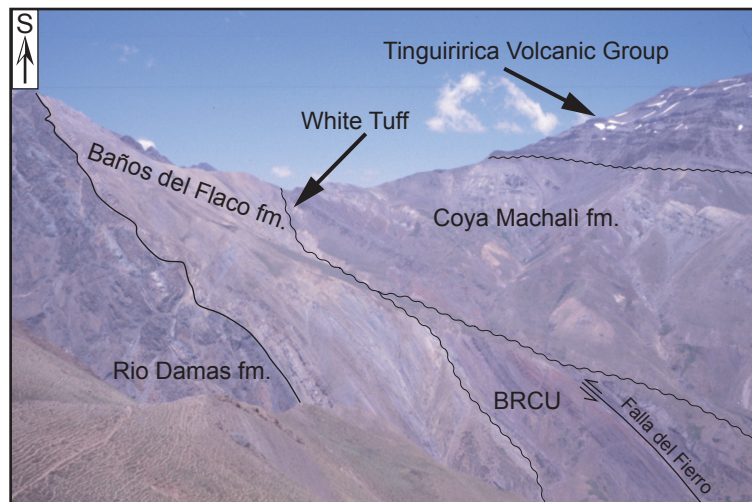
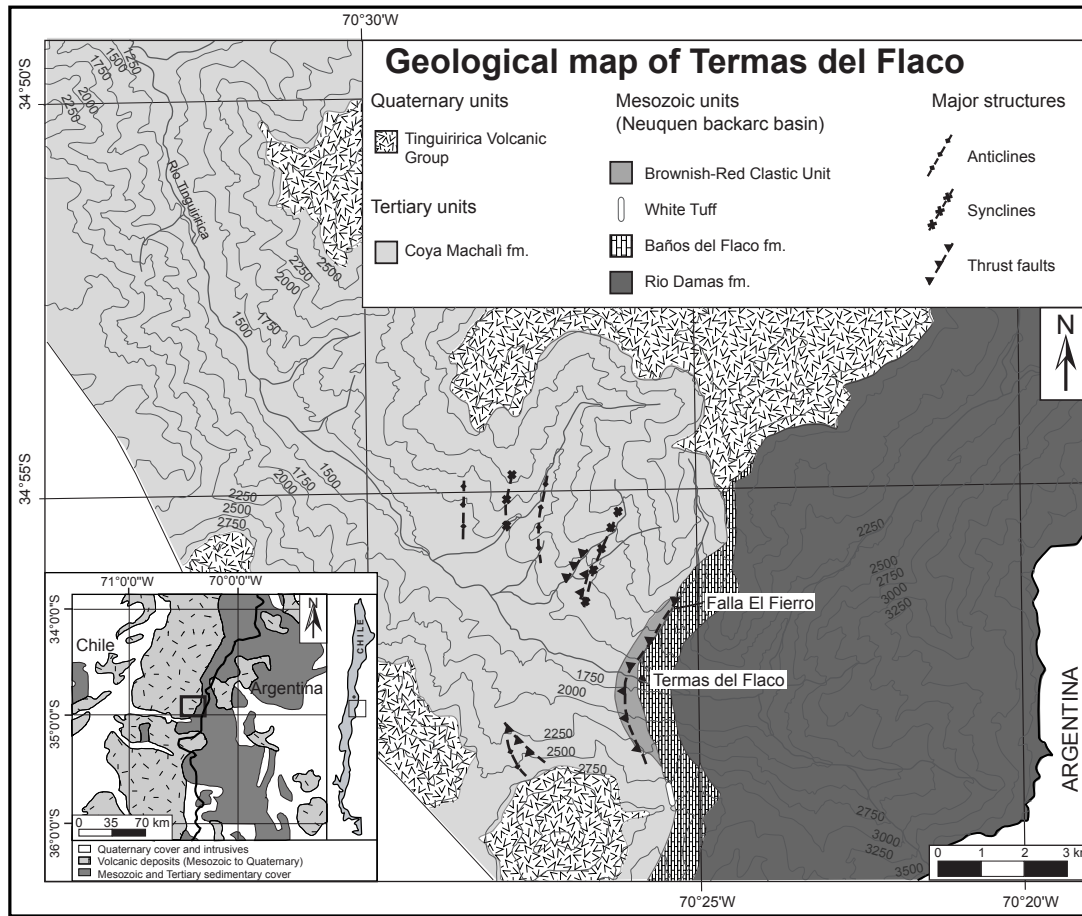


**Figure 1.2:** Geological map of the study area near the village of Termas del Flaco in the Rio Tinguiririca valley showing the stratigraphic units discussed in the text and major structural features. The photo shows a view of the southern flank of the valley. All stratigraphic units can be seen and the contacts between them have been marked for better visualisation. Wavy lines mark disconformable contacts and straight lines mark conformable contacts.





## 1.3 Key issues

### 1.3.1 Age and style of metamorphism

Many studies have addressed the mechanisms for alteration of large suites of sedimentary and volcanic or volcanoclastic rocks at low-grade metamorphic conditions in the Andes (Levi (1970); Offler et al. (1980); Levi et al. (1982); Aguirre et al. (1987, 1989); Levi et al. (1982); Vergara et al. (1993, 1994)). Levi (1970) proposed burial metamorphism as the main process and developed a model of cyclic burial metamorphism in subsiding basins for a transect east of Santiago de Chile. There, three conformable sequences of rocks are separated by stratigraphic unconformities. A continuous increase in metamorphic grade from young to old units in each sequence was observed and was considered as the main indication for burial metamorphism in subsiding basins. Inversion and uplift of the basins led to stacking of sediments belonging to different cycles, separated by stratigraphic unconformities. Sharp breaks in metamorphic grade were found over major stratigraphic unconformities and sometimes rocks altered at higher metamorphic conditions were found unconformably overlying older rocks altered at lower grades. Levi (1970) extended the model to other localities in the Central Andes. Belmar (2000) studied the low-grade metamorphism in the Rio Tinguiririca valley. He found no break in metamorphic grade over a major stratigraphic unconformity in the area but, instead, an apparently continuous increase in metamorphic grade from diagenetic to zeolites facies conditions in Tertiary units to prehnite-pumpellyite facies conditions in the Mesozoic units. Belmar (2000) proposed a long-lasting burial metamorphic event involving Cenozoic and Mesozoic rocks to account for the observed pattern of metamorphism. This is in contrast to the model proposed by Levi (1970). Also, Belmar (2000) noted that many of the rocks have a poly metamorphic history and that his model of a single burial event is not sufficient to explain all the observed alterations in the rocks.

### 1.3.2 Stratigraphy

Charrier et al. (1996) combined paleontological data, petrographic observations and paleomagnetic data with detailed mapping and Ar-Ar age determinations to reinterpret the stratigraphic sequence in the area. This reveals several character-

istic features not found in other localities that were previously misinterpreted or overlooked:

1. The Baños del Flaco Formation has been eroded in the study area and only the oldest (Tithonian) deposits are preserved. The unit that reaches a thickness of up to 2 km in other areas is only about 400 m thick in the Tinguiririca valley.
2. A white tuff layer is found lying unconformably on top of the Baños del Flaco Formation. An age of 104 Ma was determined by Ar–Ar dating and shows that the tuff neither belongs to the Baños del Flaco Formation nor to the Tertiary Coya Machali Formation.
3. Also lying unconformably on top of the Baños del Flaco Formation is the so-called Brownish–Red Clastic unit (BRCU), which has so far only been described in the Rio Tinguiririca valley.
4. Deposits lying unconformably and with a slight angular unconformity on top of the Baños del Flaco Formation, the White Tuff and the BRCU were found to contain mammal fossils (Wyss et al. (1990); Charrier et al. (1996)) constraining the unit to the Tertiary and thus showing it to belong to the Coya Machali or Abanico Formation and not, as previously thought, to the mid Cretaceous Colimapu Formation.

The ages and relative positions of the White Tuff layer and the Brownish–Red Clastic unit are still a matter of debate. Zircon fission track dating on these deposits was expected to provide information on the cooling age of the White Tuff and of volcanic material in the BRCU and therefore allow for a better constraint of their ages. Charrier et al. (1996) first described the White Tuff and the BRCU and proposed 4 possible scenarios for the setting of the White Tuff and their implications for the stratigraphy of the area:

1. The White Tuff could be a part of the Baños del Flaco Formation that was exposed during erosion. This scenario implies a stratigraphic unconformity above the White Tuff.
2. The White Tuff was deposited after erosion of the Baños del Flaco Formation but before deposition of the BRCU. Stratigraphic unconformities exist

between the Baños del Flaco Formation and the White Tuff, the White Tuff and the BRCU and the BRCU and the Coya Machali Formation.

3. The White Tuff was deposited after the BRCU but before the Coya Machali Formation. Stratigraphic unconformities would then exist between the Baños del Flaco Formation and the BRCU, the BRCU and the White Tuff and the White Tuff and the Coya Machali Formation.
4. The White Tuff forms the base of the Coya Machali Formation.

An Ar–Ar age of 104 Ma was determined for the White Tuff by Wyss et al. (1994). This is interpreted as a formation age of the tuff. Based on this, scenarios 1 and 4 can be excluded because the age does not fit either the Baños del Flaco or the Coya Machali Formation. Of the remaining two scenarios, 2 was preferred before 3 by Charrier et al. (1996) but could not be conclusively proven.

### **1.3.3 Tectonic history of the area**

The main Cordillera of the Andes at about 35° south is characterised by west-dipping Mesozoic units unconformably overlain by folded and thrustured Tertiary deposits. The Mesozoic units are hardly deformed and deformation is mainly concentrated in brittle fault zones. The angular unconformity between the Mesozoic and Tertiary units indicates that tilting of the older deposits must have begun before deposition of the younger unit. Charrier et al. (2002) collected biostratigraphic and radiometric age data from the Coya Machali Formation at different locations in the Andes in central Chile and constrained the formation of an extensional basin or series of basins to the late Eocene. Deposition in these intra-arc basins continued at least until the early Miocene.

## 1.4 Methods: fission track analysis

In the following a short overview of the concepts of fission track analysis and the methods used in this study is given, adapted from M. Steinmann (Steinmann et al. (1999)). For a comprehensive description of the concepts of fission track analysis see Wagner and Van den Haute (1992); Gallagher et al. (1998).

### 1.4.1 Fission track analysis

Fission track (FT) analysis is based on natural, spontaneous fission of the more abundant isotope of uranium ( $^{238}\text{U}$ ), which is present in trace amounts in certain minerals, especially apatite, zircon and titanite. Fission of the uranium nucleus is an explosive process, in which two highly charged, approximately equal-sized fission fragments fly apart at  $180^\circ$  to each other, stripping electrons from atoms lying in their path. The result is a linear damage trail in the enclosing atomic lattice. These so-called fission tracks accumulate within the crystal over time and, under suitable conditions, may be revealed, usually by preferential chemical etching of the weakened fission trail on an internal polished surface. The number of tracks per unit area may be counted using a high powered optical microscope and depends on:

1. the rate at which fission occurs
2. the length of time during which tracks have been accumulating
3. the uranium content of the crystal.

The uranium content is estimated by irradiating the sample with low-energy (thermal) neutrons which induce a proportion of  $^{235}\text{U}$  to fission, creating a second, induced track population. The ratio of spontaneous to induced tracks provides the ratio of uranium atoms which have fissioned naturally to the total uranium content. This ratio together with the spontaneous fission decay rate, gives the time during which tracks have been accumulating (the FT apparent age) for each individual crystal. In reality, uncertainty about the absolute value for the spontaneous fission decay constant and the complexities of absolute neutron fluence measurement have resulted in international calibration of the FT system against a series of I.U.G.S. agreed age standards. This was carried out by using a proportionality

constant zeta (Hurford and Green (1983); Hurford (1990)), which is determined by each operator as a personal value.

### **Age determinations on apatites**

23 apatite samples were analysed. However, the external detector method could only be applied for 6 samples containing enough grains with sufficient spontaneous fission tracks. For each of these 6 samples at least 20 grains were analysed and the ages are given as central ages (Galbraith and Laslett (1993)). For the remaining samples a modified population age method (see Wagner and Van den Haute (1992)) was applied: the samples were prepared after the external detector method and  $N_s$  and  $N_i$  were determined for each grain. All the  $N_s$  and  $N_i$  values were added together (within a sample) and pooled ages were then calculated for the total  $N_s/N_i$  ratio of all counted grains. The number of grains counted ranges from 19 to 60. Because of the lack of spontaneous tracks and the relatively low U content of most of these samples, the calculated ages have large  $\sigma$  errors.

The apatite PAZ is generally accepted to range from about 60 to 120 °C (Green et al. (1986, 1989); Laslett et al. (1987); Duddy et al. (1988)). Most of the ages determined for the samples from the Tinguiririca Valley are significantly younger than the stratigraphic ages of the units in question, indicating that partial or complete annealing of apatites occurred in many of the samples after deposition. Track length measurements were carried out on 4 apatite samples and thermal modelling with the software AFTSolve (Ketcham et al. (2000)) was carried out on two of these samples using the annealing model of Laslett et al. (1987) for Durango apatite (Cl-apatite). Because no chemical analyses were carried out on apatites, the model results are interpreted in terms of general shape of the temperature–time path only.

### **Age determinations on zircons**

All stratigraphic units in the study area were sampled, including the Quaternary volcanic deposits. 27 zircon samples were analysed. Four of these samples yielded less than 10 single grain ages and the central ages for these samples are given in brackets in all figures. The zircon PAZ is much less well constrained than that of apatite. Temperatures between about 180 °C and 320 °C have been derived in

various studies (Tagami and Shimada (1996); Tagami et al. (1996, 1998); Timar-Geng et al. (2004); Rahn et al. (2004)).

### 1.4.2 Method

Rock samples were crushed and sieved using conventional methods and the heavy mineral fraction was extracted by heavy liquid separation. In a last step methylene iodide (density 3.3 g/cm<sup>3</sup>) was used to separate zircons from apatites. To avoid any artificial partial annealing of the apatites, working temperatures were never allowed to exceed 50 °C during preparation. Zircon and apatite grains were then hand-picked and mounted, apatite samples in epoxy resin and zircon samples in PFA Teflon. The samples were then cut and polished. Apatite mounts were etched in 6.5% HNO<sub>3</sub> for 40 seconds at room temperature. Zircon mounts were etched in a eutectic melt of KOH–NaOH (23 : 16) at 240 °C (Gleadow et al. (1976)). Etching times for zircon varied between 4 and 24 hours. The muscovites, which were used as solid state track detectors, were etched for 45 minutes in 40% HF at room temperature. All etchings were stopped by running water. The external detector method (EDM) was used for all samples (Gleadow (1981)). The samples were irradiated at the ANSTO reactor, Lucas Heights, Australia, with a nominal total integrated flux of 1x10<sup>15</sup>n cm<sup>-2</sup> for zircons and 1x10<sup>16</sup>n cm<sup>-2</sup> for apatites. In this study, no chemical compositions were analysed.

### 1.4.3 Microscope analysis

Counting and confined track length measurements were carried out with a Zeiss optical microscope fitted with a digitizing tablet and mobile stage and the software FTStage by T. Dumitru. Zircons were counted at 1600x magnification (10x100x1.6/dry), the apatites and dosimeter muscovites with a 1000x magnification (10x100x1.0/dry). The track length measurements in apatites were carried out with the support of a digitising tablet, which was calibrated to 1 μm. Age calculations were carried out using the software Trackkey 4.1 by Istvan Dunkl (Dunkl (2002)). The following dosimeter glasses and age standards were used during irradiation:

CN1 (J. Schreuers, Corning) 39.8 ppm U

Fish Canyon Tuff (FCT), Colorado (zircon), 27.8 ± 0.4 Ma (2 σ) (Hurford and

Hammerschmidt (1985))Mc Dowell et al. (2005)

CN5 (J. Schreuers, Corning) 12.19 ppm U

Durango (DUR), Cerro de Mercado, Mexico (apatite),  $31.4 \pm 1.2$  Ma ( $2 \sigma$ )  
(Mc Dowell and Keizer (1977) <sup>1</sup>

#### 1.4.4 Age calculation

As in all radiometric dating methods, the age equation provides the base for fission track age determinations (1.1), except that, instead of a daughter product, the linear defects formed during fission are counted.

$$N_D = N_P * e^{\lambda * t - 1} \quad (1.1)$$

where

$N_D$  is the number of daughter atoms

$N_P$  is the number of parent atoms

$\lambda$  is the decay constant

t is time.

All fission tracks are assumed to be the result of spontaneous fission of  $^{238}\text{U}$ . The fission products of other isotopes such as  $^{235}\text{U}$ ,  $^{232}\text{Th}$ ,  $^{244}\text{Pu}$  as well as  $\alpha$ -recoil tracks are considered to have a negligible effect, either because of their low abundance ( $^{235}\text{U}$ ,  $^{244}\text{Pu}$ ) or their long half-life ( $^{232}\text{Th}$ ) (Fleischer et al. (1975)). The tracks can be counted under a normal optical microscope after chemical etching treatment (Price and Walker (1962)). The age equation is completed by entering the density of spontaneous tracks ( $\rho_s$ ) for Nd and the density of induced tracks ( $\rho_i$ ) for Np. Problems arise from variation in etching and counting techniques, the poorly calibrated spontaneous fission decay constant  $\lambda_f$  and the difficulty to accurately determine the thermal neutron fluence  $\phi$ . To overcome these problems Fleischer and Hart (1972); Hurford and Green (1982, 1983) introduced a personal calibration factor  $\zeta$ , which is different for every counter and every standard. To obtain this factor, ages standards and glass monitors were analysed

---

<sup>1</sup>Although newer data on the ages of the standards exist (Durango apatite: Mc Dowell et al. (2005), FCT zircon: Schmitz and Bowring (2001)), the references given here are the ones used by the software Trackkey 4.1 for age calculation

for zircons and apatites. The resulting calibration factor zeta can also be entered in the age equation 1.2.

$$t = \frac{1}{\lambda_d} * \ln\left(\lambda_d * \rho_{ratio} * \rho_d * \zeta * g + 1\right) \quad (1.2)$$

where  $t$  is the age of the sample,  $\lambda$  is the half-life value of the fission process,  $\zeta$  is the personal calibration factor of the analyst (after Hurford and Green (1983)),  $g$  is the geometry factor (0.5 for the external detector method),  $\rho_d$  is the standard density of fission tracks and  $\rho_{ratio}$  is the ratio of densities of spontaneous and induced fission tracks in the sample.

### 1.4.5 Zeta-calibration

A mean zeta value of  $339.23 \pm 12.75$  (CN 5) was established for apatite and a mean zeta value of  $143.44 \pm 8.49$  (CN1) was determined for zircon. Zeta-calibration was carried out on Durango apatites and Fish Canyon Tuff zircons (see section 1.4.3). Pooled zeta-values were calculated for each standard analysed, using the software 'ZETAFACTOR' by M. Brandon and weighted means were then calculated for all analysed standards using the software 'ZETAMEAN' by M. Brandon (Brandon (1992, 1996)).

Age determinations are based on equation 1.2 and reported as central ages (Galbraith and Laslett (1993)) unless otherwise indicated. To test whether more than one population was present a  $\chi^2$ -test was used. If the probability of passing the  $\chi^2$ -test was less than 5%, the sample was interpreted to contain more than one grain population. Radial plots (Galbraith (1990)) were used to graphically display single crystal ages of each sample.

## 1.5 Metamorphism in the study area

The rocks outcropping in the Rio Tinguiririca valley are mainly volcanic and volcanoclastic rocks and continental sediments. All the rocks have been altered at low temperatures and pressures but the pattern of metamorphism in the area is very complex and indicates a polymetamorphic history. The regional pattern is often disturbed by local effects such as contact metamorphism near intrusions. Alteration is often concentrated in areas with high permeability such as tectonised



rocks in brittle fault zones, porous sediments and vesicular volcanic rocks.

### 1.5.1 Previous work

Levi (1970) suggested a model of cyclic burial metamorphism in backarc or intra-arc basins in the Central Andes. A transect was studied East of Santiago de Chile that consisted of three sequences of rocks that show alteration at increasing metamorphic conditions with stratigraphic depth. The individual sequences of rocks are separated by major stratigraphic unconformities. Burial metamorphism was thought to be the most likely type of metamorphism because metamorphic grade increases continuously with stratigraphic age in the practically undeformed rocks. The model suggested cycles of basin formation and infill, leading to burial metamorphism at diagenetic to lower greenschist facies conditions. The basins were later inverted during periods of compression in the arc or backarc and with only very little associated deformation. During metamorphic alteration pore space in the rocks was filled with secondary minerals and the rocks were effectively sealed against fluid flow. For this reason, they were practically unaffected by later metamorphic events and the sharp breaks in metamorphic grade between the rocks of two different cycles were preserved. Levi et al. (1989) expanded the model to other parts of the Central Andes, where similar observations were made. Several later studies confirmed the model of Levi (1970); Levi et al. (1989) and higher grade metamorphic rocks were even found to overlie lower grade rocks in several different locations in the Central Andes.

In recent years, however, new insights into stratigraphic and tectonic settings of the Mesozoic and Cenozoic rocks in the Central Andes and detailed studies of metamorphic conditions across unconformities have cast doubt on the validity of such a model in some parts of the Chilean Andes (Charrier et al. (1996); Belmar (2000); Charrier et al. (2002); Bevins et al. (2003)).

Bevins et al. (2003) examined a transect East of Santiago de Chile and found continuous changes in metamorphic grade at a small scale across two stratigraphic unconformities. Their interpretation was that more refined methods would be necessary to prove a break in metamorphic grade and that some of the changes in mineral zones found by earlier authors could also be attributed to changes in whole rock chemistry. They concluded that the evidence from the available methods was not sufficient to confirm the model of Levi et al. (1989).

Belmar (2000) studied the low-grade metamorphic rocks in the Rio Tinguiririca valley. The aim of his work was to conduct a detailed study of the low-grade metamorphic rocks in that area and test the model of Levi (1970) and Levi et al. (1989). The rocks outcropping in the Rio Tinguiririca valley belong to two different basin infills, a Mesozoic sequence and a Tertiary sequence, separated by a major stratigraphic unconformity. There is a slight angular unconformity between the two sequences and the rocks of the Mesozoic sequence are very weakly deformed, whereas the rocks of the Tertiary sequence have been folded. Belmar (2000) sampled the area very densely and combined polarised light microscopy, electron microprobe analysis, fluid inclusion microthermometry, illite crystallinity and vitrinite reflectance in order to establish a pattern of metamorphic grade. He found that no visible break in metamorphic conditions occurs over stratigraphic unconformities or across major structural features such as thrust faults. Metamorphic grade appears to increase continuously from the youngest to the oldest stratigraphic units. However, the pattern is often disturbed by local effects such as contact metamorphism. Belmar (2000) proposed a polymetamorphic history for the area with an overall pattern dominated by a long-lasting burial event. This is in contrast to the models of Levi (1970) and Levi et al. (1989).

## **1.5.2 Secondary minerals found in the present study**

### **Calcic zeolites**

Calcic zeolite minerals mainly occur in the Coya Machali Formation. Here, they are concentrated in brittle fault zones, along fault planes, in tectonised rocks or in vesicular volcanic rocks. Identification of zeolites in thin section is often not possible but microprobe analyses of zeolites in 9 samples from the Coya Machali Formation allowed to identify at least 4 different zeolite minerals present (see figure 1.4): laumontite, stilbite, mordenite and cowlesite or scolecite. Some chabazite may also be present. Stilbite and scolecite are both described by Gottardi and Galli (1985) as quite common zeolites that are probably formed during hydrothermal activity. A hydrothermal genesis is also common for mordenite and chabazite according to the same authors but a so-called sedimentary genesis by alteration of volcanic glass is also possible. Laumontite has a wider range of possible settings from weathering to diagenetic or metamorphic formation to hydrothermal gene-

sis. All of these zeolites are typical of low-grade conditions. Kristmannsdottir and Tomasson (1978) described a series of zones with increasing temperature in geothermal areas in Iceland: Chabazite —  $\rightarrow$  scolecite —  $\rightarrow$  stilbite —  $\rightarrow$  laumontite. Laumontite as the highest temperature indicator in the series can still be formed at temperatures of less than 100°C (Gottardi and Galli (1985)). In a series of samples taken near and in an intrusion in the Coya Machali Formation (figure 1.5 a. and b.) stilbite and scolecite were found in the inner part of the intrusion and laumontite towards the edge indicating increasing temperatures towards the rim of the intrusion. In view of this observation it appears likely that alteration in the intrusion was connected to hydrothermal activity in the surrounding rocks and that the amount of alteration decreases from the outside in. Isolated occurrences of zeolite minerals were found in the Rio Damas Formation that is in general characterised by minerals typical of higher metamorphic conditions. In these samples zeolites cannot be identified in thin section and their presence was shown by X-ray diffraction analysis of the clay fraction ( $<2 \mu\text{m}$ ) (see Appendix A).

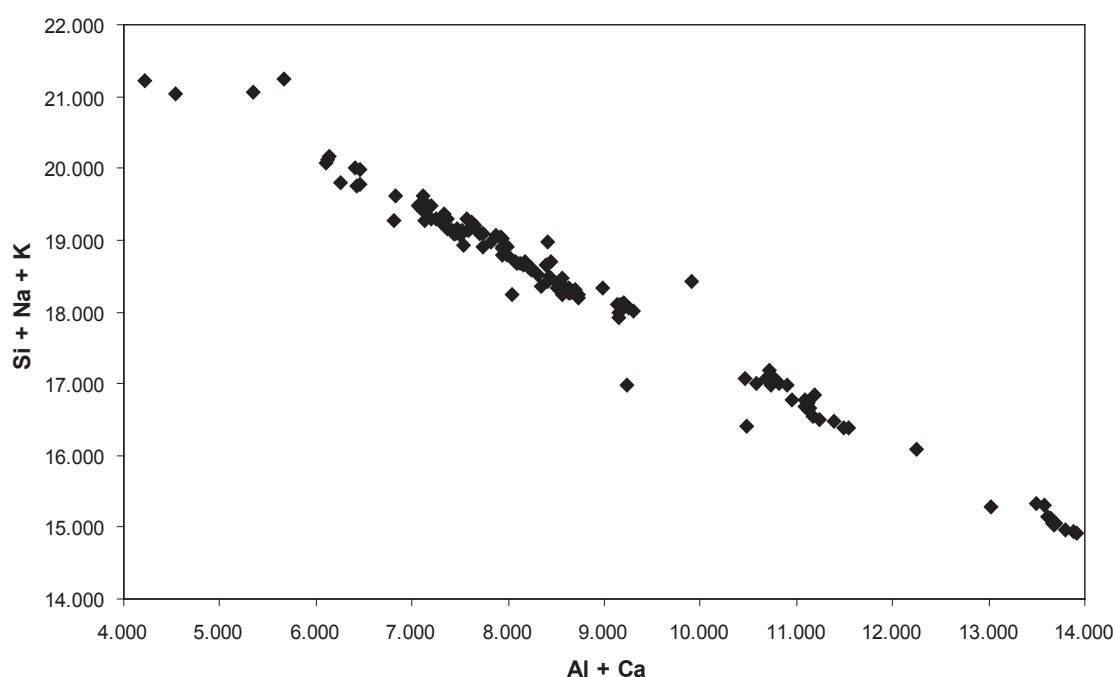


**Figure 1.4:** Microprobe analyses of zeolites in samples from the Coya Machali Fm. Analyses are recalculated for 48 O pfu. and plot along the Si+(Na,K) vs. Al+Ca exchange vector. At least 4 different zeolite minerals were analysed: mordenite, stilbite, laumontite and scolecite

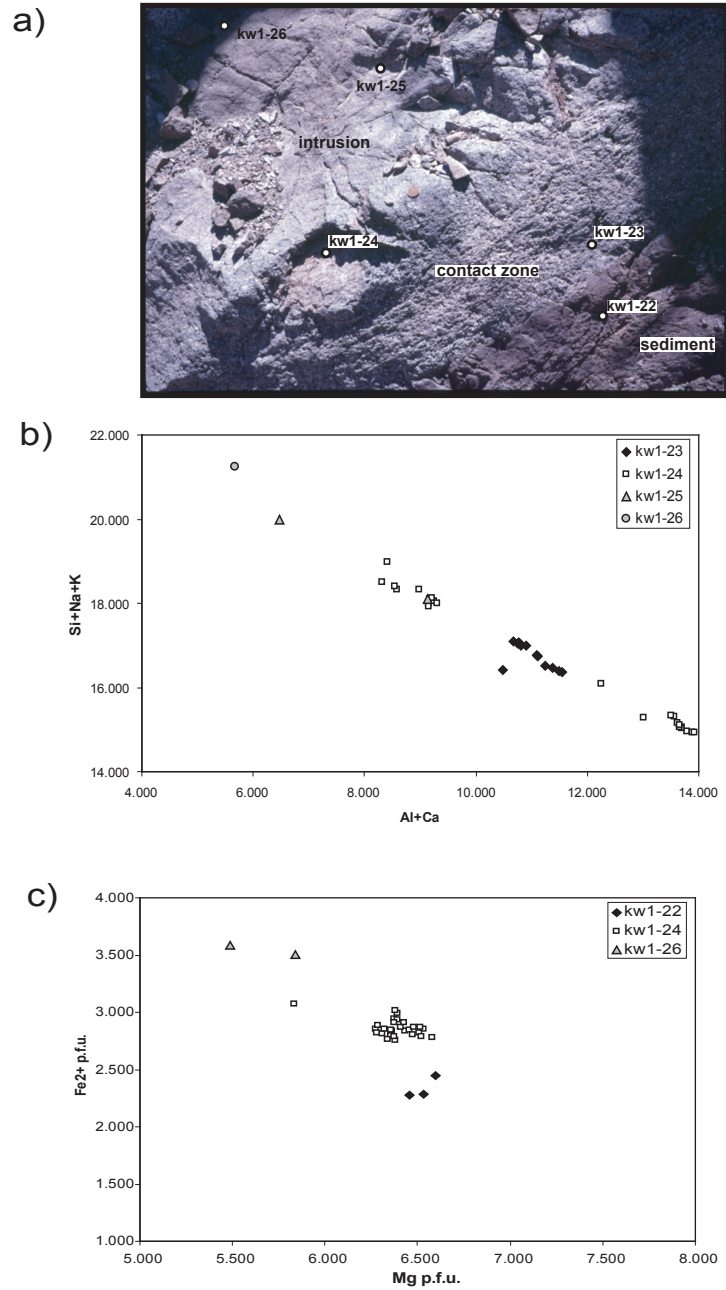


**Figure 1.5:** a. Samples taken in the contact zone between an intrusive body and the surrounding sediments of the Coya Machali Fm. b. Microprobe analyses of zeolites plotted as in figure 1.4. It can clearly be seen that at least 3 different zeolite minerals are present in the samples. c. Microprobe analyses of chlorites from the same samples show a trend of increasing  $\text{Fe}^{2+}$  values towards the inner part of the intrusion.

## Celadonite

Celadonite can be recognised in hand specimens and in thin section by its intense green–bluegreen colour. It is not an index mineral for metamorphic conditions but is generally considered to form at zeolite to prehnite–pumpellyite facies conditions. Celadonite is most commonly found in igneous rocks (mainly basalts) in vesicles or as a breakdown product of olivine or hypersthene (Odom (1984)). A hydrothermal genesis can be assumed to be common for this mineral. In the study area, celadonite occurs in great abundance in rocks of the upper Rio Damas Formation but has also been found in the Coya Machali Formation. It may sometimes be intergrown with chlorite and microprobe analyses of celadonites and chlorites in various samples indicate that a complete transition between pure chlorite and pure celadonite can be found (figure 1.6).

## Chlorite

Chlorite is a very common mineral that can be formed over a wide range of temperatures and pressures by various mechanisms including breakdown of other minerals such as feldspars, amphiboles and pyroxenes and hydrothermal activity. Chlorite was found in almost all the samples from the study area and occurs as an infill in vesicles, cracks and other small cavities in the rocks and as an alteration product, mainly in feldspar minerals. Microprobe analyses of chlorites from various samples indicate that it is often intimately intergrown with celadonite and maybe also fine-grained zeolite minerals. Appreciable amounts of Ca were often found in chemical analyses. According to (Bettison and Schiffman (1988), Ca contents of more than 0.10 cations per 28 oxygen ions indicate the presence of smectite and chlorite–smectite interlayers. A difference can be seen between chlorites from the Rio Damas and Coya Machali Formations (figure 1.7). The chlorites from the Rio Damas Formation have higher  $X_{Mg}$  values than those from the Coya Machali Formation. In a series of samples taken in an intrusion and the surrounding sediments, the  $X_{Mg}$  values increase inwards into the intrusion with increasing distance from the contact with the surrounding rocks (figure 1.5 a. and c.). The meaning of this slight change in chlorite composition is unclear but may be connected to temperature. It can be assumed that the chlorites in the Rio Damas Formation, in general, formed at higher temperatures than those in the Coya Machali Formation.

This may appear to be in contrast to the observation in the sample series in the intrusion in the Coya Machali Formation but here, the assumption is supported by the observation that zeolites analysed in these samples also imply decreasing temperatures towards the inner part of the intrusion.

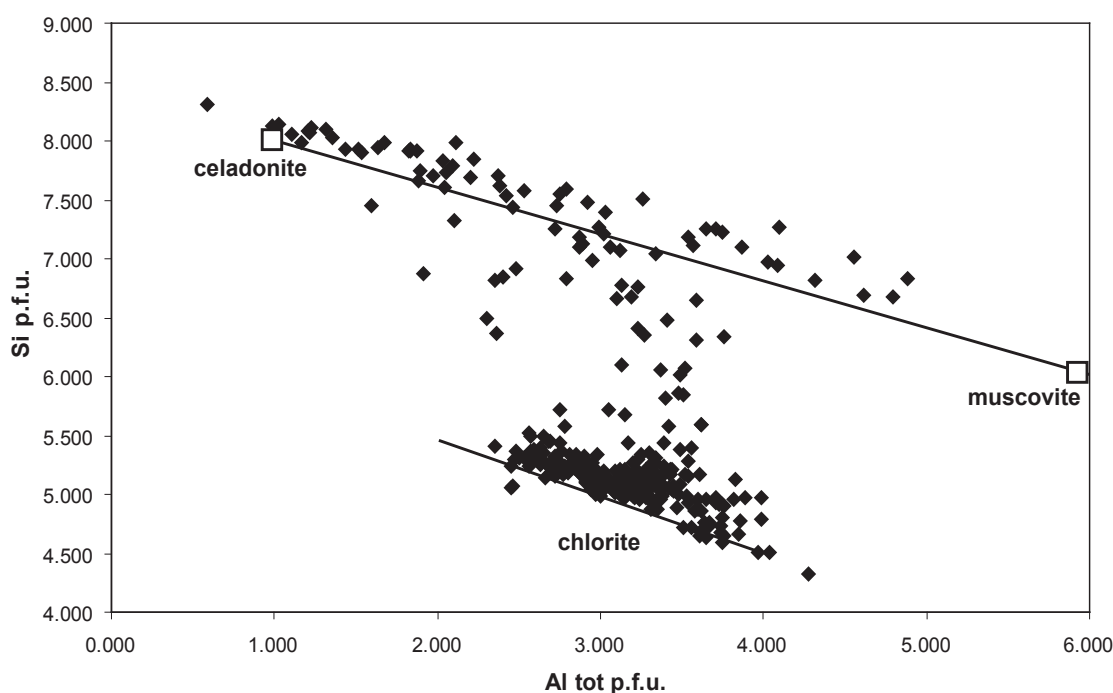


**Figure 1.6:** Microprobe analyses of phyllosilicates recalculated for 22 O pfu. Pure celadonite was found and also a wide range of celadonitic micas plotting along the cel–ms exchange vector. Clinocllore was found in great abundance and the analyses show a spread between about 2 and 4  $Al_{tot}$ . Analyses plotting between the chlorite and mica exchange vectors indicate (probably) mixed analyses. These may represent physical intergrowth of the 2 minerals.

## Epidote

Epidote occurs in samples from all over the study area. It is often present as slick-fibres along brittle fault planes in the Rio Damas and Coya Machali Formations but also as an infill in cracks and vugs in the rocks mainly in the Rio Damas Formation or as a replacement of feldspar or other primary minerals. Epidote is not an index mineral for any specific metamorphic conditions but, like chlorite, can exist over a fairly large temperature range. The combined occurrence of epidote and pumpellyite, however, appears in rocks of a wide range of compositions to be diagnostic of temperatures between about 240 and 290 °C (Potel et al. (2002)).

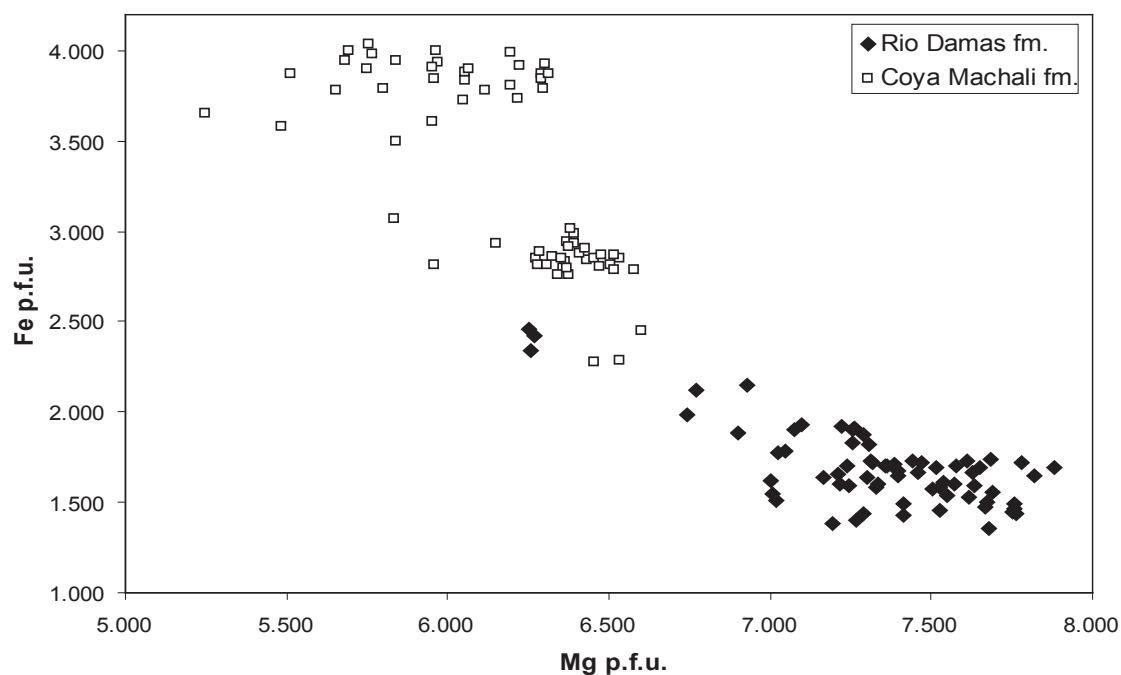


**Figure 1.7:** Microprobe analyses of chlorites from the Rio Damas and Coya Machali Formations recalculated for 28 O pfu. Chlorites from the Coya Machali Formation, in general, contain slightly more Fe than samples from the Rio Damas Formation.

Epidote is only found in direct contact with pumpellyite in the lower Rio Damas Formation.

### Pumpellyite

Pumpellyite was found mainly in the rocks of the Rio Damas Formation. Here, it occurs in great abundance in vesicles and cracks and together with chlorite and sometimes epidote as a replacement of feldspar. Belmar (2000) reported isolated occurrences of pumpellyite in the Coya Machali Formation near intrusions. He interpreted these occurrences to be due to contact metamorphism near the intrusions. In general, the occurrence of pumpellyite can be taken as an indication of prehnite–pumpellyite facies conditions. In this study, pumpellyite was not found together with prehnite although occurrences of prehnite in the Rio Damas Formation were reported by Belmar (2000). As mentioned above, pumpellyite sometimes occurs with epidote. This assemblage is restricted to a fairly narrow temperature range. No actinolite was found in any of the samples and thus it can be assumed that pumpellyite–actinolite or even greenschist facies conditions were not reached in the area.

### **1.5.3 Metamorphic conditions in the study area**

#### **Rio Damas Formation**

Metamorphic grade increases in the Rio Damas from the top toward the bottom of the formation. Near the top, celadonite is the dominant secondary mineral. Celadonite is thought to represent zeolite facies to prehnite–pumpellyite facies conditions. Slightly lower down in the formation, pumpellyite becomes the main index mineral indicating prehnite–pumpellyite facies conditions. In the lowest samples from the Rio Damas Formation, pumpellyite is found together with epidote, indicating temperatures above about 240 °C (Potel et al. (2002)). However, zeolite minerals have been identified in a sample from near the top and in a sample from the lowest part of the Rio Damas Formation. Also, zonation within filled vesicles in the rocks sometimes indicates decreasing temperatures instead of increasing metamorphic conditions (Belmar (2000)). Such effects cannot be attributed to contact metamorphism but rather appear to document later hydrothermal activity at slightly lower temperatures.

#### **Baños del Flaco Formation**

The Baños del Flaco Formation mainly consists of limestones and sands. Chlorite, quartz and calcite are mainly found as secondary minerals but do not give any constraints on metamorphic grade in the unit. Belmar (2000) found a temperature of 222 °C from fluid inclusions in the Baños del Flaco Formation and proposed late diagenetic conditions in this unit.

#### **BRCU**

In the BRCU also no index minerals were identified. Chlorite and quartz are widely found but give little indication of metamorphic grade. Again, Belmar (2000) proposed late diagenetic conditions for the unit based on vitrinite reflectance data.

#### **Coya Machali Formation**

In the Coya Machali Formation, the main index minerals are zeolites. 4 or 5 different zeolites were identified in various samples by electron microprobe analysis in thin sections. Chlorite, quartz, calcite, epidote and celadonite were also widely



found in the rocks of the Coya Machali Formation. Zeolite minerals are especially concentrated in areas where the rocks underwent brittle deformation. They occur as slickofibres on fault planes and in cracks and other cavities in the rocks. In extreme cases, zeolite minerals occur as a kind of cement that holds together tectonic breccias. Zeolite facies conditions appear to have been prevalent in the Coya Machali Formation but there are indications of several phases of mineralization (see figure 2.5). Amygdales are often filled with several generations of secondary minerals, such as chlorite, calcite and zeolite minerals, or are later offset by younger cracks that have since been filled with secondary minerals. Zeolite minerals and celadonite are typical of hydrothermal alteration at fairly low (<100 °C) temperatures. Probably, very low grade burial metamorphism occurred in the unit but has since been overprinted by several more localised events, such as circulation of hot fluids in brittle fault zones. No such clear evidence of an increase of metamorphic grade with stratigraphic age can be seen in the unit because the Coya Machali Formation has been folded and thrust. However, no sharp breaks in metamorphic grade have been found either. This indicates that pulses of hydrothermal activity have occurred during and after deformation.

### 1.5.4 Pattern of metamorphism

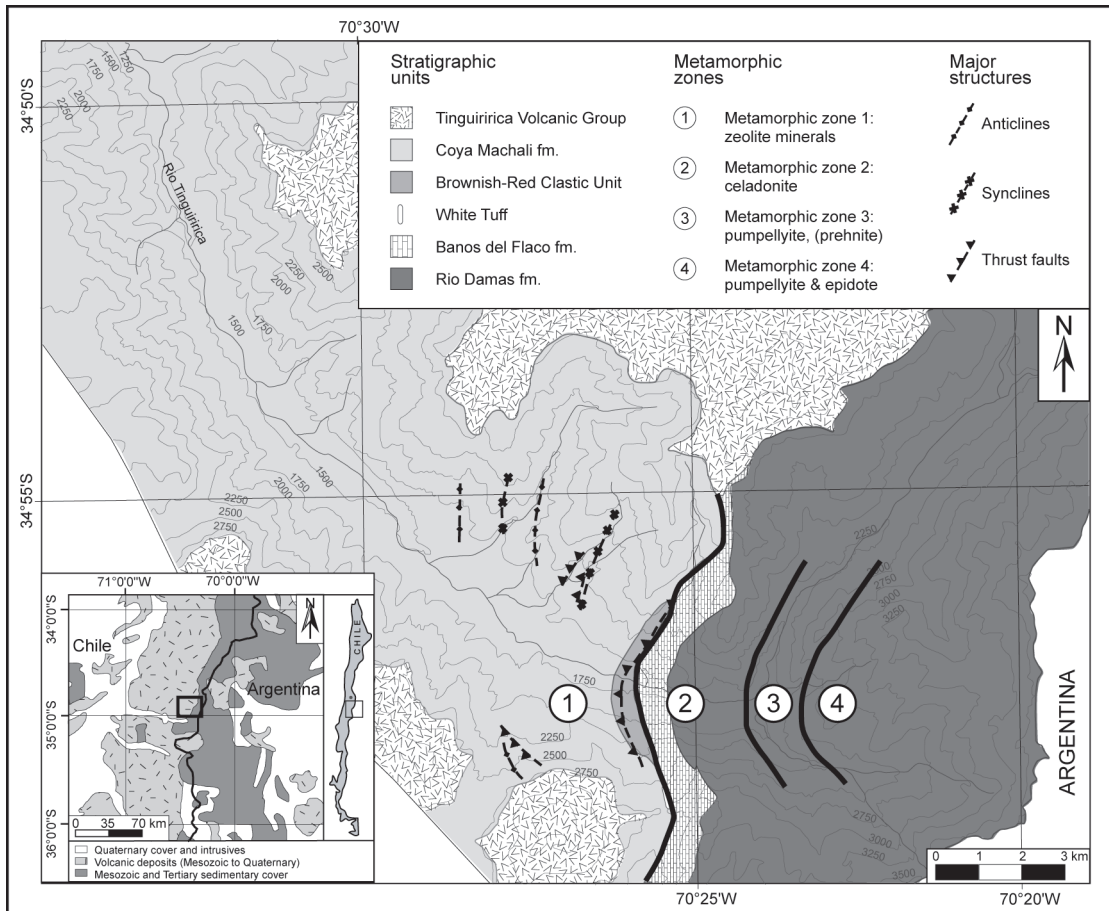


**Figure 1.8:** As described by Belmar (2000) there appears to be an increase in metamorphic grade from west to east in the study area. Here, 4 different zones with major occurrences of different minerals or mineral assemblages have been distinguished. However, the overall pattern is often disturbed by minor inconsistencies.

The pattern of metamorphism in the Rio Tinguiririca valley is very complex. The rocks were altered at very low-grade conditions and differences in metamorphic facies are not very large. In general, an increase in metamorphic conditions with stratigraphic depth from zeolite facies conditions in the Coya Machali Formation to prehnite–pumpellyite or even pumpellyite–epidote facies conditions in the lower part of the Rio Damas Formation can be observed. The increase in metamorphic grade is most pronounced within the Rio Damas Formation where there is a definite increase in temperature from the top to the bottom of the unit. An Ar–Ar age of  $101.3 \pm 2.9$  Ma was determined by Belmar (2000) 2000 in a sample

from near the top of the Rio Damas Formation. The age was interpreted to be a formation age of celadonite. This indicates that metamorphism in this part of the Rio Damas Formation occurred well before deposition of the Coya Machali Formation and probably also of the BRCU. Accordingly, at least two metamorphic events must be distinguished in the area; an older one in the Rio Damas and possibly Baños del Flaco Formations and a much younger one in the Coya Machali Formation and the BRCU that may also have affected the older units to some extent. Figure 1.8 shows zones of different predominant index minerals or diagnostic assemblages.

**Metamorphic zone 1** encompasses the Coya Machali Formation and probably the BRCU and Baños del Flaco Formation. It is characterised by metamorphic conditions corresponding to the zeolite facies and zeolite minerals are the main index minerals present in this zone (figure 1.10). However, there are indications that several episodes of zeolite facies metamorphism occurred (figure 2.5) at different times since older structures are sometimes overprinted by younger mineralizations.

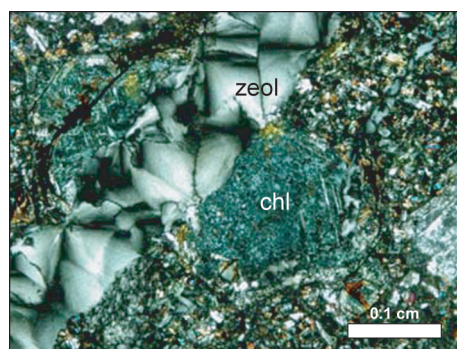


**Figure 1.9:** Photomicrograph of an amygdale in a sample from the Coya Machali Fm. under crossed Nicols. The amygdale is filled with chlorite. The rock was cracked after mineralisation in the amygdale and the crack was later filled with zeolite minerals.

**Metamorphic zone 2** is in the upper part of the Rio Damas Formation. The main index mineral in this zone is celadonite (figure 1.10), which occurs in very large quantities and is easily recognisable by its vivid green to bluish-green colour. Celadonite forms at zeolite to prehnite–pumpellyite facies conditions and does not give any clear constraints on metamorphic grade. Belmar (2000) interpreted the

preferred occurrence of celadonite rather than zeolite minerals to be an effect of a change in rock chemistry rather than an increase in metamorphic conditions. Since the formation of celadonite apparently predates the formation of zeolite minerals in the younger rocks, both metamorphic conditions and whole rock chemistry may have had an effect.

**Metamorphic zone 3** is characterised by the occurrence of pumpellyite (figure 1.10). Occurrences of prehnite from the same area were documented by Belmar (2000) but no prehnite was found in this study.

**Metamorphic zone 4** shows the highest metamorphic conditions and is characterised by the occurrence of pumpellyite together with epidote (figure 1.10). This mineral association has only been found in the lower part of the Rio Damas Formation.

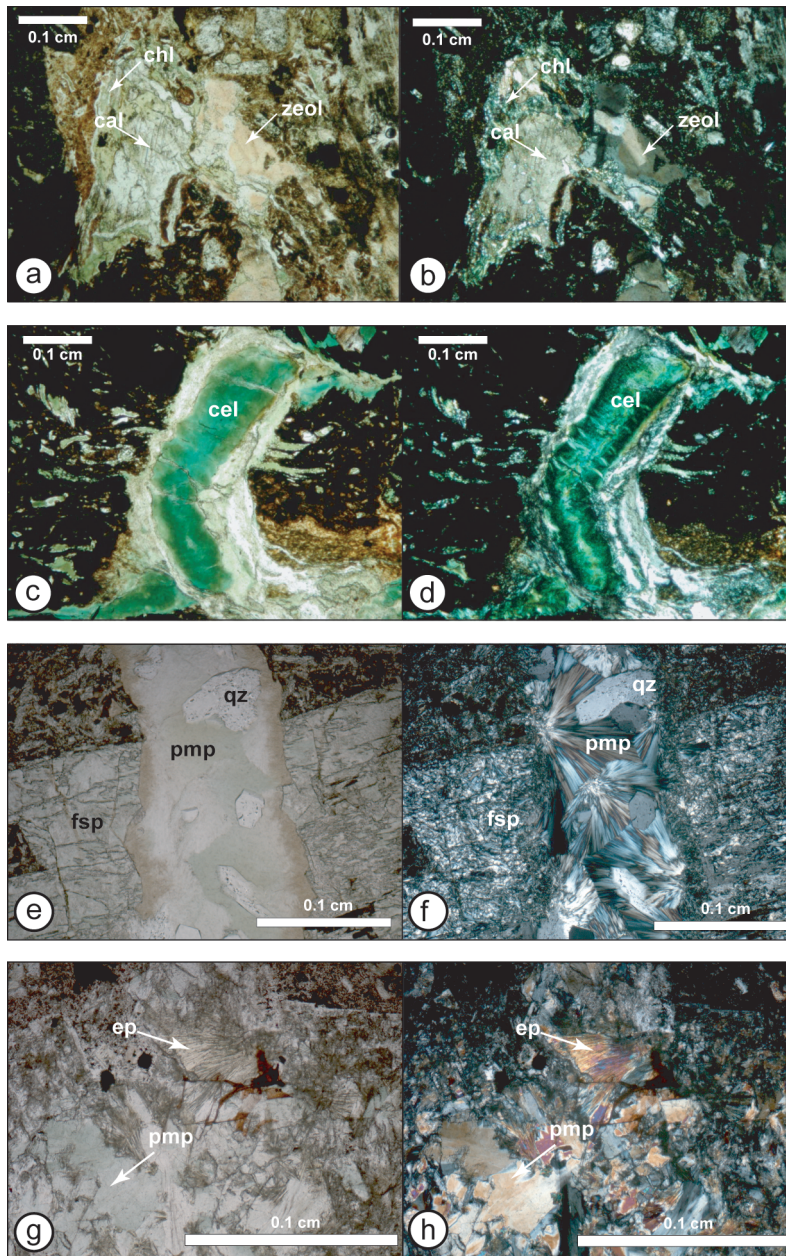


**Figure 1.10:** Photomicrographs of metamorphic minerals found in various samples from the Tinguiririca river valley. (a), (c), (e), (g) were taken with plane parallel light, (b), (d), (f), (h) with crossed Nicols. (a) and (b) show zeolite minerals (laumontite) in a sample from the Coya Machali Fm., (c) and (d) show celadonite in a sample from the Coya Machali Fm. This mineral is easily recognised by its vivid green colour. (e) and (f) show pumpellyite (and quartz) filling a crack in a sample from the Rio Damas Fm. (g) and (h) show epidote and pumpellyite in close contact in a sample from the Rio Damas Fm.



## Chapter 2

# Fission track analysis and low-grade metamorphism in the Rio Tinguiririca valley in the central Chilean Andes

### 2.1 Abstract

Fission track analysis on zircons and apatites from the Rio Tinguiririca valley in the Andes of central Chile has shown that the apparent increase in metamorphic grade in the rocks from West to East, which has hitherto been interpreted as a pattern caused by a long-lasting burial metamorphic event is in fact the result of several heating events at different times. Burial metamorphism may have occurred in subsiding basins but has since been overprinted by local thermal events that caused considerable heating of the rocks even quite close to the surface. The different stratigraphic units in the study area underwent different thermal histories and no regional metamorphic event affecting all units leading to a regional gradient could be demonstrated. Metamorphic grade in the area ranges from diagenetic to subgreenschist facies (prehnite–pumpellyite facies) conditions. Previous studies on the low-grade metamorphism have shown that maximum temperatures during metamorphism must have been around 300 °C in the eastern part of the study area. These temperature estimates are confirmed by fission track analysis since fission tracks in zircon from the eastern part of the study area were sub-

stantially, although not fully annealed sometime during the Cretaceous. In the stratigraphically younger units (the BRCU and the Coya Machali Formation) almost no annealing of zircon fission tracks has occurred. Temperatures in excess of 200 °C were probably only reached for very short times due to contact metamorphism near intrusions.

## 2.2 Introduction

Based on the detailed mapping of Zapatta Nicolis (1995), Belmar (2000) carried out a metamorphic study of the rocks in the Rio Tinguiririca valley in the main Cordillera of the Andes of central Chile (about 35° South). Based on the mineral assemblages, illite crystallinity, fluid inclusion microthermometry and mineral chemistry in the area, Belmar (2000) found increasing metamorphic conditions from west to east, that is from stratigraphically younger to older units in the study area. In the western part of the area, zeolite minerals are abundant and temperature estimates from various methods indicate diagenetic to zeolite facies conditions. In the eastern part of the transect prehnite and pumpellyite were found and temperature estimates confirmed upper subgreenschist facies conditions. Belmar (2000) proposed a long-lasting burial event in the late Tertiary as a mechanism to produce this metamorphic pattern because there are no abrupt changes in metamorphic grade either across stratigraphic or tectonic boundaries. This model contrasts with earlier models for low-grade metamorphism in the Andes (Aguirre et al. (1987, 1989); Levi (1970); Levi et al. (1989); Offler et al. (1980)). Levi (1970) first proposed a model of cyclic burial metamorphism in subsiding basins. Subsequent inversion and uplift of these basins led to stacking of sediments belonging to different cycles separated by stratigraphic unconformities. Sharp breaks in metamorphic grade were found over stratigraphic unconformities, whereas within the individual sequences of sediments a continuous increase in metamorphic grade from younger to older rocks was observed. In later studies (e.g. Aguirre et al. (1987); Levi et al. (1989)) it was shown that porous rocks that underwent low-grade metamorphism are often sealed by the formation of secondary minerals. During later metamorphic cycles, such rocks are no longer permeable and fluids cannot circulate. Only little formation of new minerals takes place and the rocks show only minor traces of the later event. The observation of Belmar (2000) of an apparently continuous



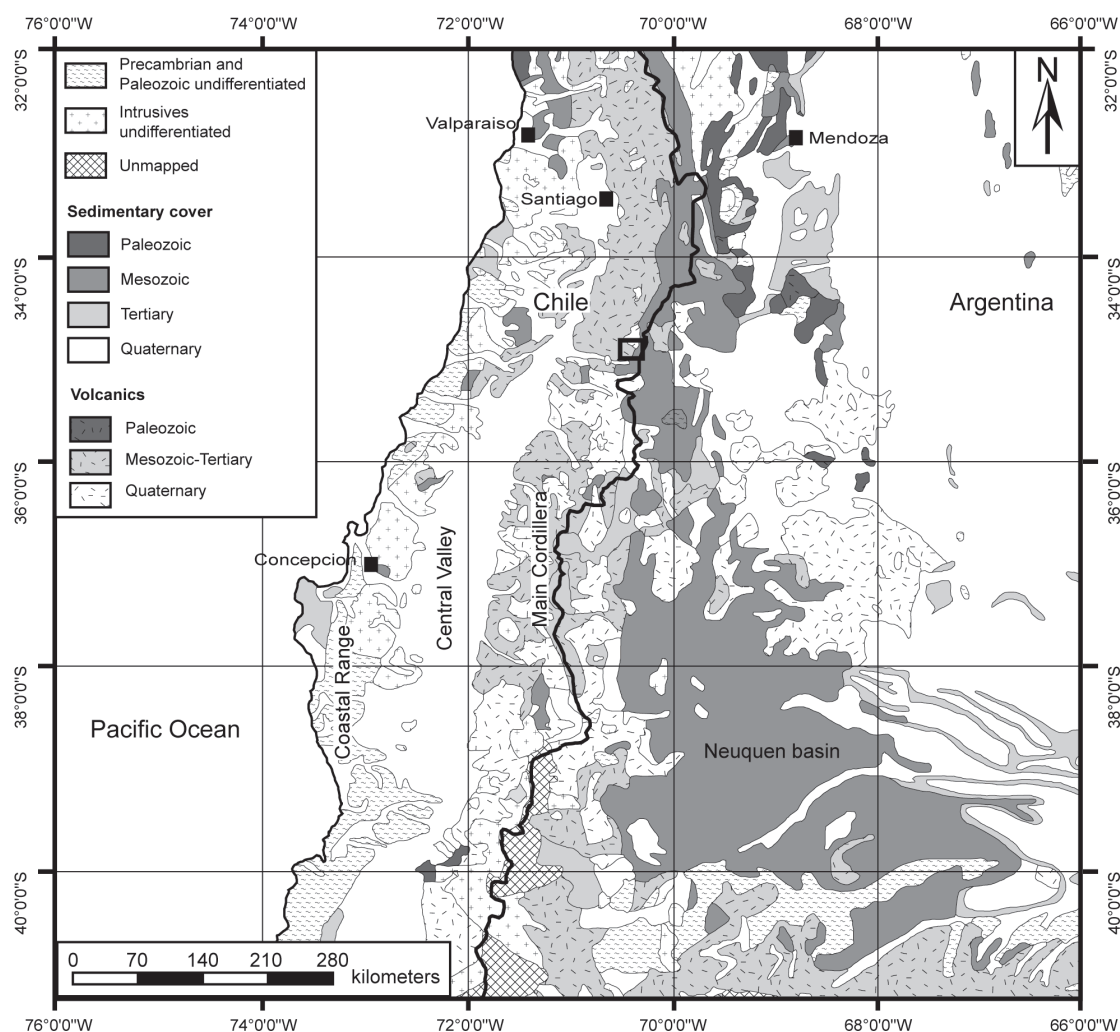
increase in metamorphic grade within sediments belonging to two separate cycles of infill of extensional basins is thus in sharp contrast to the previous models. The aim of the present study was to test the model of a single burial event proposed by Belmar (2000) using fission track analysis on apatites and zircons from the same study area and complementing the data set with further petrological studies, such as additional data on mineral chemistry from electron microprobe analysis and identification of phyllosilicates with X-ray diffraction analysis. The Rio Tinguiririca Valley was chosen for this study because its geology and stratigraphy have already been described in detail by Charrier et al. (1996); Zapatta Nicolis (1995) and the metamorphic conditions are known from the study of Belmar (2000). Also, the area was found to be relatively little disturbed by intrusive activity compared to areas to the North and South in the main Cordillera of the Chilean Andes.

### 2.2.1 Geological setting

The study area is located in the main Cordillera of the Andes in central Chile at about 35° South (see figure 2.1). A 25 km transect in the Rio Tinguiririca valley from near the Argentinean border in the East to the confluence of the Rio Tinguiririca and the Rio Azufre in the West was investigated.

Figure 2.1 shows a geological overview of the setting of the study area near the village of Termas del Flaco. It is at the western edge of the Neuquen back arc basin in the Main Cordillera of the Andes. The area is at the transition of two segments of the Andes that have distinctly different Mesozoic histories. To the North a sedimentary platform (the Aconcagua platform) developed in the back arc during the Jurassic. In the Early Cretaceous an aborted marginal basin developed West of the platform and large volumes of basalts and andesites were erupted. In the middle Cretaceous a fold and thrust belt was formed in the back arc area (Aconcagua fold and thrust belt) and the magmatic arc migrated to the West during the Late Cretaceous and Early Tertiary. To the South a large ensialic back arc basin (Neuquen basin, see figure 2.1) developed in the Early Jurassic and was active until the Early Cretaceous. In the Cretaceous a fold and thrust belt also formed in the back arc area. The magmatic arc remained more or less stationary up to the present and active volcanism continued until recent times (see Mpodozis and Ramos (1989)).

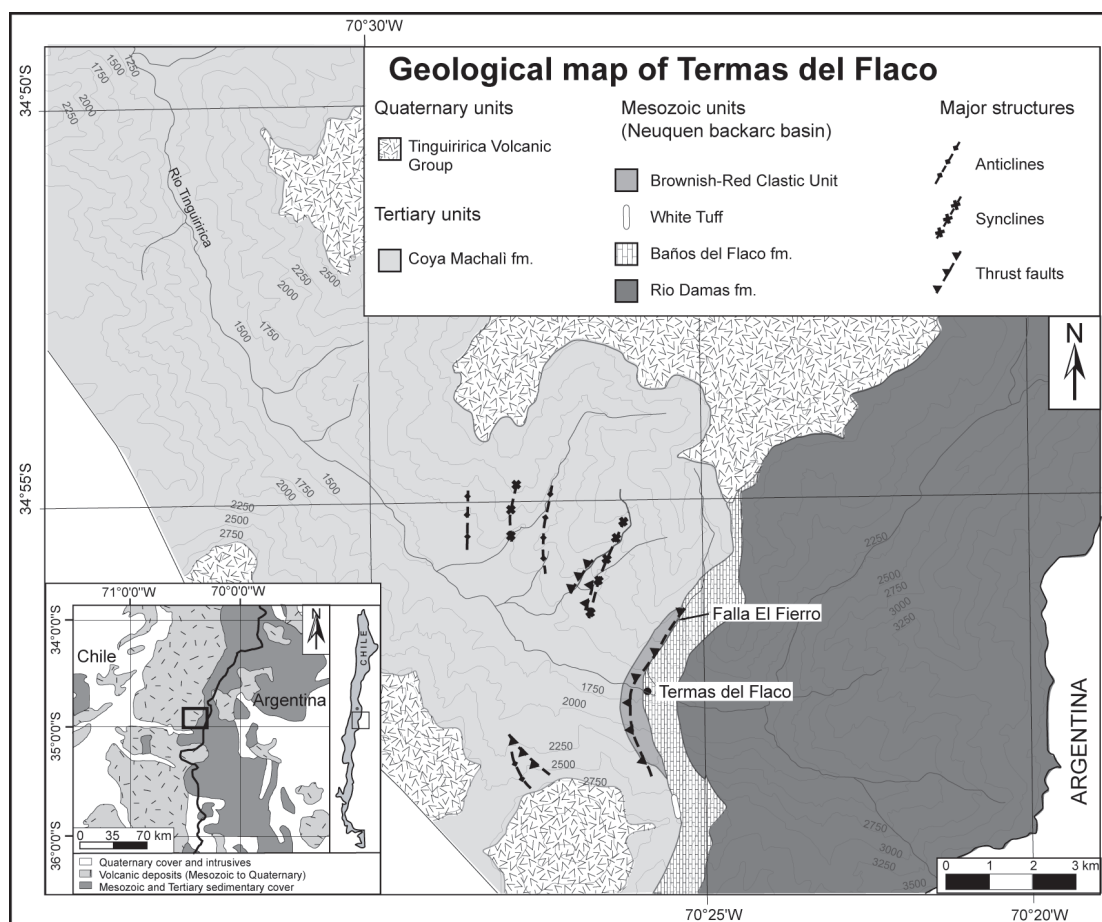
The Mesozoic units outcropping in the study area were deposited along the



**Figure 2.1:** Location of the study area (black box) in the Main Cordillera of the Andes at about 35° south. The study area lies at the transition between the deposits of the Neuquen backarc basin to the east and the Mesozoic to Tertiary volcanic deposits in the Main Cordillera of the Andes.

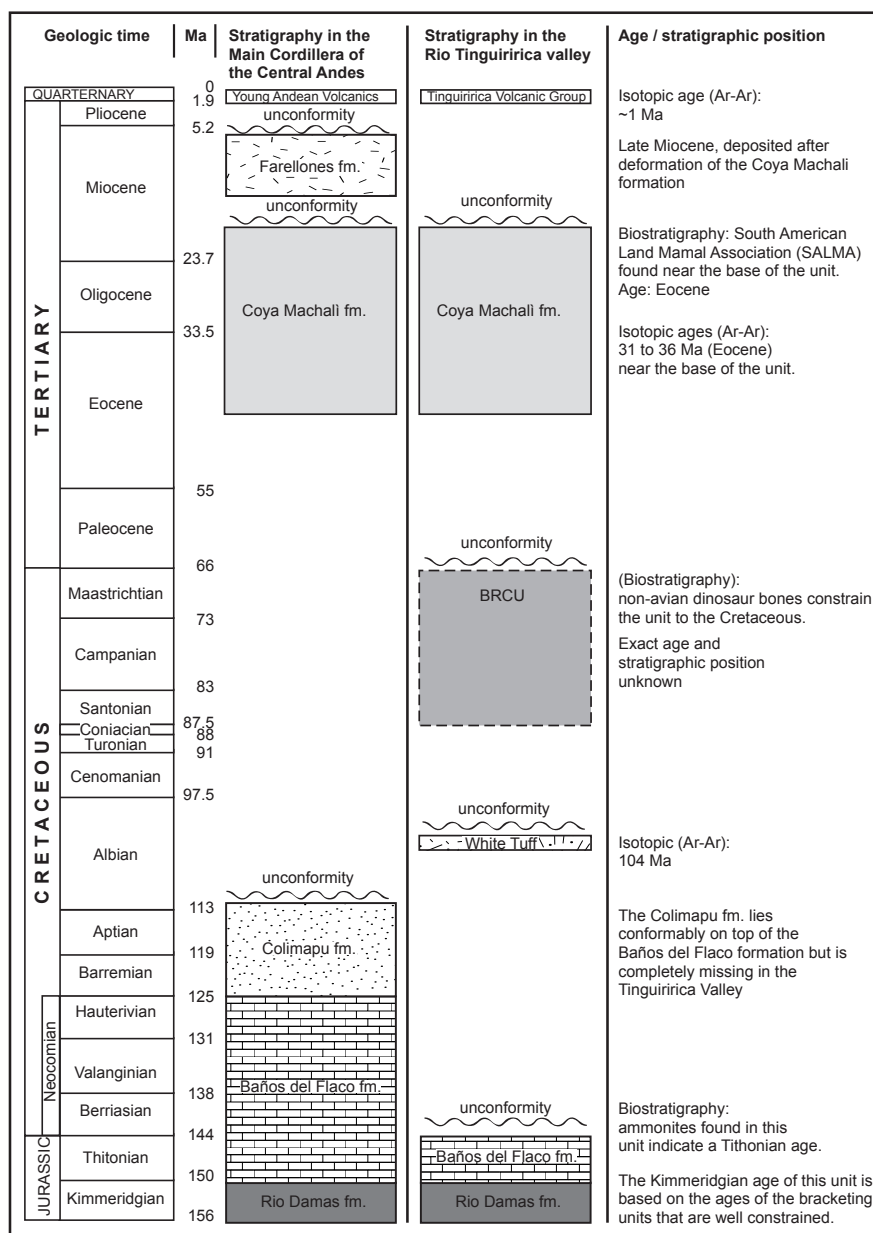
western edge of the Neuquen back arc basin and are unconformably overlain by deposits from a Tertiary intra-arc basin that formed to the west of the Neuquen basin. This second basin was active from the Late Eocene to Late Oligocene or Early Miocene and was then deformed during a period of compression in the Miocene.

Figure 2.2 shows a geological map of the study area near the village of Termas del Flaco. The middle Jurassic to Early Cretaceous stratigraphic sequence in the Neuquen back arc basin consists of two transgression-regression cycles with marine and continental clastic sediments. The oldest deposits of the series, the Nacientes del Teno Formation (Oxfordian), are not exposed in the study area. They consist



**Figure 2.2:** Geological map of the study area near the village of Termas del Flaco in the Rio Tinguiririca valley showing the stratigraphic units discussed in the text and major structural features.

of an 800–1000 m thick sequence of marine sandstones and limestones capped by a gypsum upper member (Charrier et al. (1996)). The Kimmeridgian Rio Damas Formation is the oldest unit exposed in the study area (figure 2.2) and consists of a 3700 m thick sequence of continental sandstones and conglomerates with a high percentage of volcanic material and of lavas. The Baños del Flaco Formation conformably overlies the continental deposits of the Rio Damas Formation and consists mainly of marine sandstones and limestones showing a transgression from platform to shelf sediments. Deposition of this unit was from the Tithonian to the Neocomian (Early Cretaceous) and the unit reaches thicknesses of up to 2000 m, but in the study area only the Tithonian deposits (about 400 m thick) are preserved and the upper part of the formation has been eroded (Charrier et al. (1996)). At other localities, the Aptian to Albian Colimapu Formation conformably overlies



**Figure 2.3:** Stratigraphic column showing the ages of the units outcropping in the study area. The second column shows a simplified column of units found in other parts of the Central Andes. The BRCU has hitherto only been found in the Tinguiririca river valley and its exact age is not known. Fig. modified after Charrier et al. (1996).

the Baños del Flaco Formation. However, it is completely missing in the study area (figure 2.3). It is not known whether the unit was deposited and later eroded or if local erosion began earlier and deposition did not take place. Instead, a unit consisting of well-bedded brown and red continental clastic sediments, the so-called Brownish-Red Clastic Unit (BRCU), lies without angular unconformity on top of the erosional surface of the Baños del Flaco Formation. This unit has no continuation to the North and South and has not hitherto been described in any other locality in the Central Andes. The exact stratigraphic position and age of the BRCU are still a matter of debate (see Charrier et al. (1996)).

The deposits of the Tertiary intra-arc basin are represented in the study area by the Coya Machali Formation, a thick (about 1500 m) sequence of continental sediments and volcanic and volcanoclastic rocks. The age of these deposits is given as late Eocene to early Miocene based on fossils and radiometric age data (Charrier et al. (1996); Wyss et al. (1990)). Charrier et al. (2002) showed that the oldest ages for the Coya Machali Formation appear to differ laterally and that the onset of sedimentation was probably not at the same time in all parts of the basin. The deposits of the Coya Machali Formation were later folded and thrust in the Miocene.

A suite of Quaternary volcanics, radiometrically dated at 1.1 Ma (Charrier et al. (1996); Arcos et al. (1988)) lies discordantly on top of all the deformed Mesozoic and Tertiary units. These consist mainly of basalts and pyroclastic flows and belong to the Tinguiririca Volcanic Group.

The Mesozoic units in the study area are all tilted to the West with dip angles of about  $50^\circ$ . Although there is a major stratigraphic unconformity between the Baños del Flaco Formation and the BRCU, there is no significant angular unconformity between the units. Tilting must have occurred after deposition of the BRCU and prior to deposition of the Coya Machali Formation, however, because there is an angular unconformity of  $15$  to  $20^\circ$  between the Baños del Flaco Formation and the overlying Coya Machali Formation. Another sharp angular unconformity separates Mesozoic and Tertiary units and the Quaternary volcanics, which lie almost horizontally on top of all the other units. Folding is only observed in the deposits of the Coya Machali Formation. The pre-Tertiary, deformation is documented by the steeply inclined strata and rarely observed thrusts, while no major folds could be observed at the investigated scale. The most prominent structure in the study

area is the Falla el Fierro fault (see figure 2.2) that cuts the BRCU and the Baños del Flaco Formation. Although offset along this fault is not very large (in the range of meters or tens of meters) it can be traced in other localities to the North and South of the study area. Charrier et al. (2002) suggested that the Falla el Fierro thrust is a reactivated normal fault that formed during basin formation in the Late Eocene.

One of the most enigmatic units in the study area is a 3–4 m thick layer of white tuff found directly on top of the Baños del Flaco Formation on the South side of the valley (figures 2.2, 2.3). This tuff layer has been dated with Ar–Ar chronometry at 104 Ma (see Charrier et al. (1996); Wyss et al. (1994)). The age was interpreted as a formation age of the tuff and shows that the layer can neither belong to the Baños del Flaco Formation (Tithonian to Neocomian, see figure 2.3) nor the overlying Coya Machali Formation (Eocene to Miocene, see figure 2.3). Stratigraphically, the white tuff layer takes the same position as the BRCU between the Baños del Flaco Formation and the overlying Coya Machali Formation. Yet field evidence does not allow constraint of the relative ages of the White Tuff and the BRCU.

### **2.2.2 Distribution of metamorphic minerals and facies assemblages**

The pattern of metamorphism in the study area was described in detail by Belmar (2000). Only a brief summary of the most important results from this study will be given in the following. A more detailed discussion is given in chapter 1.

Belmar (2000) observed an increasing gradient in metamorphic conditions from diagenetic to zeolite facies in the West (Coya Machali Formation) to prehnite–pumpellyite facies in the East (Rio Damas Formation). However, locally individual occurrences of minerals did not fit with the overall pattern. Pumpellyite was sometimes found in the Coya Machali Formation and was thought to be an indicator of contact metamorphism near large intrusions.

The rocks in the study area were metamorphosed at fairly low temperatures and pressures (subgreenschist facies). The area can be roughly divided into four zones with different typical index minerals or mineral assemblages (see figure 2.4). From West to East the metamorphic zones are:

1. zeolite
2. celadonite
3. pumpellyite as the dominant secondary phase
4. pumpellyite and epidote occur together indicating the highest metamorphic conditions found in the study area.

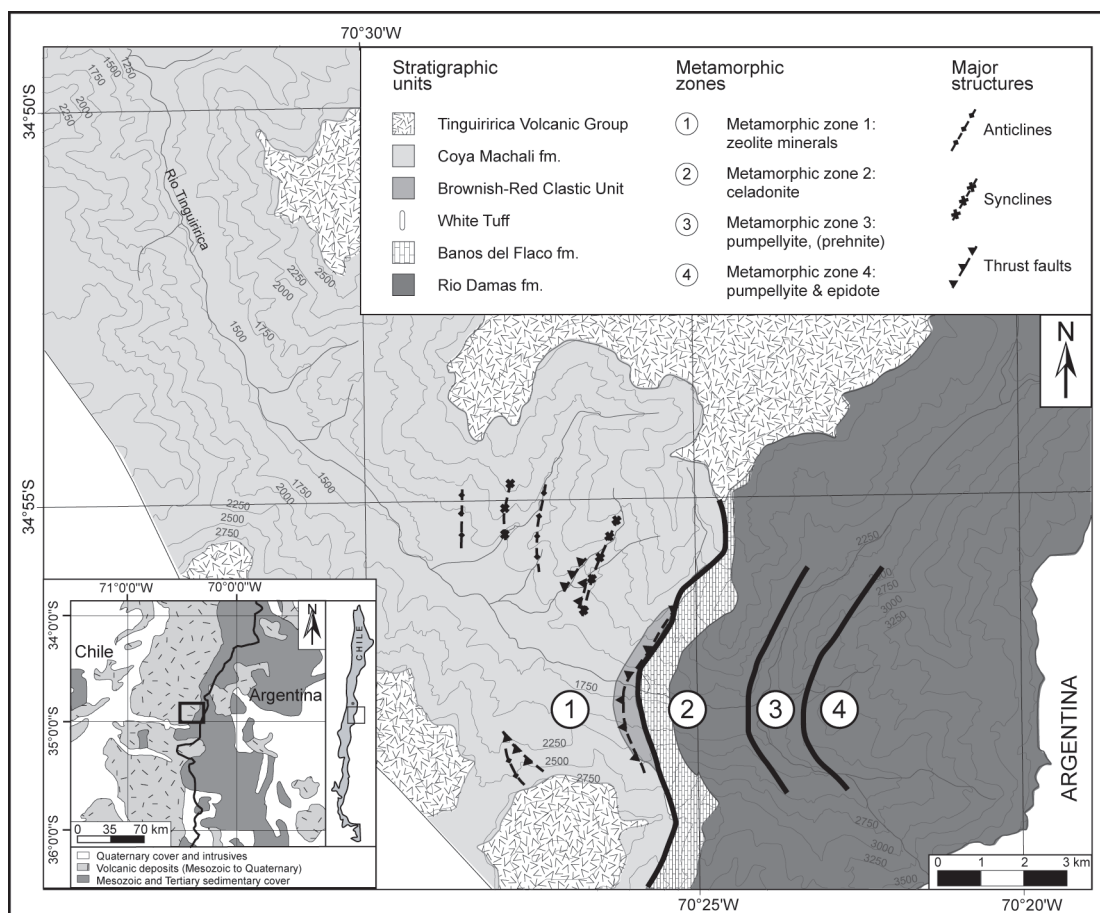


**Figure 2.4:** As described by Belmar (2000) there appears to be an increase in metamorphic grade from west to east in the study area. Here, 4 different zones with major occurrences of different minerals or mineral assemblages have been distinguished (see section 1.5.4 for a more detailed description). However, the overall pattern is often disturbed by minor inconsistencies.

Metamorphic zone 1 (Coya Machali Formation and BRCU, see figure 2.4)

Samples from this zone often contain zeolite minerals in cracks and vesicles and concentrated along fault planes. Belmar (2000) identified at least 6 different zeolite minerals in the study area, including laumontite, stilbite, mordenite, chabazite and scolecite. Of these, mordenite and scolecite are especially indicative of hydrothermal alteration at low temperatures (Gottardi and Galli (1985)). Chlorite, calcite, quartz, epidote and celadonite have also been found in rocks from this part of the study area. In some of the samples zeolite can clearly be seen to be a 'late' formation as it occurs in cracks that offset earlier mineralization, i.e. chlorite and quartz. Figure 2.5 shows a micrograph of an amygdale filled with chlorite that is cut by a crack, which in turn has been filled with zeolite minerals. Several phases of alteration at similar temperature conditions probably occurred in this part of the study area.

Metamorphic zone 2 (upper Rio Damas Formation and possibly Baños del Flaco Formation, see figure 2.4) Celadonite is the dominant secondary mineral in the rocks of the upper Rio Damas Formation. It occurs in very large amounts and is easily recognised by its intense green to blue-green colour. Celadonite is not an index mineral for specific temperature and pressure conditions but is mostly associated with conditions of the zeolite to prehnite-pumpellyite facies. The occurrence of celadonite is more specifically linked to whole rock chemistry (Odom (1984)) and is typically found in basalts or other igneous rocks or as a breakdown product of olivine. Samples from the Baños del Flaco Formation are mostly carbonates and do not contain celadonite. However, a similar metamorphic history can be assumed for these rocks to that of the upper Rio Damas Formation because no large difference in age, stratigraphic depth or structure exists between the rocks of the upper Rio Damas and lower Baños del Flaco Formation.

Metamorphic zone 3 (middle part of the Rio Damas Formation, see figure 2.4) In this zone pumpellyite is the main secondary mineral. Occurrences of prehnite in the same zone were described by Belmar (2000) but prehnite was not found in the present study. Metamorphic grade must have reached prehnite-pumpellyite conditions in this part of the study area and temperature estimates made by Belmar (2000) using fluid inclusion microthermometry and illite crystallinity in this area confirm temperatures of roughly 200 to 250 °C. Chlorite often occurs with pumpellyite but is not as abundant as in samples from the other zones.



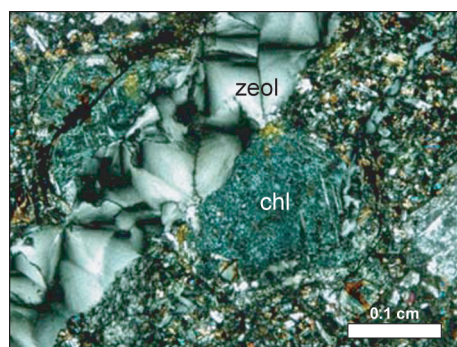


**Figure 2.5:** Photomicrograph of an amygdale in a sample from the Coya Machali Fm. under crossed Nicols. The amygdale is filled with chlorite. The rock was cracked after mineralisation in the amygdale and the crack was later filled with zeolite minerals.

Quartz is often present in vesicles and cracks and calcite is sometimes found as a secondary mineral.

Metamorphic zone 4 (lower Rio Damas Formation) In the lower part of the sequence, pumpellyite often occurs together with epidote, either in cracks and vugs or as alteration products in feldspars. The occurrence of epidote together with pumpellyite in basic rocks has been shown by Potel et al. 2002 to be confined to a fairly narrow temperature range between about 220 and 290 °C for appropriate whole-rock compositions. This mineral assemblage documents the highest metamorphic conditions so far found in the study area.

On a large scale, the metamorphic grade appears to increase from West to East in the study area. Yet a closer look reveals that many of the rocks apparently underwent polymetamorphism (i.e. figure 2.5) and local effects such as contact metamorphism near intrusions often overprint the overall pattern. Belmar (2000) reported occurrences of pumpellyite in the Coya Machali Formation that he interpreted to represent the effects of contact metamorphism near intrusions. Mineralisation of zeolite and epidote along brittle fault planes indicates preferred circulation of metamorphic fluids in fault zones and associated mineralization.

## 2.3 Results from fission track analysis

The methods used for fission track analysis are described in chapter 1. 31 samples were prepared for fission track analysis (tabs 2.1 and 2.2). 19 samples yielded enough zircon and apatite for study, while in the remaining samples only one of

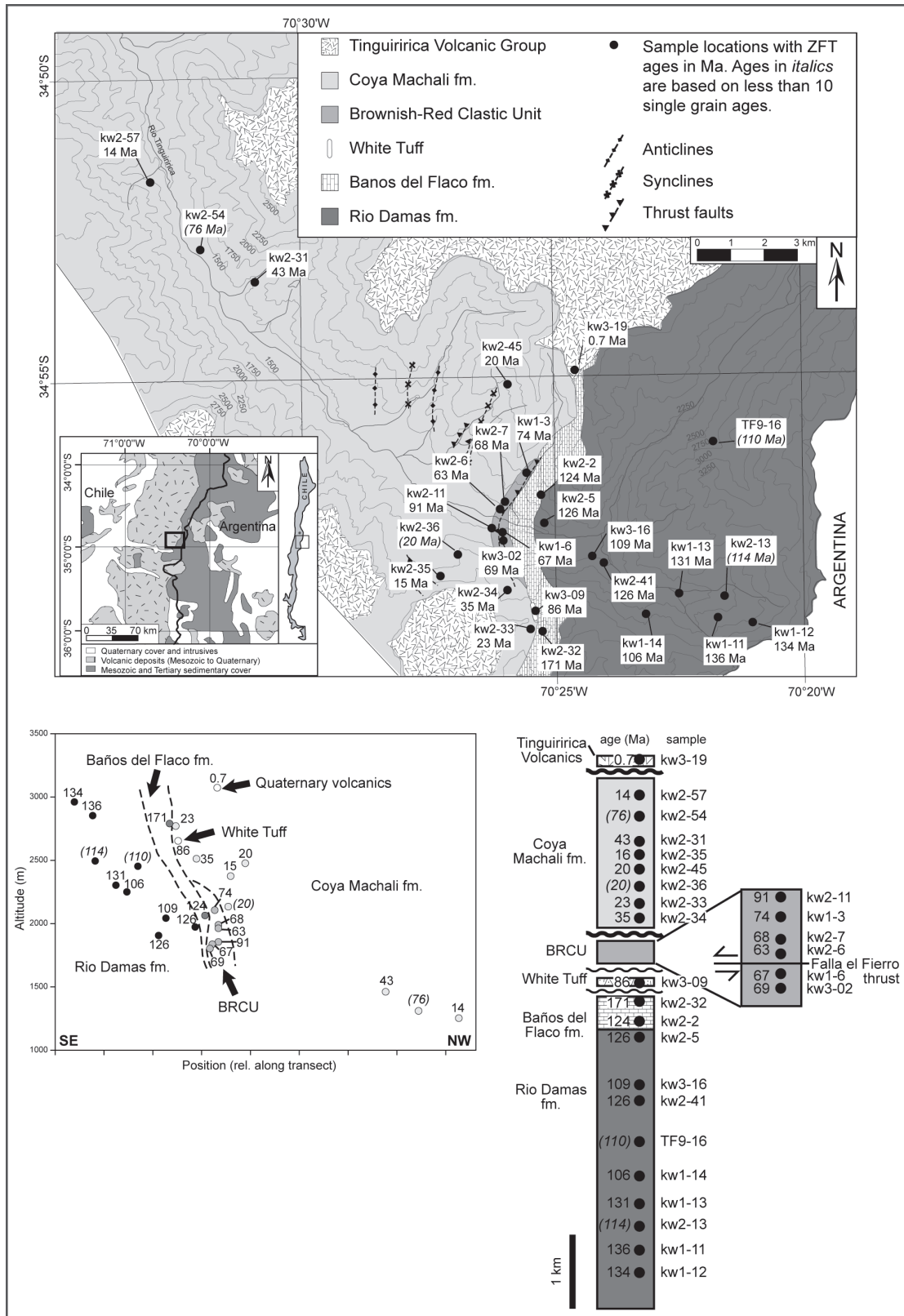
the two minerals could be analysed. All stratigraphic units in the study area were sampled, including the Quaternary volcanic deposits. Samples were analysed with the external detector method (see Wagner and Van den Haute (1992)). Ages were calculated with the software Trackkey 4.1 by Dunkl (2002) and are given as central ages (Galbraith and Laslett (1993)) with  $1-\sigma$  errors for all zircon samples and for several apatite samples (kw1–12, kw2–13, kw2–20, kw2–22, kw2–32, kw2–35). Ages shown in brackets and *italics* are based on fewer than 10 single grain ages. For the remaining apatite samples ages were calculated and are shown as pooled ages because single grain age dating was not possible (see section 1.4.1). Pooled ages are also given with  $1-\sigma$  errors. Radial plots in figs. 2.7, 2.10, 2.11, 2.13, 2.15, 2.17 show single grain ages with  $\sigma$  errors on the left vertical, relative errors of the single grain ages on the horizontal and age in Ma on the right part of the plot. The oldest and youngest single grain ages of each sample are indicated (right). The plots are arranged in stratigraphic order with the stratigraphically highest plot at the top. Grey bars or areas in the plots mark deposition ages of the units in question.

### 2.3.1 Zircon fission track data

27 zircon samples were prepared and irradiated for fission track analysis. Four of these samples yielded less than 10 single grain ages and the central ages for these samples are given in brackets in figures 2.6, 2.7, 2.15. Results are summarised in table 2.1. Figure 2.6 shows the distribution of zircon fission track central ages in the study area together with their position in the stratigraphic column and in a position altitude plot along a NW–SE transect (shown in Appendix A).

**Table 2.1:** Zircon fission track data of samples from all stratigraphic units in the study area: QV: Quaternary Volcanics (Tinguirrica Volcanic Group), CM: Coya Machali Formation, BRCU: Brownish-Red Clastic Unit, WT: White Tuff, BdF: Baños del Flaco Formation, RD: Rio Damas Formation.  $N_S$ ,  $N_I$  and  $N_D$  are numbers of tracks counted.

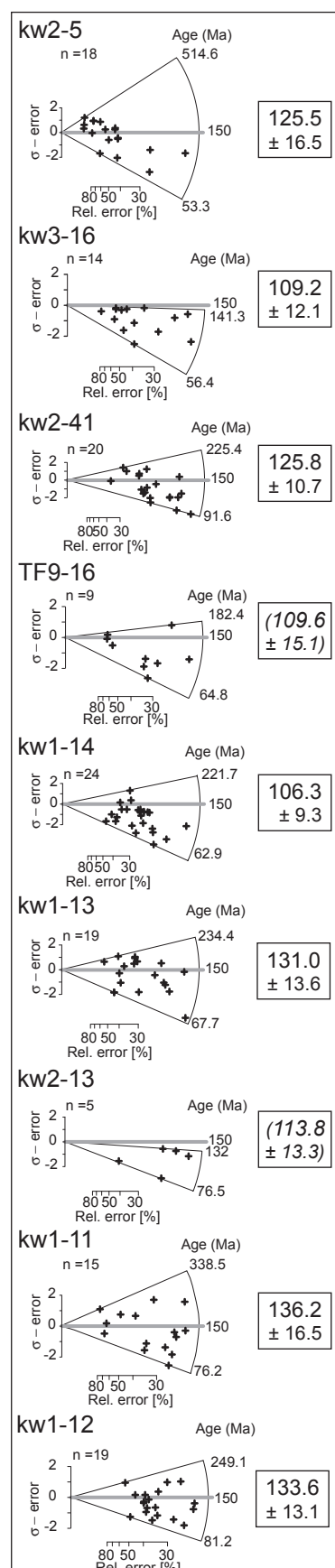
Sample number	Strat. unit	Latitude (S)	Longitude (W)	Altitude (m)	Grains	Spont. track density ( $\times 10^5 \text{ cm}^{-2}$ )	$(N_S)$	Ind. track density ( $\times 10^5 \text{ cm}^{-2}$ )	$(N_I)$	Std. track density ( $\times 10^5 \text{ cm}^{-2}$ )	$(N_D)$	$P(\chi^2)$ (%)	Central Age $\pm 1\sigma$ (Ma)	U (ppm)
kw3-19	QV	34° 54' 24.3"	70° 25' 00.0"	3070	20	1.59	(84)	48.677	(2572)	2.7759	(1366)	50.88	0.7 ± 0.1	806.84
kw2-31	CM	34° 53' 38.3"	70° 31' 11.7"	1458	19	95.043	(1912)	24.755	(498)	3.121	(1366)	<5	42.6 ± 10.5	353.58
kw2-33	CM	34° 59' 16.6"	70° 25' 37.1"	2767	37	20.887	(2014)	32.315	(3116)	4.9384	(2103)	<5	23.0 ± 1.9	262.66
kw2-34	CM	34° 58' 53.5"	70° 26' 09.1"	2509	16	33.968	(232)	25.476	(174)	3.7087	(1800)	97.39	35.4 ± 4.2	298.25
kw2-35	CM	34° 58' 33.1"	70° 27' 37.2"	2372	20	14.261	(371)	24.908	(648)	3.7124	(1800)	12.36	15.5 ± 1.5	311.43
kw2-36	CM	34° 58' 19.6"	70° 27' 22.0"	2131	7	31.375	(150)	42.042	(201)	3.705	(1800)	47.21	19.8 ± 2.5	444.88
kw2-45	CM	34° 55' 23.4"	70° 26' 13.0"	2474	20	23.655	(517)	31.525	(689)	3.6977	(1800)	<5	19.5 ± 1.9	369.74
kw2-54	CM	34° 52' 48.7"	70° 32' 29.5"	1307	5	124.704	(271)	34.512	(75)	3.0864	(1366)	<5	76.3 ± 17.1	473.76
kw2-57	CM	34° 51' 50.6"	70° 33' 13.1"	1250	21	24.621	(798)	38.475	(1247)	3.0519	(1366)	<5	14.2 ± 1.6	500.55
kw1-3	BRCU	34° 56' 53.4"	70° 25' 39.1"	2103	20	69.84	(1418)	32.014	(650)	4.9204	(2103)	<5	73.6 ± 7.0	282.00
kw1-6	BRCU	34° 57' 57.2"	70° 26' 05.4"	1834	12	54.742	(1244)	30.407	(691)	5.1187	(2103)	<5	66.5 ± 6.1	236.10
kw2-6	BRCU	34° 57' 15.4"	70° 26' 06.0"	1960	20	68.498	(1042)	29.056	(442)	3.7307	(1800)	52.53	62.8 ± 5.4	316.55
kw2-7	BRCU	34° 57' 10.3"	70° 25' 57.2"	1987	20	69.139	(777)	27.584	(310)	3.727	(1800)	<5	67.7 ± 10.4	298.34
kw2-11	BRCU	34° 57' 57.7"	70° 26' 17.6"	1852	23	64.122	(1704)	23.782	(632)	4.7761	(2103)	<5	90.5 ± 10.9	218.09
kw3-02	BRCU	34° 57' 44.4"	70° 26' 01.0"	1800	11	83.032	(995)	25.035	(300)	2.9829	(1366)	<5	68.7 ± 7.6	324.74
kw3-09	WT	34° 58' 52.7"	70° 25' 25.1"	2650	20	110.226	(1403)	26.476	(337)	2.9139	(1366)	65.00	86.4 ± 7.7	357.83
kw2-2	BdF	34° 57' 16.9"	70° 25' 51.3"	2061	14	122.103	(978)	34.583	(277)	4.7942	(2103)	<5	124.1 ± 13.8	288.76
kw2-32	BdF	34° 59' 16.8"	70° 25' 28.5"	2787	20	105.962	(1579)	16.106	(240)	3.716	(1800)	<5	170.5 ± 20.2	193.56
kw1-11	RD	34° 59' 13.9"	70° 22' 08.1"	2850	15	76.162	(785)	19.792	(204)	5.1006	(2103)	5.55	136.2 ± 16.5	153.99
kw1-12	RD	34° 59' 17.6"	70° 21' 49.0"	2958	19	78.809	(871)	20.449	(226)	4.8843	(2103)	75.88	133.6 ± 13.1	201.73
kw1-13	RD	34° 58' 30.4"	70° 22' 31.5"	2300	19	92.784	(1181)	25.533	(325)	5.0646	(2103)	<5	131.0 ± 13.6	215.14
kw1-14	RD	34° 58' 51.1"	70° 23' 11.5"	2247	24	49.119	(1470)	15.972	(478)	4.8663	(2103)	15.00	106.3 ± 9.3	134.45
kw2-5	RD	34° 57' 29.8"	70° 25' 31.7"	1970	18	88.435	(604)	19.327	(132)	3.7344	(1800)	20.44	125.5 ± 16.5	170.11
kw2-13	RD	34° 58' 49.2"	70° 22' 02.0"	2491	5	65.735	(551)	15.271	(128)	3.7197	(1800)	29.06	113.8 ± 13.3	250.18
kw2-41	RD	34° 58' 09.8"	70° 24' 10.2"	1903	20	87.526	(3690)	18.478	(779)	3.7013	(1800)	<5	125.8 ± 10.7	217.25
kw3-16	RD	34° 58' 01.6"	70° 24' 17.7"	2040	14	122.031	(788)	22.61	(146)	2.8449	(1366)	86.83	109.2 ± 12.1	293.49
TF9-16	RD	34° 56' 01.6"	70° 22' 03.9"	2450	9	51.038	(469)	12.079	(111)	3.7417	(1800)	30.09	109.6 ± 15.1	184.77



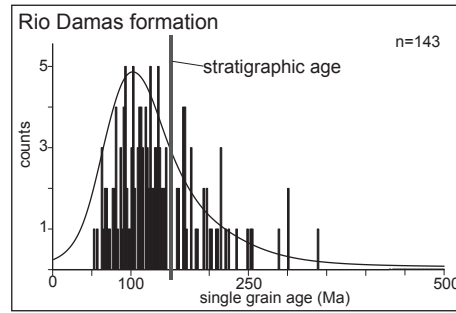
**Figure 2.6:** Central ages determined for zircon fission track samples from the Tinguiririca river valley, top: in map view, bottom: in an age vs. position plot along the transect shown in Appendix A and in a schematic stratigraphic column. Ages in brackets and *italics* are based on less than 10 single grain ages (see tab. 2.1).

## Rio Damas Formation

9 samples from the Rio Damas Formation were analysed (see table 2.1, figures 2.6, 2.7, 2.8). They cover a range from close to the top of the unit to the lower part (the base is not exposed in the study area) and the difference in stratigraphic depth between the highest and lowest samples is about 3500 m. The relatively consistent central ages range between 106.3 and 136.2 Ma with no trend of increasing or decreasing age either with stratigraphic depth or with sample–elevation (table 2.1, figure 2.6). Radial plots of the individual samples are shown in figure 2.7. Central ages determined in the Rio Damas Formation are all significantly younger than the inferred stratigraphic age (Kimmeridgian, 156–150 Ma) of the unit. Single grain age spreads in the individual samples are all similar and grains preserving ages older than the stratigraphic age of the unit are still found in most samples (figure 2.7). Figure 2.8 shows a histogram of all single grain ages of samples from the Rio Damas Formation. The maximum in the distribution is at about 100 Ma and thus clearly younger than the stratigraphic age. This, together with the fact that numerous grains older than the deposition age are still preserved, is indicative of partial annealing. The 100 Ma maximum is tentatively interpreted as roughly approximating the time of metamorphic overprint.



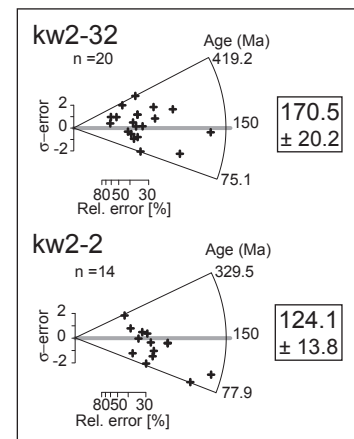
**Figure 2.7:** Radial plots of samples from the Rio Damas Fm.



**Figure 2.8:** Bar chart showing all ZFT single grain ages measured in samples from the Rio Damas Fm. The distribution shows a maximum at about 100 Ma, which is significantly younger than the stratigraphic age of the unit. Youngest single grain ages are at about 50 to 55 Ma.

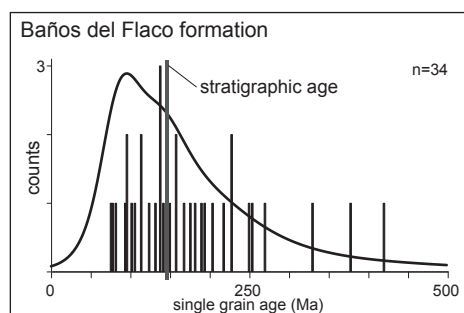
### Baños del Flaco Formation

Two samples from the Baños del Flaco Formation (kw2-2 and kw2-32) yielded central ages of 124.1 Ma and 170.5 Ma respectively (table 2.1, figure 2.6, 2.10). Kw 2-2 is from near the base of the unit on the North side of the valley and shows similar characteristics to samples from the Rio Damas Formation. The central age is younger than the stratigraphic age of the unit (Tithonian, 150–144) indicating at least partial annealing. The spread of single grain ages is also similar to those of samples from the Rio Damas Formation and grains with ages older than the stratigraphic age of the unit show that no total annealing of the sample occurred. Kw2-32 is from close to the top-most preserved part of the Baños del Flaco Formation in the vicinity of the unconformably overlying White Tuff. Although the difference in stratigraphic depth between these two samples is not very large (about 300 m), kw2-32 has a significantly older central age than any of the other samples from the Rio Damas or Baños del Flaco Formations. The central age (170.5 Ma) is much older than the stratigraphic age of the unit. However, the single grain age distribution of the sam-



**Figure 2.9:** Radial plots of two ZFT samples from the Baños del Flaco Fm. The horizontal grey bar marks the approximate deposition age of the unit. The samples are shown in stratigraphic order with the stratigraphically highest sample at the top.

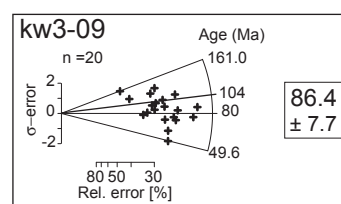
ple (figure 2.10 b.) shows that the sample also contains individual grains younger than the stratigraphic age, thus indicating that partial annealing occurred in this sample as well.



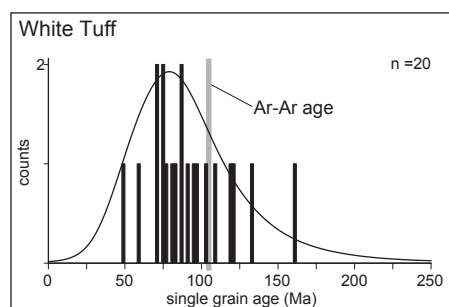
**Figure 2.10:** Bar chart showing all single grain ages measured in samples from the Baños del Flaco Fm.

## White Tuff

The White Tuff layer (kw3-09, see table 2.1), which lies directly on top of the erosional surface of the Baños del Flaco Formation, has a zircon fission track central age of  $86.4 \pm 7.7$  Ma. The sample passes the  $\chi^2$  -test and the age is interpreted as a cooling age. Figure 2.11 shows the single grain age distribution of the White Tuff.



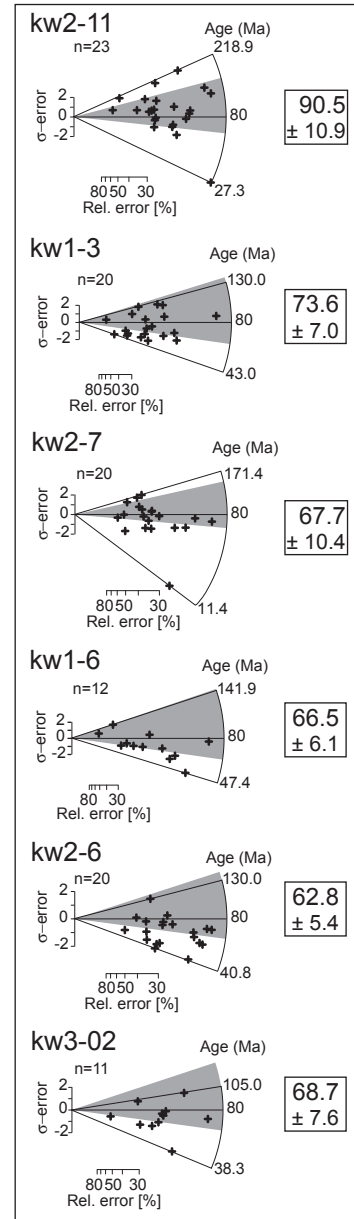
**Figure 2.11:** Radial plot of the ZFT sample from the White Tuff.



**Figure 2.12:** Bar chart showing the single grain ages measured in the sample from the White Tuff.

### Brownish–Red Clastic Unit

6 samples from the BRCU were analysed (table 2.1, figures 2.6, 2.13). 2 samples are from the footwall of the Falla el Fierro thrust (kw1–6 and kw3–02, see figure 2.6) and 4 from the hanging wall. The samples are all sediments containing volcanic material but some of the zircons from these samples are rounded indicating that they were reworked and transported before deposition. The 5 stratigraphically lower samples (figure 2.6) yielded central ages ranging between 62.8 and 73.6 Ma. An older age of 90.5 Ma was determined for the uppermost sample from the highest stratigraphic level, near the top of the unit. Because there is no independent indication that heating and annealing of fission tracks in zircon occurred after deposition, these ages are thought to represent detrital ages grains from the source areas. However, a histogram of the single grain ages from all six samples (see figure 2.13 a.) shows that most of the individual grains have late Cretaceous ages. The central ages are surprisingly similar and the sediments deposited in the BRCU appear to have come from a restricted source area where active volcanism occurred in the late Cretaceous.





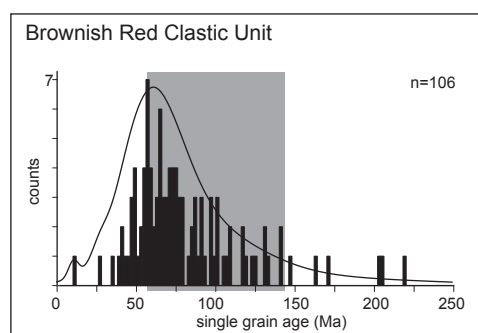


**Figure 2.14:** Bar chart showing all ZFT single grain ages measured in the 6 samples from the BRCU.

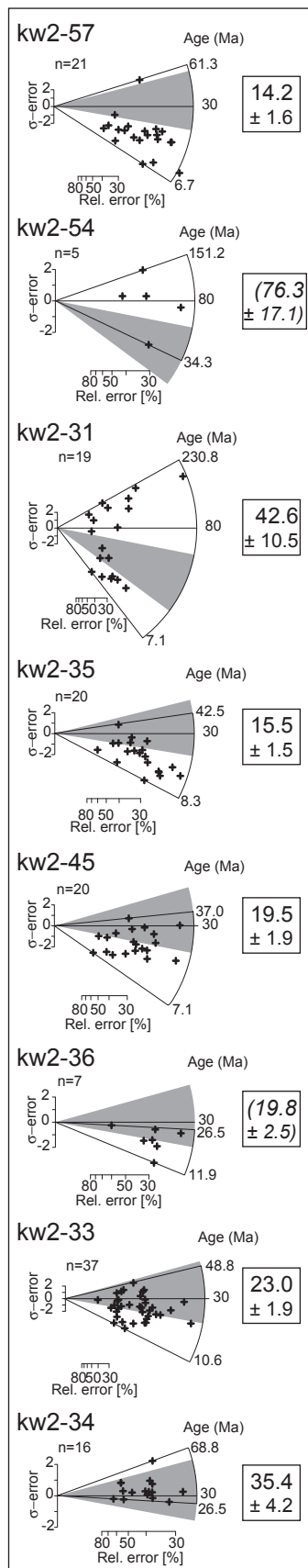


**Figure 2.15:** Radial plots of 8 ZFT samples from the Coya Machali Fm.

## Coya Machali Formation

8 samples from the Coya Machali Fm were analysed (tab. 2.1 figs 2.6, 2.15, 2.16). Central ages range from  $14.2 \pm 1.6$  Ma to  $76.3 \pm 17.1$  Ma. Fig. 2.16 shows a histogram of all single grain ages from the Coya Machali Fm. There is a pronounced peak at about 20 Ma but also a significant number of grains with ages much older than the stratigraphic age of the Coya Machali Fm. Fig. 2.15 shows radial plots of the individual samples from the Coya Machali Fm. Samples kw2–34 and kw2–33 are from the lower levels of the Coya Machali Fm. and central ages of 35.4 and 23 Ma were determined for these two samples. Samples kw2–36 and kw2–45 have ages of 19.8 and 19.5 Ma respectively. All these ages fit with the period of active extension and sedimentation in the basin, from the Late Eocene to Early Miocene. Kw2–31 has a central age of 42.6 Ma and clearly contains at least two different grain populations (see fig. 2.15). The age is therefore interpreted as a mixed age of detrital grains transported into the basin from outside and grains formed during volcanism associated with basin formation. Kw2–54 also contains detrital grains with ages much older than the deposition of the Coya Machali Fm. (tab. 2.1, fig. 2.15). The remaining two samples, kw2–35 and kw2–57 both show ages that are younger than the generally accepted stratigraphic age of the Coya Machali Fm. Since there is no indication of substantial post-depositional heating, the samples possibly show that the stratigraphic range of the Coya Machali Fm has to be extended towards the middle Miocene.

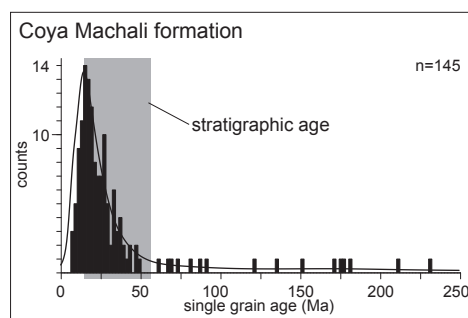


**Figure 2.16:** Bar chart showing all ZFT single grain ages measured in samples from the Coya Machali Fm. The grey bar marks the time-span of deposition of the unit (Eocene to early Miocene). There is a maximum in the distribution at about 20 Ma (early Miocene) but a number of grains show ages significantly older than the given deposition age of the unit.

### Tinguiririca Volcanic Group

One sample (kw3-19) from a tuff layer in the Quaternary volcanic rocks was dated to  $0.7 \pm 0.1$  Ma (table 2.1, figures 2.6, 2.17), well in agreement with other radiometric data (see Charrier et al. (1996)).

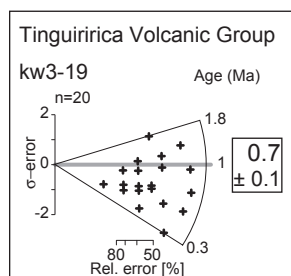


**Figure 2.17:** Radial plot of a ZFT sample from the Quaternary volcanics.

### 2.3.2 Apatite ages

23 apatite samples were analysed (see tab. 2.2, fig. 2.18). However, single grain age dating could only be applied to 6 samples containing enough grains with sufficient spontaneous fission tracks. For each of these 6 samples at least 20 grains were analysed and the ages are given as central ages (tab. 2.2). For the remaining samples a modified population age method (see section 1.4.1, Wagner and Van den Haute (1992)) was applied: all grains with good surfaces were counted, including

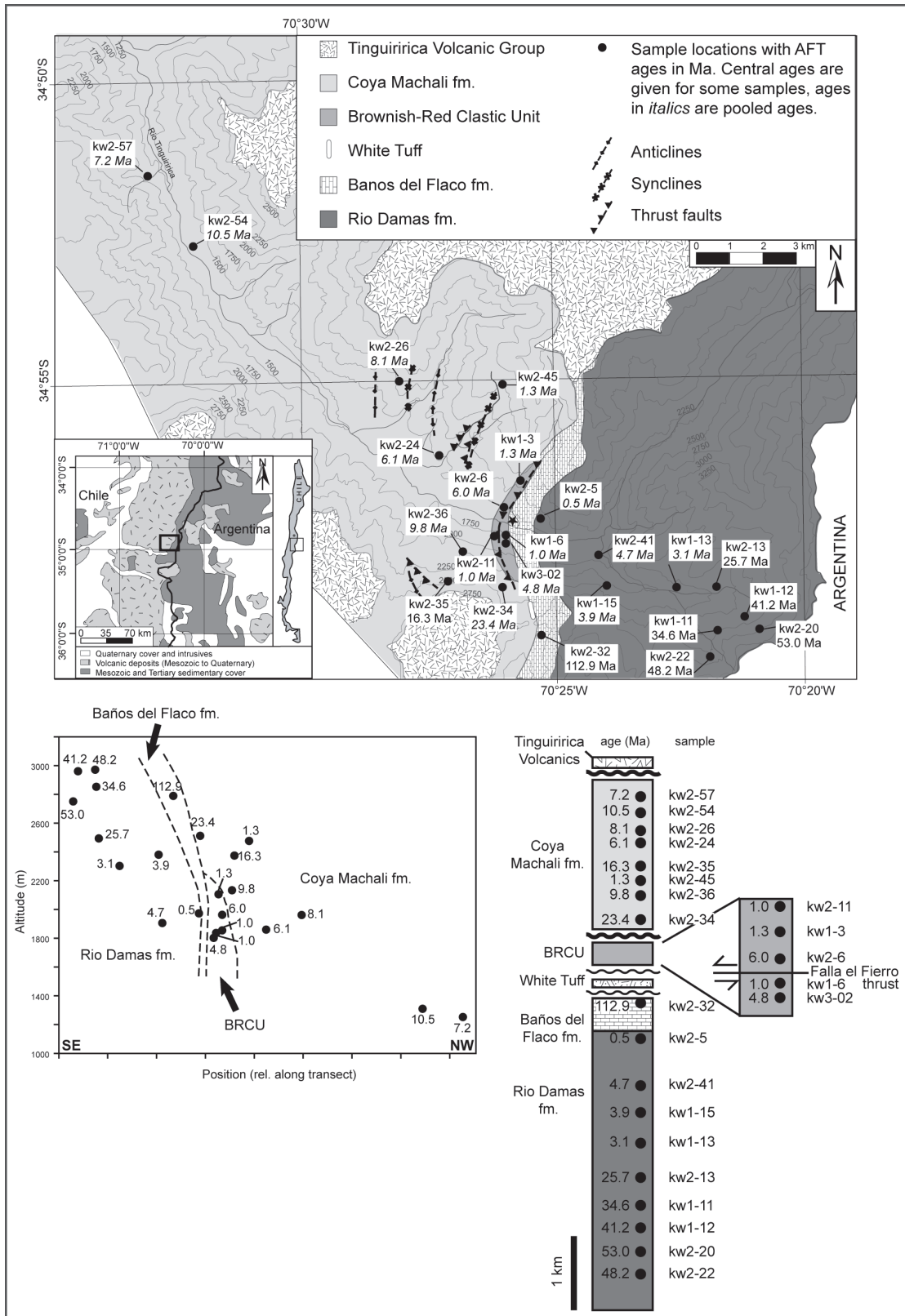


**Figure 2.18:** Apatite fission track data in the Tinguiririca river valley. Ages are given as central ages or pooled ages (see tab. 2.2). top: map view, bottom: position (rel. position along the transect shown in Appendix A) vs. altitude plot and in a schematic stratigraphic column.

those grains with no spontaneous tracks. Pooled ages were then calculated for the total  $N_s/N_i$  ratio of all counted grains. The number of counted grains ranges from 19 to 60. Because of the lack of spontaneous tracks and the relatively low U content of most of these samples, the calculated ages have large relative errors (see tab. 2.2).

**Table 2.2:** Apatite fission track data: CM: Coya Machali Formation, BRCU: Brownish-Red Clastic Unit, BdF: Baños del Flaco Formation, RD: Rio Damas Formation.  $N_S$ ,  $N_I$  and  $N_D$  are numbers of tracks counted. Pooled ages are given for samples that contained too few spontaneous tracks for single grain age dating, central ages are given for samples where enough individual grains could be dated.

Sample number	Strat. unit	Latitude (S)	Longitude (W)	Altitude (m)	Grains	Spont. track den-sity ( $\times 10^5 \text{ cm}^{-2}$ )	$(N_S)$	Ind. track den-sity ( $\times 10^5 \text{ cm}^{-2}$ )	$(N_I)$	Std. track den-sity ( $\times 10^5 \text{ cm}^{-2}$ )	$(N_D)$	$F(\chi^2)$ (%)	Pooled Age (Ma)	Central Age $\pm 1\sigma$ (Ma)	U (ppm)	mean track length ( $\mu\text{m}$ )	std. dev. length ( $\mu\text{m}$ )
kw2-57	CM	34°51'50.6"	70°33'13.1"	1250	33	0.221	(12)	5.864	(318)	11.1907	(4148)	84.13	7.2±2.1		6.30		
kw2-54	CM	34°52'48.7"	70°32'29.5"	1307	45	0.177	(16)	3.275	(296)	11.4417	(4148)	69.64	10.5±2.7		3.86		
kw2-26	CM	34°55'08.5"	70°28'27.4"	1959	30	0.180	(8)	4.476	(199)	11.9437	(4148)	81.04	8.1±3.0		4.98		
kw2-35	CM	34°58'33.1"	70°27'37.2"	2372	20	0.613	(77)	7.582	(952)	11.8396	(2159)	21.31	16.2±2.0	<b>16.3±2.1</b>	7.95	13.8	1.7
kw2-36	CM	34°58'19.6"	70°27'22.0"	2131	40	0.169	(17)	3.587	(361)	12.2572	(2159)	84.08	9.8±2.5		3.62		
kw2-24	CM	34°56'23.8"	70°26'55.1"	1857	40	0.119	(18)	4.193	(633)	12.6748	(2159)	55.45	6.1±1.5		4.23		
kw2-11	BRCU	34°57'57.7"	70°26'17.6"	1852	40	0.033	(5)	3.898	(586)	7.2047	(3564)	53.87	1.0±0.5		6.13		
kw2-45	CM	34°55'23.4"	70°26'13.0"	2474	40	0.032	(7)	4.905	(1068)	11.7005	(2159)	41.97	1.3±0.5		5.15		
kw2-34	CM	34°58'53.5"	70°26'09.1"	2509	60	0.377	(79)	3.380	(709)	12.3964	(2159)	<5	23.4±3.0		4.02		
kw2-6	BRCU	34°57'15.4"	70°26'06.0"	1960	60	0.098	(22)	3.721	(837)	13.3707	(2159)	<5	6.0±1.3		3.80		
kw1-6	BRCU	34°57'57.2"	70°26'05.4"	1834	29	0.042	(6)	5.877	(847)	8.5586	(3564)	74.42	1.0±0.4		8.48		
kw3-02	BRCU	34°57'44.4"	70°26'01.0"	1800	40	0.063	(13)	2.400	(494)	10.6887	(4148)	47.53	4.8±1.4		2.96		
kw1-3	BRCU	34°56'53.4"	70°25'39.1"	2103	50	0.035	(5)	3.921	(562)	8.3651	(3564)	99.95	1.3±0.6		6.18		
kw2-5	RD	34°57'29.8"	70°25'31.7"	1970	28	0.018	(2)	5.871	(654)	9.5256	(3564)	98.22	0.5±0.4		7.72		
kw2-32	BdF	34°59'16.8"	70°25'28.5"	2787	52	4.726	(956)	8.820	(1784)	12.5356	(2159)	<5	112.9±6.7	<b>112.9±7.6</b>	9.18		
kw2-41	RD	34°58'09.8"	70°24'10.2"	1903	39	0.105	(41)	4.559	(1779)	11.9788	(2159)	10.72	4.7±0.8		4.79		
kw1-15	RD	34°58'43.7"	70°23'59.5"	2378	24	0.178	(11)	6.124	(378)	7.9783	(3564)	<5	3.9±1.2		10.02		
kw1-13	RD	34°58'30.4"	70°22'31.5"	2300	18	0.120	(4)	5.207	(173)	7.7877	(3082)	46.05	3.1±1.5		8.35		
kw1-11	RD	34°59'13.9"	70°22'08.1"	2850	12	1.974	(54)	10.124	(277)	10.4927	(3564)	93.66	34.6±5.3	<b>34.6±5.3</b>	10.19		
kw2-13	RD	34°58'49.2"	70°22'02.0"	2491	24	0.975	(135)	8.394	(1162)	13.0923	(2159)	56.82	25.7±2.6	<b>25.7±2.6</b>	7.03		
kw2-22	RD	34°59'43.0"	70°21'59.7"	2969	20	2.383	(524)	10.711	(2355)	12.8140	(2159)	52.07	48.2±3.1	<b>48.2±3.1</b>	10.21	9.9	1.5
kw1-12	RD	34°59'17.6"	70°21'49.0"	2958	21	1.242	(71)	4.758	(272)	9.3322	(3564)	73.57	41.2±5.7	<b>41.2±5.7</b>	6.56	11.5	1.9
kw2-20	RD	34°59'14.1"	70°21'36.7"	2748	19	2.501	(466)	10.316	(1922)	12.9531	(2159)	73.19	53.0±3.6	<b>53.0±3.6</b>	9.67	9.5	2.0

## Samples analysed with the external detector method

Four samples from the Rio Damas Formation, one sample from the Baños del Flaco Formation and one sample from the Coya Machali Formation could be analysed with the external detector method (see figs 2.19, 2.21, 2.22).

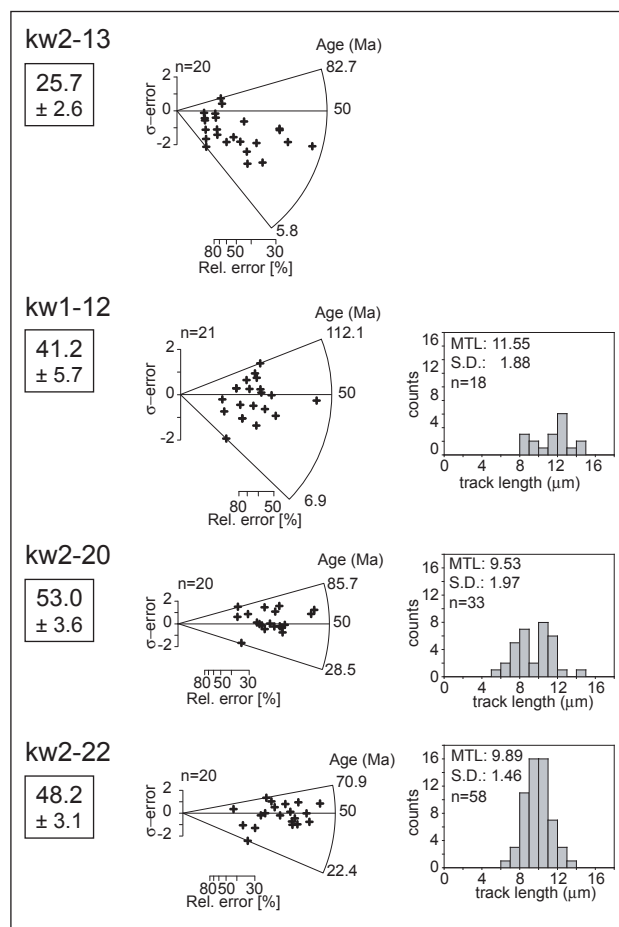


**Figure 2.19:** Radial plots of 4 AFT samples from the Rio Damas Fm. Ages are given as central ages in Ma with  $1-\sigma$  errors. The plots are in stratigraphic order with the stratigraphically highest sample at the top. Track length data was measured in three of the samples (see tab. 2.2) and track length distributions are plotted next to the radial plots. MTL: mean track length, S.D.: standard deviation of MTL, n: number of horizontal tracks measured. In all three samples, tracks  $>15\mu\text{m}$  were scarce or absent.

The four samples from the lower part of the Rio Damas Formation, yielded central ages between 25.7 and 53 Ma and all pass the  $\chi^2$ -test (tab. 2.2, figures 2.18, 2.19). Radial plots of the samples are shown in figure 2.19. Track length distributions of confined horizontal tracks were measured in three sam-

ples (kw1–12, kw2–20 and kw2–22, see figs 2.19, 2.20) and thermal modelling of temperature–time–paths was carried out using the software AFTSolve (Ketcham et al. (2000)). Fig. 2.20 shows a model run and track length distribution of sample kw2–22. Interestingly, in all three samples long fission tracks ( $>15 \mu\text{m}$ ) are completely missing. Mean track lengths are between 9 and 10  $\mu\text{m}$ . Modelling of temperature time paths (figure 2.20) shows rapid cooling of the samples in the late Cretaceous. The samples cooled below the apatite PAZ in the Early Tertiary. After a slight T–increase, possibly due to burial, the samples were heated in very recent times to temperatures within the apatite PAZ. Reheating is immediately followed by rapid cooling to surface temperatures. Based on the modelling results, the Eocene central ages of the samples are interpreted to be meaningless and the samples underwent a two–stage cooling history with late Cretaceous cooling followed by slight Tertiary reheating and a final late Tertiary/Quaternary heating pulse.

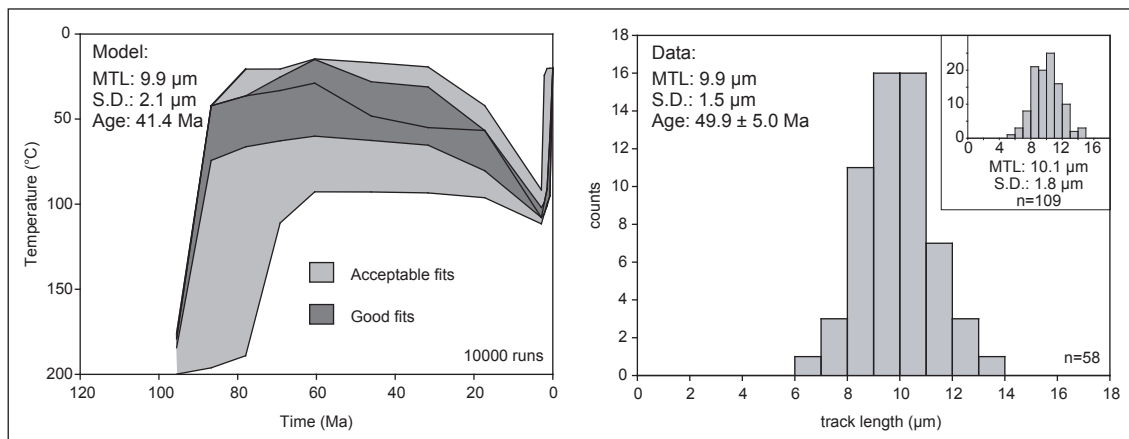


**Figure 2.20:** left: Temperature time path modelled for sample kw2–22 with the software AFTSolve (Ketcham et al. (2000)). Constraints were set as follows: Temperature within the zircon PAZ at 95 Ma ( $>180^\circ\text{C}$ ), temperature less than  $80^\circ\text{C}$  at 60 Ma (cooling of the sample), temperature between  $25^\circ\text{C}$  and  $120^\circ\text{C}$  at 3 Ma. 10000 model runs were calculated using a Monte Carlo modelling scheme and the apatite annealing model of Laslett et al. (1987) (Durango apatite). The light grey area shows acceptable solutions, the dark grey area marks good fits, the black line is the best fit found in this run. right: Track lengths measured in sample kw2–22. There are no tracks longer than  $15 \mu\text{m}$ . MTL: mean track length, S.D.: standard deviation of MTL, n: number of horizontal tracks measured. inset: Track lengths measured in three samples (kw1–12, kw2–20, kw2–22) from the lower Rio Damas Formation.

Sample kw2–32 from the Baños del Flaco Formation, just below the eroded surface of the unit, yielded a central age of 112.9 Ma. The sample fails the  $\chi^2$



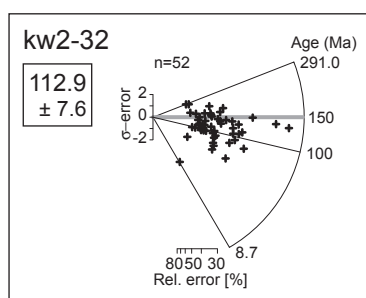


**Figure 2.21:** Radial plot of an AFT sample from the Baños del Flaco Fm. The age is given as a central ages in Ma with a  $1\text{-}\sigma$  error.

–test and shows a very large spread in single grain ages (see fig. 2.21). No track length measurements were possible in this sample. However, a single very young grain could possibly indicate that this sample also underwent late reheating.

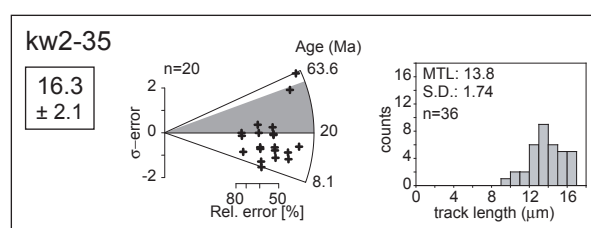


**Figure 2.22:** Radial plot of an AFT sample from the Coya Machali Fm. The age is given as a central ages in Ma with a  $1\text{-}\sigma$  error. The track length distribution was measured and is plotted beside the radial plot. MTL: mean track length, S.D.: standard deviation of MTL, n: number of horizontal tracks measured.

Sample kw2–35 from the Coya Machali Formation (table 2.2, figure 2.22) has a central age of 16.3 Ma. Fig. 2.23 b. shows a confined track length–histogram for this sample. In contrast to the samples from the Rio Damas Formation, long tracks are present. Modelling of this sample with AFTSolve (figure 2.23 a.) shows cooling of the sample in the middle Miocene followed almost immediately by reheating to temperatures within the apatite PAZ and then slow cooling during the late Miocene. Final cooling below the apatite PAZ could have been between about 7 and 3 Ma ago. Following the interpretation of the zircon fission track data, the rapid cooling is probably related to synsedimentary volcanic activity in the source area of the sediments. Detrital grains were then rapidly deposited in the Coya Machali Formation. Because there are no independent constraints on cooling or heating events for this sample, the results from modelling can only be considered

as one possible solution.

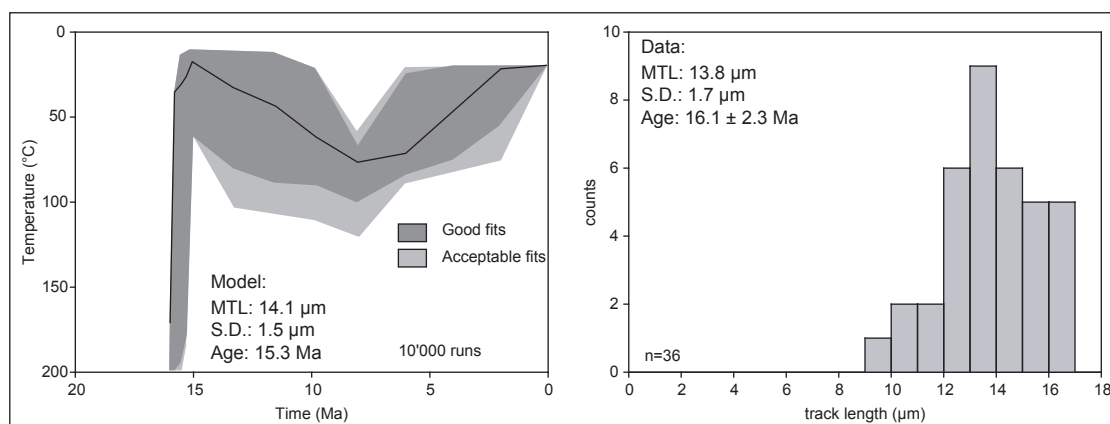


**Figure 2.23:** left: Temperature time path modelled for sample kw2–35 with the software AFT-Solve (Ketcham et al. (2000)). Constraints were set as follows: Temperature within the zircon PAZ at 17 Ma ( $>180^{\circ}\text{C}$ ), temperature less than  $60^{\circ}\text{C}$  at 15 Ma (cooling of the sample), temperatures between 20 and  $120^{\circ}\text{C}$  at 8 Ma. 10000 model runs were calculated using a Monte Carlo modelling scheme and the apatite annealing model of Laslett et al. (1987) (Durango apatite). The light grey area shows acceptable solutions, the dark grey area marks good fits, the black line is the best fit found in this run. right: Track lengths measured in sample kw2–35. MTL: mean track length, S.D.: standard deviation of MTL, n: number of horizontal tracks measured.

### Apatite samples counted with the modified population method

17 apatite samples contained a large number of grains with no spontaneous tracks (see tab. 2.2). All grains with suitable surfaces were counted and pooled ages were calculated for the samples.  $1\sigma$  errors on the ages calculated by this method are larger than on ages determined by single grain age dating.

In the central part of the study area, near the village of Termas del Flaco and the hot springs and near the Quaternary volcanics very young ages ( $<2$  Ma) were determined in apatites from all the stratigraphic units. With increasing distance from this area, apatite ages increase to Eocene to Cretaceous ages. This pattern most likely evidences the decreasing effect of a local heat-source due to hydrothermal activity that occurred in the Quaternary and affected apatite crystals to different degrees depending on their distance from the heat-source. Since the degree of thermal overprint cannot be constrained for the individual samples, no information about possible earlier events in the area can be gained from the samples.

## 2.4 Discussion

The rocks outcropping in the study area represent parts of a stratigraphic sequence ranging from the Late Jurassic to Quaternary. Different thermal histories must be assumed for the different stratigraphic units. The Rio Damas and Baños del Flaco Formations were deposited in a subsiding basin in the Late Jurassic. The White Tuff and BRCU were both deposited unconformably on top of the Jurassic units and probably did not experience any significant burial. The Coya Machali was deposited unconformably on top of the already tilted Mesozoic units. According to Charrier et al. (2002) the older units probably formed a scarp along the Eastern edge of the Tertiary extensional basin and no renewed burial of the older units occurred. The Quaternary volcanics were deposited unconformably on top of all the other units.

### 2.4.1 Constraints on the thermal history of the units derived from the fission track data

#### Rio Damas and Baños del Flaco Formations

Partial annealing of zircon fission tracks occurred in the deposits of the Rio Damas and Baños del Flaco Formations in the middle Cretaceous. This is inferred from the distribution of single grain ages from these two units, which shows a maximum at about 100 Ma (see figure 2.7). The zircon PAZ is generally accepted to lie between about 180 and 320 °C (Tagami and Shimada (1996); Tagami et al. (1996, 1998); Timar-Geng et al. (2004)). Temperatures within this range correspond to conditions within the prehnite–pumpellyite metamorphic facies and minerals typical of these conditions are in fact found in the Rio Damas Formation (see figure 2.4). Belmar (2000) determined an Ar–Ar age of  $101.3 \pm 2.9$  Ma on a celadonite from the upper Rio Damas Formation, which he interpreted as a formation age of the celadonite. The timing of this crystallisation fits very well with the middle Cretaceous timing of peak metamorphism inferred from the fission track data. Apatite samples from the lower part of the Rio Damas Formation have Early to Late Eocene cooling ages (figure 2.18). Thermal modelling (see figure 2.20) shows rapid cooling of these samples during the Late Cretaceous to Early Tertiary and a short, late heating event in the Pleistocene or Quaternary. Thus, it can be inferred

that cooling and denudation of the rocks, possibly associated with the beginning of tilting of the units, occurred in the Late Cretaceous to Early Tertiary following the metamorphic event in the middle Cretaceous. Heating then occurred again in the latest Tertiary to Quaternary. It is thought that this heating event is due to a local heat-source in the Tinguiririca valley associated with the geothermal system that is evidenced by the present-day hot springs and possibly connected to Quaternary volcanism.

Sample kw2-32 from near the eroded surface of the Baños del Flaco Formation preserves a Cretaceous apatite fission track age. This implies that the sample probably was at near surface depths in the middle to late Cretaceous and since then was never reheated to temperatures above the apatite PAZ either by renewed burial or hydrothermal activity.

### **BRCU and the white tuff layer**

There is no indication of annealing of fission tracks in zircon either in the White Tuff layer or in the BRCU. The ZFT age of the White Tuff layer is thought to represent the final cooling below the zircon partial annealing zone and the ages from the BRCU are probably mixed ages of detrital grains that were reworked and deposited in the basin. There is a disagreement between the Ar-Ar age of 104 Ma determined for the White Tuff (Wyss et al. (1994)) and the zircon fission track cooling age of 86.4 Ma. Either one of the ages is inaccurate or active volcanism continued for at least 20 Ma and the two ages represent samples from different levels in the tuff. In any case, the Tuff was deposited on top of the already eroded Baños del Flaco Formation and indicates that erosion was already ongoing or even completed by 100 Ma the time when peak temperatures were reached in the underlying units. If no annealing of fission tracks in zircon occurred in the BRCU, then temperatures remained below the zircon PAZ after deposition of this unit. This is in accordance with the metamorphic minerals found in the unit; chlorite, calcite and quartz occur as secondary minerals but do not indicate any distinctive temperature or pressure conditions. The absence of secondary minerals such as prehnite and pumpellyite in the unit supports the assumption that temperatures did not exceed 180°C in this unit. Apatites were dated in five samples from the BRCU. Three of these were completely reset during Quaternary reheating, the other two can be assumed, because of their proximity to the heat-source, to have

been at least partially reset during the same event and the AFT ages therefore do not give any direct information on the thermal history of the unit between the Cretaceous and Late Tertiary. However, total annealing of apatites in the unit indicates that temperatures above the apatite PAZ must have been reached. The apatite PAZ is generally accepted to be between about 60 and 120 °C (Green et al. (1986, 1989); Laslett et al. (1987); Duddy et al. (1988)). Temperatures between 120 °C (upper limit of the apatite PAZ) and 180 °C (lower limit of the zircon PAZ) thus were reached during the Quaternary. No apatites were counted in the sample from the White Tuff layer.

### **Coya Machali Formation**

In most of the zircon fission track samples from the Coya Machali Formation, no indication of annealing of fission tracks can be seen. Two samples contain detrital grains that preserve ages much older than the deposition of the Coya Machali Formation and 4 others have central ages that probably are connected to active volcanism associated with basin formation. The remaining two samples have ZFT ages that are younger than deposition of the Coya Machali Formation. Either partial annealing of fission tracks occurred locally in these samples, e.g. due to contact metamorphism near intrusions or sedimentation continued on into the middle Miocene. No secondary minerals indicating exceptionally high temperatures have been found in either sample and based on this it is impossible to tell if local heating occurred or not. Sample kw2-35 was taken fairly close to a large intrusion and has a ZFT age of 15.5 Ma. However, another sample, kw2-36, was taken even closer to the same intrusion and has a ZFT age of 19.8 Ma and shows no sign of partial annealing. From the zircon fission track data it is evident that temperatures above 180 °C were not reached in the Coya Machali Formation except, maybe, locally. Thermal modelling of an apatite sample from the Coya Machali Formation showed rapid cooling in the middle Miocene to temperatures just within the apatite PAZ, a change to very slow cooling at just after 15 Ma and final cooling below the apatite PAZ between about 8 and 4 Ma. However, because independent information on the thermal history of the unit is very scarce, the results of the model are very vague and can only be treated as one possible scenario. With the exception of kw2-35, where the AFT and ZFT ages are almost the same indicating very rapid cooling of this sample in the middle Miocene (see

figure 2.23 and tables 2.1, 2.2), apatite fission track ages in the samples from the Coya Machali Formation are significantly younger than zircon ages. This shows that temperatures above the apatite PAZ must have been reached at some stage. The influence of the Quaternary heating event on the individual samples cannot be estimated but from the pattern of ages, this does not appear to be the only event that led to annealing of fission track in apatite. However, the dataset is not good enough to allow for a more accurate estimate of the timing of heating but the results from thermal modelling imply that temperatures within the apatite PAZ persisted during much of the middle Miocene. There is no trend in the apatite fission track ages that implies a regional metamorphic event such as burial metamorphism or large-scale hydrothermal heating in the Coya Machali Formation. On the contrary, the impression of a number of local effects at different times and with overlapping areas of influence on the rocks is supported. It is proposed that hydrothermal activity within the subsiding basin and also during later compression and basin inversion led to a number of local heating events and associated formation of minerals such as zeolites in the rocks.

#### **2.4.2 Type of metamorphism: Burial or no burial?**

Burial metamorphism in subsiding basins has generally been accepted to be the main mechanism to produce large volumes of rocks altered at low grades in the Central Andes (Levi (1970); Levi et al. (1989); Aguirre et al. (1987)). In the study area, Belmar (2000) found a continuous increase in metamorphic grade from west to east, that is from younger to older deposits. He proposed burial metamorphism as a likely mechanism for such a pattern but observed that the rocks in the area have a polymetamorphic history and that the overall pattern is disturbed by local events such as contact metamorphism near intrusions. However, based on the fission track data and on geological observations, the idea of a single burial metamorphic event in the study area has to be abandoned. The units outcropping in the study area belong to two separate cycles of basin formation and infill and there are major stratigraphic unconformities and also an angular unconformity between older and younger deposits. The concept of a single vertical stack of sediments does not fit with geological evidence in the field. In the Jurassic Rio Damas and Baños del Flaco Formations, metamorphism took place long before the Coya Machali Formation was deposited. This is implied by the evidence of

partially reset fission tracks in zircon as well as by the formation age of  $101.3 \pm 2.9$  Ma determined by Belmar (2000) in a celadonite from the upper Rio Damas Formation. Furthermore, this metamorphic event cannot be only attributed to burial of these sediments. The samples from the Rio Damas and Baños del Flaco Formation were heated to temperatures within the zircon partial annealing zone in the middle Cretaceous and deposition of the White Tuff layer on top of the already eroded Baños del Flaco Formation took place at more or less the same time that peak temperatures were apparently reached. Burial, therefore, is not a possible explanation for the heating. Much more likely is that heating at quite shallow levels occurred due to geothermal activity associated, maybe, with the volcanism that erupted the White Tuff layer. The fact that there is no clear trend in the ZFT ages in the Rio Damas Formation with increasing depth is also an indication that heating in these rocks occurred within the same timespan but was not consistent over the whole area. Some samples were less affected or cooled earlier than others. Thermal modelling of samples from the lower part of the Rio Damas Formation indicates rapid cooling after the Cretaceous metamorphic event and no later heating until the Quaternary. Burial metamorphism due to deposition of the Coya Machali Formation can therefore be excluded. Samples from the Cretaceous White Tuff layer and the BRCU show no indication of annealing of fission tracks in zircon. Fission tracks in apatite were partially or completely annealed during the Quaternary (figure 2.24).

In the Coya Machali Formation there is also no evidence of annealing of fission tracks in zircon. The Coya Machali Formation (up to 2000 m) is not thick enough to account for heating to temperatures within the zircon PAZ, even under high geothermal gradients. Thermal modelling of an apatite sample from the Coya Machali Formation implies that reheating occurred after deposition and that temperatures did not drop below the partial annealing zone of apatite till later than 10 Ma. The elevated temperatures may be partially due to burial in the basin but it is also likely that pulses of hydrothermal activity took place at various times and at various localities in the basin. There is no trend in the apatite ages of samples from the Coya Machali Formation to indicate a pattern of classical burial and exhumation.

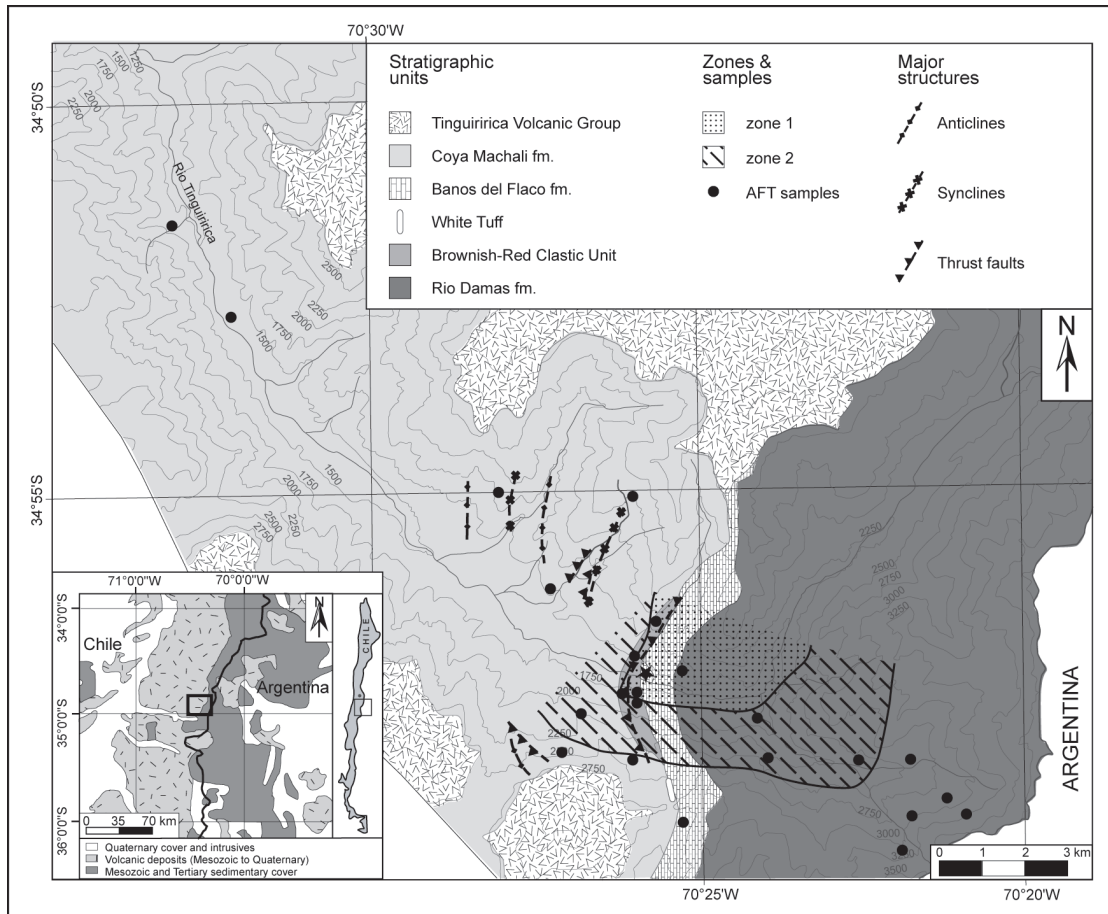


**Figure 2.24:** Zones of thermal overprint of AFT samples during Quaternary heating. In zone 1, fission tracks in apatite were almost completely annealed, in zone 2 fission tracks were substantially annealed. Thermal overprinting also occurred outside these zones as evidenced by thermal modelling (see fig. 2.20 but to a lesser extent).



## 2.5 Conclusions

A new model is proposed for the low-grade metamorphism in the Tinguiririca valley. At least 2 cycles of metamorphism in subsiding basins have taken place. In the Rio Damas and Baños del Flaco Formations a major heating event occurred during the middle Cretaceous. Temperatures above 200 °C were reached as was shown by Belmar (2000) using fluid inclusion microthermometry and also confirmed by the observed partial annealing of fission tracks in zircon. Peak temperatures during this event were reached at about 100 Ma. The heating cannot have been due to burial alone because the presence of the White Tuff layer with a middle Cretaceous formation age shows that erosion of the Baños del Flaco Formation was already ongoing or completed during peak temperatures conditions. A very high geothermal gradient due to magmatic and hydrothermal activity is proposed as the most likely cause of heating at shallow depths and also accounts for the irregular pattern of ZFT ages in the Rio Damas and Baños del Flaco Formations as heating would not have been uniform over a large area. Hydrothermal activity may have been associated with the active volcanism that erupted the White Tuff layer. Cooling to temperatures below the apatite PAZ in the Late Cretaceous to Early Tertiary was then followed by a long period of little thermal activity in the Rio Damas and Baños del Flaco Formations. Little information was gained on the thermal history of the Cretaceous deposits, the White Tuff formation and the BRCU. No indication of annealing of fission tracks in zircon can be seen in either unit. Apatite samples from the BRCU were reset during a Quaternary heating event. The deposits of the Coya Machali Formation were not pervasively heated to temperatures within the zircon PAZ, although contact metamorphism may have caused high temperatures locally. This assumption is supported by the secondary minerals found in the rocks of the Coya Machali Formation: zeolite minerals, indicating alteration at low temperatures, chlorite, quartz and calcite are commonly found in samples from the Coya Machali Formation but minerals indicating higher temperatures such as prehnite or pumpellyite are only rarely found near large intrusions. Heating to temperatures within or even above the partial annealing zone of apatite certainly occurred. Sadly, the pattern of apatite ages and the unknown effect of overprinting during the Quaternary heating event do not allow for any detailed model on the timing of the heating event. Burial metamorphism in the Tertiary extensional

basin may have occurred but the pattern of apatite ages is not typical of a classical burial and exhumation. Instead, hydrothermal activity, probably concentrated in brittle fault zones or along other conduits, has imposed a very complex pattern of overlapping localised heating events and associated formation of secondary minerals on the rocks of the Coya Machali Formation. Localised heating during the Quaternary, close to the present-day hot springs of Termas del Flaco caused complete annealing of fission tracks in apatite near the village and the Falla el Fierro thrust fault. Samples further away from the heat source were only partially reset but the effects of the heating can be seen even in samples from the lower part of the Rio Damas Formation as can be shown by thermal modelling. The amount of resetting in the individual apatite samples cannot be quantified. The Quaternary heat-source was located almost exactly at the transition between the Mesozoic and Tertiary deposits in the study area. The two sets of rocks with two separate thermal histories were both overprinted by the same event. The difference in metamorphic grade between the older rocks (prehnite–pumpellyite facies) and the younger deposits (zeolite facies) was probably considerably blurred by this late heating and isolated occurrences of zeolite minerals in the rocks of the Rio Damas Formation can probably also be attributed to this event.

Finally, it is worth noting that in the Rio Tinguiririca valley, hydrothermal activity in the middle Cretaceous, during the Miocene and in the Quaternary appears to be mainly responsible for the low-grade alteration of the rocks. Burial metamorphism, that has often been termed the main mechanism for such alteration, appears to have played only a very minor role in this area.

## Chapter 3

# Constraining the age of the Brownish–Red Clastic Unit: new evidence from fission track dating

### 3.1 Introduction

In their paper Charrier et al. (1996) described a new unit, the so-called Brownish–Red Clastic Unit (BRCU), in the Rio Tinguiririca valley in the main Cordillera of the Andes of central Chile. Stratigraphically this unit lies between the late Jurassic Baños del Flaco Formation and the Tertiary Coya Machali Formation and is only exposed over a distance of about 4 to 5 km before it wedges out both to the North and South. No biostratigraphically significant fossils have been found in the deposits of the BRCU that enable an exact dating of the unit. However, non-avian dinosaur bones found in the upper part of the unit (Charrier et al. (1996)) constrain it to the Cretaceous.

#### 3.1.1 Geological setting

In the Rio Tinguiririca valley in the main Cordillera of the Andes at 35° South a discontinuous stratigraphic sequence from the Late Jurassic to the Miocene can be found. An overview of the stratigraphic sequence in the Tinguiririca valley is given in figure 3.1.

The oldest unit in the area is the Rio Damas Formation. It consists of conti-

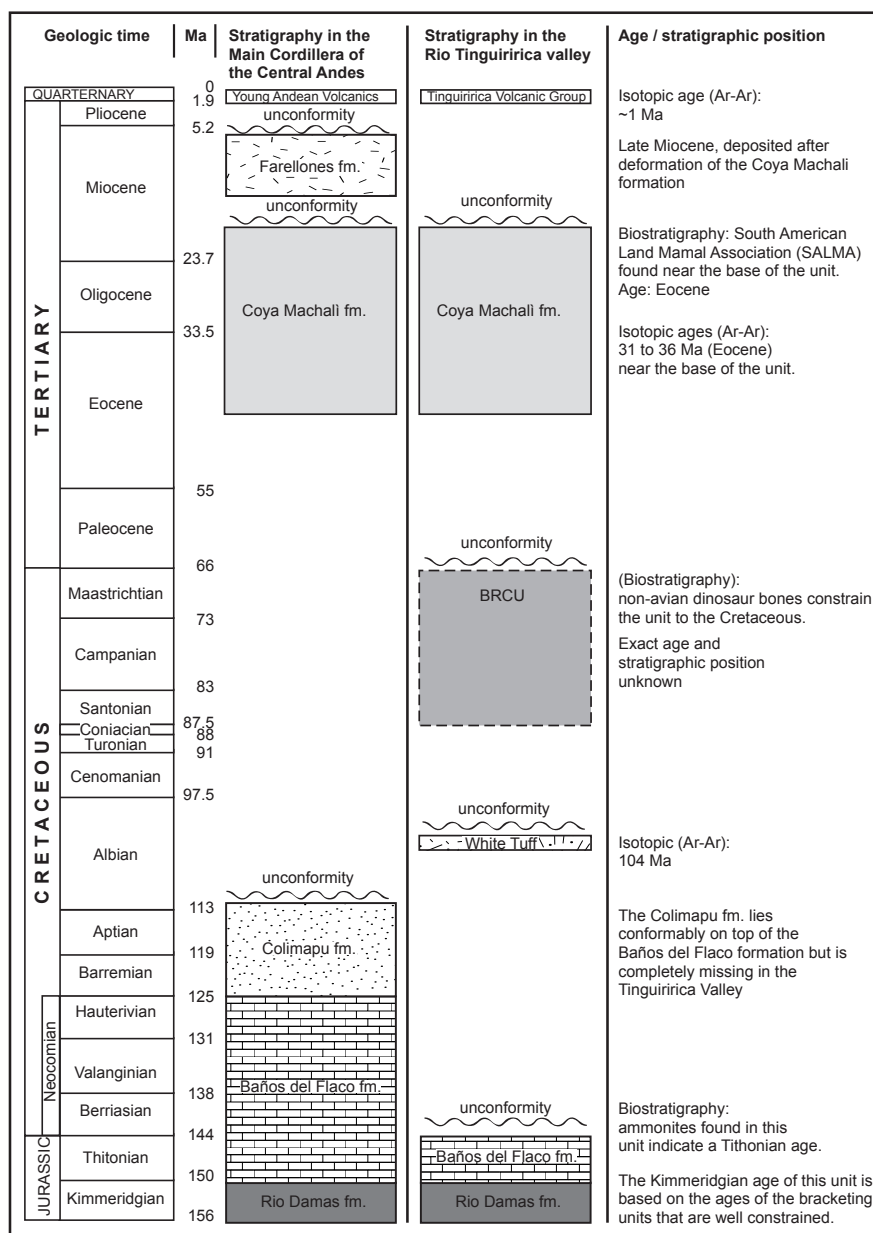


**Figure 3.1:** Stratigraphic column showing the ages of the units outcropping in the study area. The second column shows a simplified column of units found in other parts of the Central Andes. The BRCU has hitherto only been found in the Tinguiririca river valley and its exact age is not known. Fig. modified after Charrier et al. (1996).

mental sandstones and conglomerates and lavas and is 3700 m thick in the study area (Charrier et al. (1996)). The age of the Rio Damas Formation is known to be Kimmeridgian based on the well defined ages of its bracketing units. The marine deposits of the Baños del Flaco Formation lie conformably on top of the Rio Damas Formation. They consist mainly of marine sandstones and limestones and contain abundant fossils. The Baños del Flaco Formation has been dated as Tithonian based on stratigraphically significant ammonite species found in the unit. In the study area, the Baños del Flaco Formation is about 400 m thick and the top was eroded. To the north and south, the Baños del Flaco Formation is up to 2000 m thick and deposition is known to have continued to the Neocomian (Early Cretaceous). The BRCU unconformably overlies the deposits of the Baños del Flaco Formation. It consists of fan deposits and alluvial plane deposits and reaches a maximum thickness of about 250 m. The Tertiary Coya Machali Formation lies unconformably on top of the BRCU and the Baños del Flaco Formation with a slight angular offset. It consists mainly of continental sediments, lavas and pyroclastics and is about 1600 m thick.

South of where the BRCU wedges out, a white tuff layer is exposed along the contact between the Baños del Flaco Formation and the Coya Machali Formation. This tuff layer is absent along the contact between the Baños del Flaco Formation and the BRCU and the relative stratigraphic positions of the tuff layer and the BRCU cannot be established from field evidence. An isotopic age for this white tuff is given as  $104 \pm 0.5$  Ma (Wyss et al. (1994); Charrier et al. (1996)) and the tuff can therefore neither be a part of the Baños del Flaco Formation (Tithonian) nor of the Coya Machali Formation (Eocene to Early Miocene) but was deposited on top of the already eroded Baños del Flaco Formation. The Coya Machali Formation lies with a slight angular unconformity on top of the BRCU, the white tuff and the Baños del Flaco Formation. Mammal fossils found near the base of this unit (Wyss et al. (1994)) confirm an Eocene age for this unit. Deposition continued to the late Oligocene or early Miocene (Charrier et al. (2002)) and the unit was then folded during a Miocene phase of compression in the area.

Charrier et al. (1996) suggested 4 possible scenarios for the position of the BRCU and the White Tuff based on field evidence:

1. The White Tuff is an intercalation within the Baños del Flaco Formation that was exposed when the overlying members were eroded in the Cretaceous.

2. The White Tuff was deposited after local erosion on top of the Baños del Flaco Formation and before the deposition of the BRCU. This would imply an unconformity between the Baños del Flaco Formation and the White Tuff and another between the White Tuff and the BRCU.
3. The White Tuff was deposited after the deposition and local erosion of the BRCU but before deposition of the Coya Machali Formation. This scenario would also imply two unconformities, one between the BRCU and the White Tuff and another between the White Tuff and the Coya Machali Formation.
4. The White Tuff is the lowest part of the Coya Machali Formation.

Scenarios 1 and 4 were termed unlikely by the authors on account of the fairly exact age brackets given for the Baños del Flaco and Coya Machali Formations. Neither of these fits with the 104 Ma age determined for the White Tuff and it is unlikely that this deposit is a member of either the overlying or underlying formation. Of the other two possibilities, scenario 2 was preferred to scenario 3 but could not be conclusively proven to be true based on the available field evidence.

**Table 3.1:** Zircon fission track data of samples from the Brownish-Red Clastic Unit (BRCU) and the White Tuff (WT).  $N_S$ ,  $N_I$  and  $N_D$  are numbers of tracks counted.

Sample number	Strat. unit	Latitude (S)	Longitude (W)	Altitude (m)	Grains	Spont. track density ( $\times 10^5 \text{ cm}^{-2}$ )	$(N_S)$	Ind. track density ( $\times 10^5 \text{ cm}^{-2}$ )	$(N_I)$	Std. track density ( $\times 10^5 \text{ cm}^{-2}$ )	$(N_D)$	$P(\chi^2)$ (%)	Central Age $\pm 1\sigma$ (Ma)	U (ppm)
kw1-3	BRCU	34° 56' 53.4"	70° 25' 39.1"	2103	20	69.84	(1418)	32.014	(650)	4.9204	(2103)	<5	73.6 ± 7.0	282.00
kw1-6	BRCU	34° 57' 57.2"	70° 26' 05.4"	1834	12	54.742	(1244)	30.407	(691)	5.1187	(2103)	<5	66.5 ± 6.1	236.10
kw2-6	BRCU	34° 57' 15.4"	70° 26' 06.0"	1960	20	68.498	(1042)	29.056	(442)	3.7307	(1800)	52.53	62.8 ± 5.4	316.55
kw2-7	BRCU	34° 57' 10.3"	70° 25' 57.2"	1987	20	69.139	(777)	27.584	(310)	3.727	(1800)	<5	67.7 ± 10.4	298.34
kw2-11	BRCU	34° 57' 57.7"	70° 26' 17.6"	1852	23	64.122	(1704)	23.782	(632)	4.7761	(2103)	<5	90.5 ± 10.9	218.09
kw3-02	BRCU	34° 57' 44.4"	70° 26' 01.0"	1800	11	83.032	(995)	25.035	(300)	2.9829	(1366)	<5	68.7 ± 7.6	324.74
kw3-09	WT	34° 58' 52.7"	70° 25' 25.1"	2650	20	110.226	(1403)	26.476	(337)	2.9139	(1366)	65.00	86.4 ± 7.7	357.83

## 3.2 Discussion

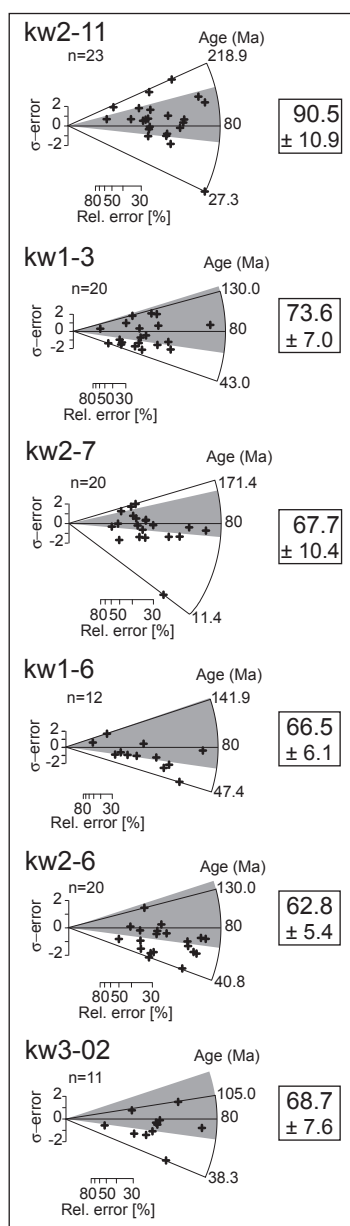
Tab. 3.1 gives an overview of the zircon fission track (ZFT) data for samples from the White Tuff and the BRCU.

The zircon fission track central age for the White Tuff is  $86.4 \pm 7.7$  Ma and passes the chi square-test. Thus it can be treated as a cooling age. This age is younger by about 20 Ma than the age of 104 Ma determined by Ar–Ar chronometry. Since the tuff is only about 3–4 m thick, cooling would normally be expected to have been fairly fast and the ZFT age should not be much younger than the Ar–Ar age. Several possible explanations exist:

1. The ZFT age is inaccurate.
2. The Ar–Ar age is inaccurate.
3. The Tuff layer was originally much thicker and possibly covered with more deposits that were later eroded. Cooling in this thick pile of volcanic deposits took more than 10 Ma.
4. The formation age of 104 Ma is correct and a later heating event occurred that caused partial or complete annealing of fission tracks in zircon and reset the sample to a younger age.
5. Both age determinations are accurate and reflect a long-lasting volcanic activity with only small amounts of volcalcanoclastics deposited.

The zircon sample was prepared, etched and irradiated according to the methods described in chapter 1. There is no obvious reason why the ZFT age for the white tuff should be less accurate than the ages of any of the other samples. The grains contain enough Uranium to give reasonable count statistics, 20 individual grains were dated and the sample passes the chi square test. The only possible issue is that the grains are rather small and accordingly only fairly small areas were counted on each grain. However, this should not have a large impact on the central age and the  $\sigma$ -error for the age is on the scale of 10%, which is acceptable and was found in most of the other zircon samples analysed.





According to Charrier et al. (1996), there are no other major volcanic deposits of mid Cretaceous age reported from the Andes in central Chile. The White Tuff is only found locally and is only 3 – 4 m thick. There is no indication that it was once thick enough to explain such a slow cooling as would be necessary to neatly explain the difference between Ar–Ar and ZFT ages of about 20 Ma.

The partial annealing zone for zircon is generally accepted to be between about 180 and 320 °C (Tagami and Shimada (1996); Tagami et al. (1996, 1998); Timar-Geng et al. (2004)). Such temperatures cannot easily be expected close to the surface. Thus a significant amount of burial would have to be expected in order to allow for temperatures in the range between 180 and 320 °C to cause annealing of fission tracks in zircon. Possible mechanisms for generating such high geothermal gradients include contact metamorphism near an intruding pluton and/or hydrothermal activity. Again, there is no indication that the Tuff was buried to any great extent before deposition of the Coya Machali Formation. Also, a sample from near the erosive surface of the Baños del Flaco Formation, close to the White Tuff, has an apatite age of 112.9 Ma. If the Tuff layer had been heated to temperatures within the zircon partial annealing zone (about 180 to 320 °C, see Tagami and Shimada (1996); Tagami et al. (1996, 1998); Timar-Geng et al. (2004)) any time after 100 Ma, this apatite sample would have been affected also and fission tracks in apatite would have been annealed if temperatures

within the apatite PAZ, about 60 to 120 °C, were reached (Green et al. (1986, 1989); Laslett et al. (1987); Duddy et al. (1988)).

Analysed samples from the BRCU are all sediments. Fission track central ages for detrital zircons from these sediments range from 62.8 to 90.5 Ma. With one exception these samples do not pass the chi square test. The spread in single grain ages is not very large in most of the samples but individual grains show considerably older or younger ages than the bulk of the grains (see figure 3.2). There is no direct indication that heating and annealing of fission tracks in zircon occurred in the BRCU. Firstly, most of the samples do not pass the chi square test and thus possibly reflect the cooling of the detrital source area. Secondly, there is no indication of a heating event in the late Cretaceous neither in the Baños del Flaco Formation nor in the White Tuff layer discussed above. The BRCU is only about 250 m thick. If temperatures of over 200 °C had been reached, one would expect to find evidence in the underlying units also.

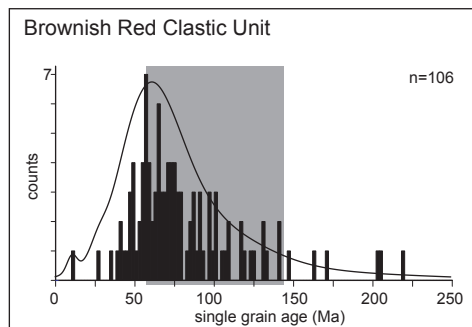


**Figure 3.4:** Bar chart showing all ZFT single grain ages measured in the 6 samples from the BRCU. The grey bar marks the supposed time-span in which the unit was deposited (Cretaceous). The maximum of the distribution is at about 60 to 70 Ma, in the late Cretaceous.

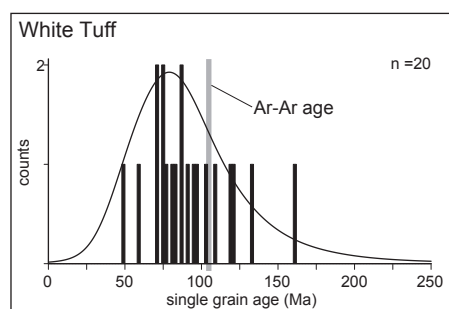


**Figure 3.5:** Bar chart showing the single grain ages measured in the sample from the White Tuff.

Most of the grains from the BRCU are between about 60 and 80 Ma old. Since the samples are all sediments and no heating and annealing of the samples is assumed after deposition, detrital grain ages must be older than the age of deposition. Most of the grains are not much rounded and corroded and therefore were probably not transported very far. Erosion and deposition of most of the detrital grains in the BRCU is suggested to have occurred fairly soon after initial deposition of the volcanic source material.

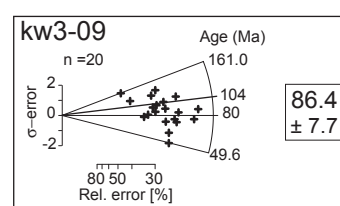


**Figure 3.3:** Radial plot of the ZFT sample from the White Tuff. The sample passes the  $\chi^2$ -test (see tab. 2.1) and the central age is therefore thought to represent cooling of the tuff directly after deposition.

Thus the late Cretaceous zircon fission track ages are suggested to quite accurately date the deposition of the BRCU as late Cretaceous, in good agreement with the Cretaceous fossils found in the upper part of the unit.

Figure 3.6 shows enveloping curves for single grain ages from all analysed units in the area. The grains from the Rio Damas and Baños del Flaco Formations have a maximum frequency at about 100 Ma, those from the White Tuff at about 80 Ma and the grains from the BRCU have a maximum at about 60 Ma. Grains from the Coya Machali Formation are, with the exception of several detrital grains, much younger and have a marked maximum at about 20 Ma. This sequence probably represents the relative positions of the units with the White Tuff deposited sometime before the BRCU (figure 3.7).

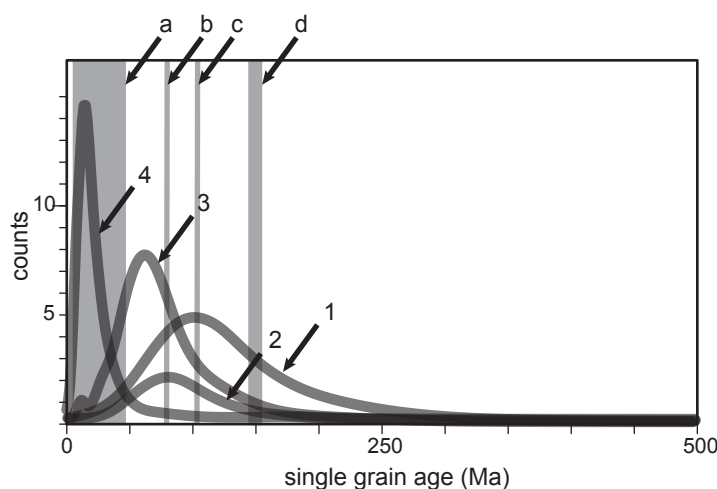


**Figure 3.6:** Enveloping curves of the single grain age distributions of 1. the Rio Damas and Baños del Flaco Fms, 2. the White Tuff layer, 3. the BRCU and 4. the Coya Machali Fm. The grey bars mark a. the deposition age of the Coya Machali Formation, b. and c. the possible deposition ages of the White Tuff (see text) and d. the deposition of the Baños del Flaco and Rio Damas Fms.

### 3.3 Conclusions

The White Tuff was deposited in the mid to late Cretaceous on to the eroded top of the Baños del Flaco Formation. The available age data, taken as accurately dating formation and fast cooling of volcanic deposits respectively, constrain the time of volcanic activity to 104 to 86 Ma. The White Tuff was clearly deposited before the BRCU.

Central ages for samples from the BRCU are mainly late Cretaceous. These detrital ages do not directly date the age of deposition of the BRCU because the samples are sediments and the ages of the zircon grains date the time of cooling in volcanic deposits that were later eroded and redeposited in the BRCU. Thus, the inferred upper limit for the age of the BRCU is the late Cretaceous. Therefore, a late Cretaceous age has to be assumed for the BRCU. This was obviously deposited before tilting of the older units because there is no angular unconformity between the BRCU and the Baños del Flaco Formation.

The results support the hypothesis of Charrier et al. (1996), who proposed that the BRCU was deposited in the late Cretaceous and, accordingly, that there is an unconformity between the Baños del Flaco Formation and the White Tuff, another between the White Tuff and the BRCU and another between the BRCU and the Coya Machali Formation.

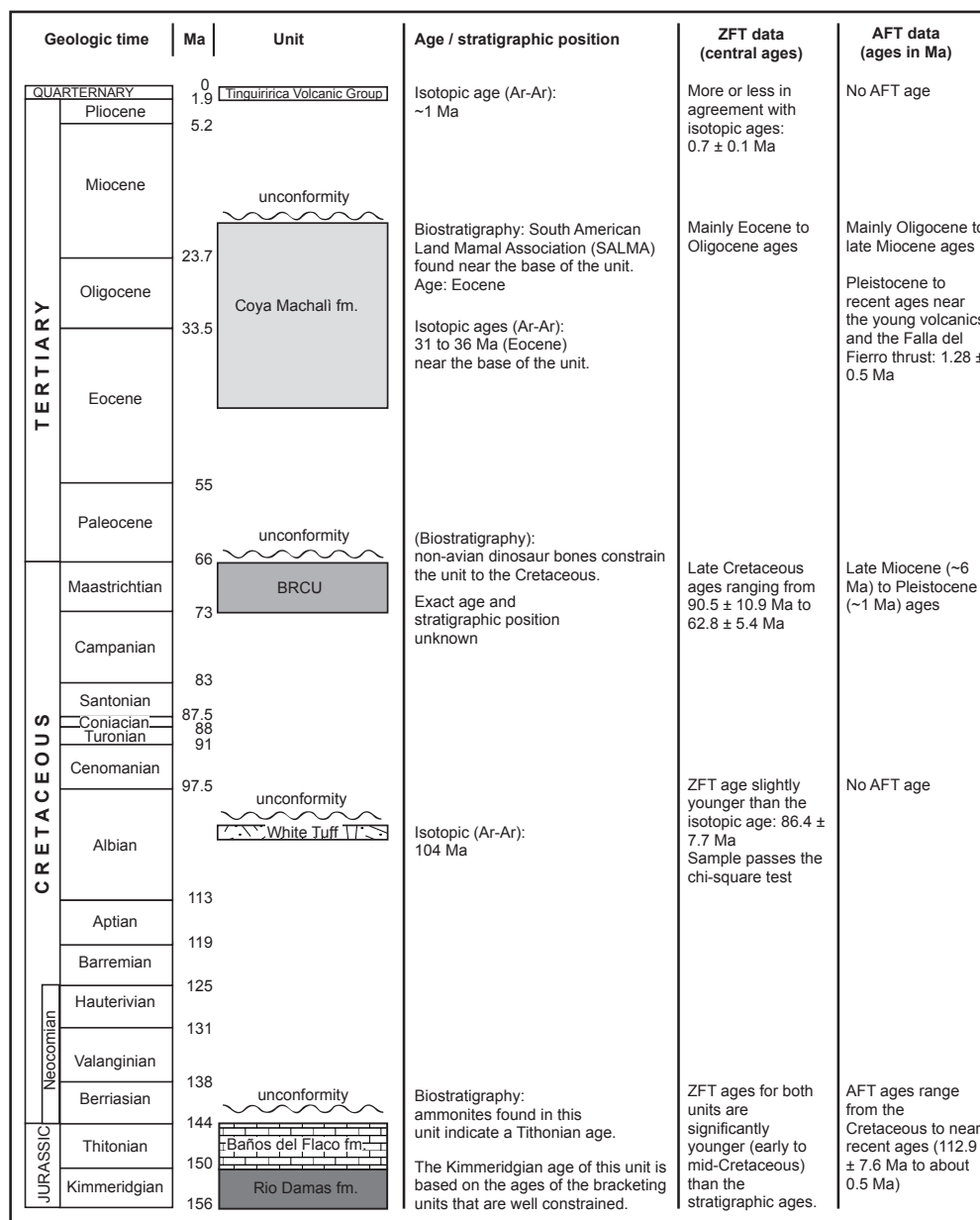


**Figure 3.7:** Compilation of data from previous publications (see section 3.1, ZFT and AFT allows more accurate constraints on the ages and relative positions of some of the units in the Tinguiririca river valley. The BRCU can be set in the late Cretaceous and is younger than the White Tuff (see fig. 3.6), deposition of the Coya Machali Fm. probably continued to the middle Miocene. The exact age of the White Tuff remains uncertain but a middle to late Cretaceous age is supported by evidence from FT analysis.



## Chapter 4

# New insights into the tectonic development of the Rio Tinguiririca valley area, in the main Cordillera of the Andes, 35° south, from fission track dating

### 4.1 Abstract

Fission track analysis was carried out on zircon and apatite mineral separates from the stratigraphic units outcropping in the Rio Tinguiririca valley in the main Cordillera of the Andes of central Chile. The data allow more accurate constraints of the tectonic and metamorphic history of the area. A model for the Mesozoic to Quaternary tectonic evolution of the area is proposed, based on the fission track data from this study and earlier work by Charrier et al. (1996) and Charrier et al. (2002). Metamorphic alteration of rocks in the Rio Tinguiririca valley appears to be mainly due to hydrothermal activity associated with active magmatism and/or volcanism. Burial metamorphism did not play a major role.

## 4.2 Introduction

In the Rio Tinguiririca valley in the main Cordillera of the Andes of central Chile parts of a stratigraphic sequence ranging from the late Jurassic to the Quaternary are exposed. Originally, the units were thought to represent a more or less continuous sequence from the late Jurassic to late Cretaceous. However, the discovery of Tertiary mammal fossils in a unit previously mapped as Cretaceous (Wyss et al. (1990)) and further work by Charrier et al. (1996) led to a reinterpretation of the stratigraphic sequence in the area. The relationships are more complex than originally thought and the Rio Tinguiririca valley has several distinctive features that do not occur in other locations (see section 4.3).

### 4.2.1 Geological setting

An overview of the tectonic setting of the study area is given in chapter 1. It is located in the main Cordillera of the Andes in central Chile at about 35° South (see figure 4.1). A 25 km transect in the Rio Tinguiririca valley from near the Argentinean border in the East to the confluence of the Rio Tinguiririca and the Rio Azufre in the West was investigated.

Figure 4.1 shows a geological overview of the setting of the study area. It is at the western edge of the Neuquen back arc basin in the Main Cordillera of the Andes. The area is at the transition of two segments of the Andes that have distinctly different Mesozoic histories. To the North a sedimentary platform developed in the back arc during the Jurassic. In the Early Cretaceous an aborted marginal basin developed west of the platform and large amounts of basalts and andesites were erupted. In the middle Cretaceous a fold and thrust belt was formed in the back arc area and the magmatic arc migrated to the West during the Late Cretaceous and Early Tertiary. To the South a large ensialic back arc basin (Neuquen basin, see figure 4.1) developed in the Early Jurassic and was active until the Early Cretaceous. In the Cretaceous a fold and thrust belt also formed in the back arc area. The magmatic arc remained more or less stationary up to the present and active volcanism continued until recent times (see Mpodozis and Ramos (1989)). The Mesozoic units outcropping in the study area were deposited along the western edge of the Neuquen back arc basin and are unconformably overlain by deposits from a Tertiary intra-arc basin that formed to the west of



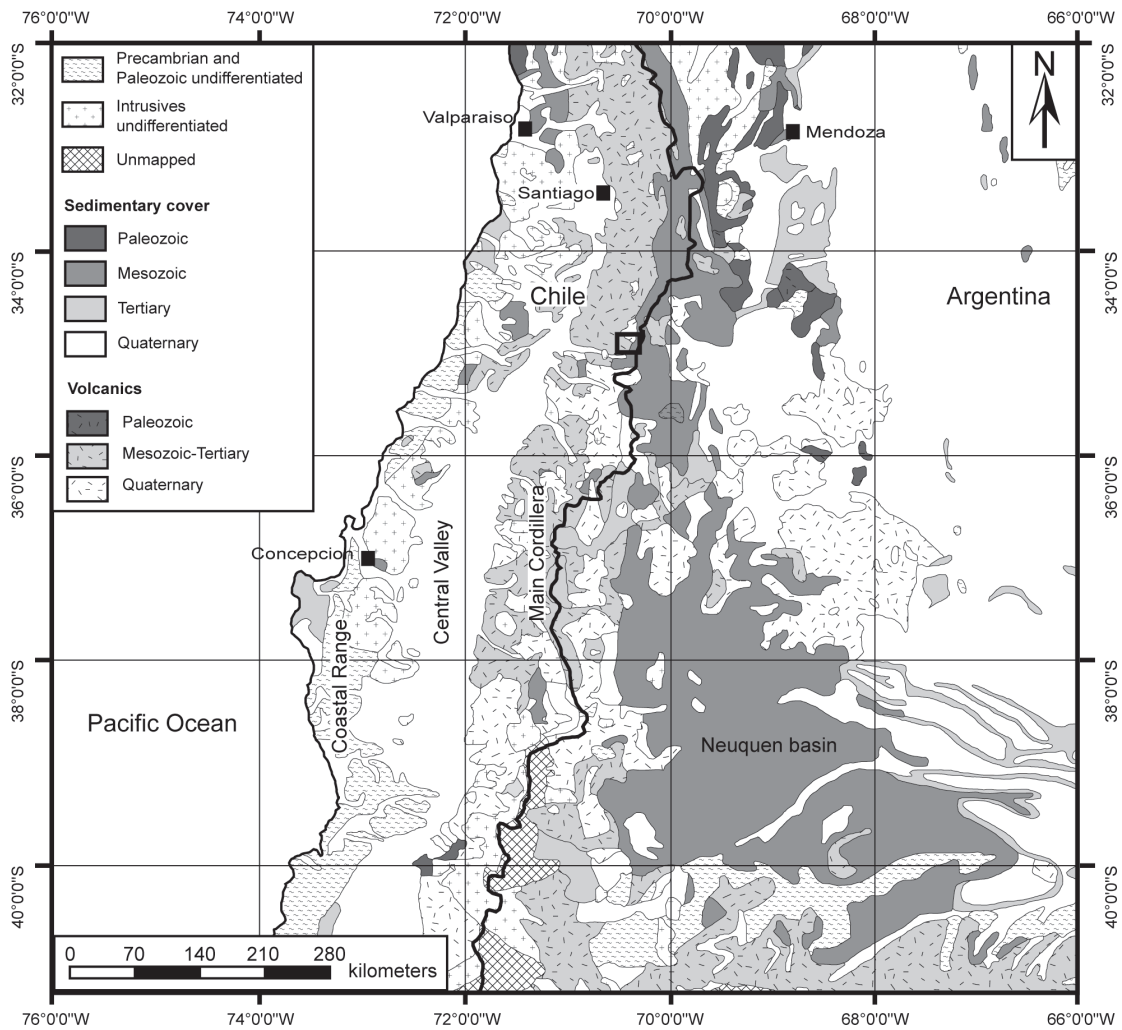


**Figure 4.1:** Location of the study area (black box) in the Main Cordillera of the Andes at about 35° south. The study area lies at the transition between the deposits of the Neuquen backarc basin to the east and the Mesozoic to Tertiary volcanic deposits in the Main Cordillera of the Andes.

the Neuquen basin. This second basin was active from the Late Eocene to Late Oligocene or Early Miocene and was then deformed during a period of compression in the Miocene.

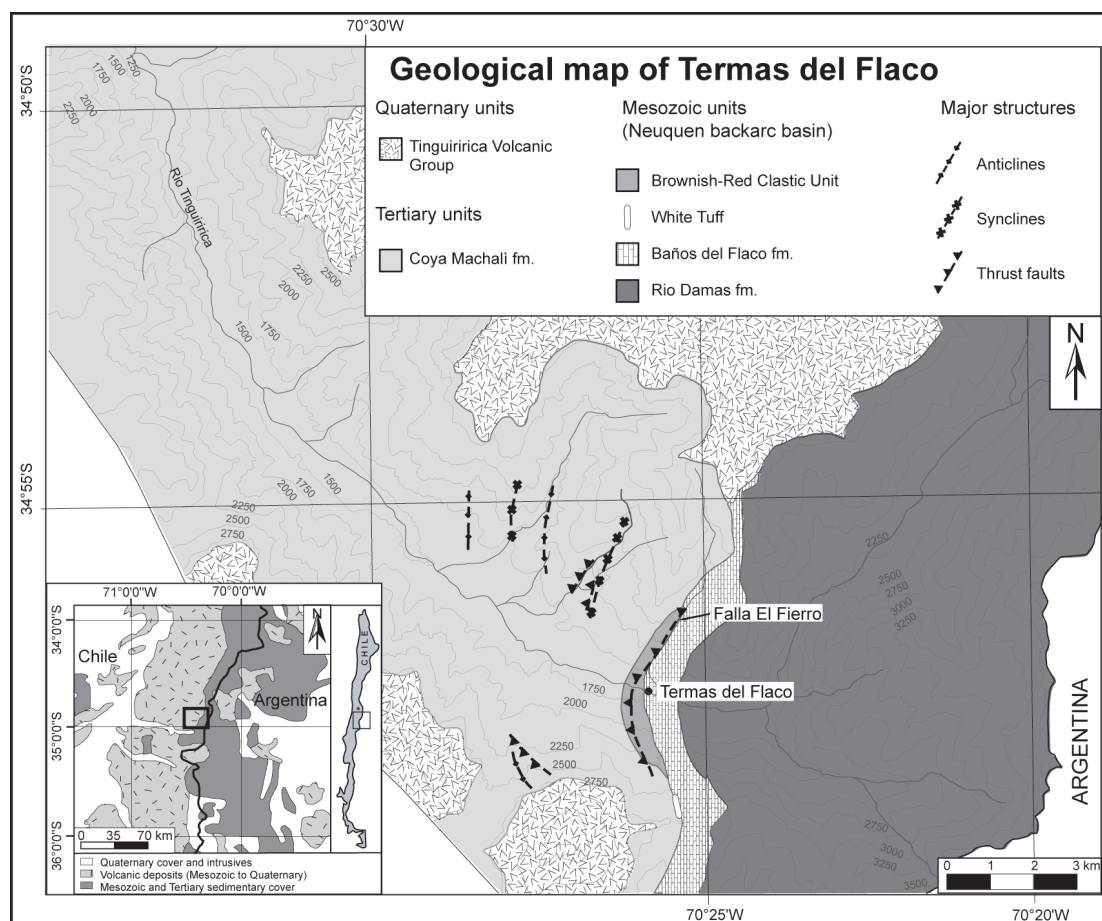


**Figure 4.2:** Geological map of the study area near the village of Termas del Flaco in the Rio Tinguiririca valley showing the stratigraphic units discussed in the text and major structural features.

Figure 4.2 shows a geological map of the study area near the village of Termas del Flaco. The middle Jurassic to Early Cretaceous stratigraphic sequence in the Neuquen back arc basin consists of two transgression–regression cycles with marine and continental clastic sediments. The oldest deposits of the series, the Nacientes del Teno Formation (Oxfordian), are not exposed in the study area. They consist of an 800–1000 m thick sequence of marine sandstones and limestones capped by a gypsum upper member (Charrier et al. (1996)). The Kimmeridgian Rio Damas Formation is the oldest unit exposed in the study area (figure 4.2) and consists

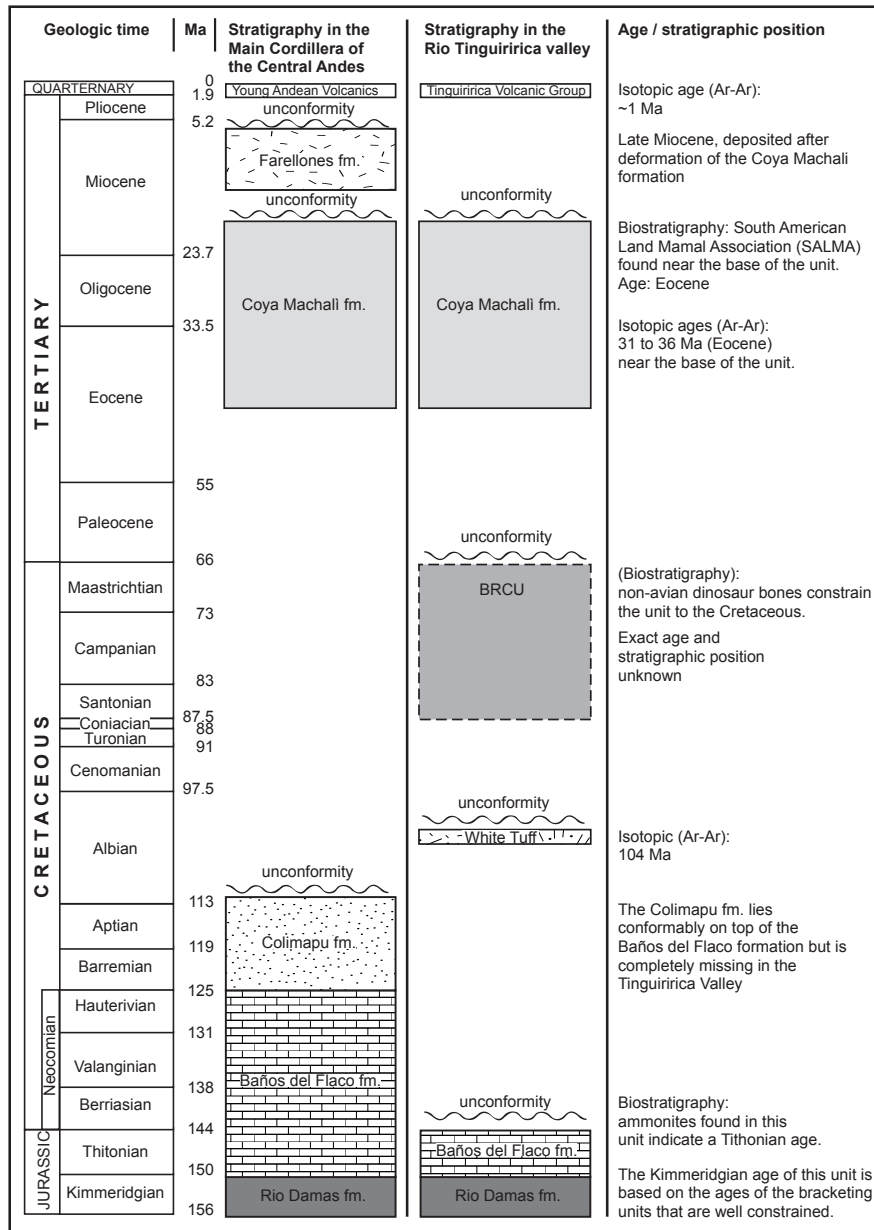


**Figure 4.3:** Stratigraphic column showing the ages of the units outcropping in the study area. The second column shows a simplified column of units found in other parts of the Central Andes. The BRCU has hitherto only been found in the Tinguiririca river valley and its exact age is not known. Fig. modified after Charrier et al. (1996).

of a 3700 m thick sequence of continental sandstones and conglomerates with a high percentage of volcanic material and of lavas. The Baños del Flaco Formation conformably overlies the continental deposits of the Rio Damas Formation and consists mainly of marine sandstones and limestones showing a transgression from platform to shelf sediments. Deposition of this unit was from the Tithonian to the Neocomian (Early Cretaceous) and the unit reaches thicknesses of up to 2000 m, but in the study area only the Tithonian deposits (about 400 m thick) are preserved and the upper part of the formation has been eroded (Charrier et al. (1996)). At other localities, the Aptian to Albian Colimapu Formation conformably overlies the Baños del Flaco Formation but it is completely missing in the study area (figure 2.3). It is not known whether the unit was deposited and later eroded or if local erosion began earlier and deposition did not take place. Instead, a unit consisting of well-bedded brown and red continental clastic sediments, the so-called Brownish-Red Clastic Unit (BRCU), lies without angular unconformity on top of the erosional surface of the Baños del Flaco Formation. This unit has no continuation to the North and South and has not hitherto been described in any other locality in the Central Andes. The exact stratigraphic position and age of the BRCU are still a matter of debate (see Charrier et al. (1996)).

The deposits of the Tertiary intra-arc basin are represented in the study area by the Coya Machali Formation, a thick (about 1500 m) sequence of continental sediments and volcanic and volcanoclastic rocks. The age of these deposits is given as late Eocene to early Miocene based on fossils and radiometric age data (Charrier et al. (1996)). Charrier et al. (2002) showed that the oldest ages for the Coya Machali Formation appear to differ laterally and that the onset of sedimentation was probably not at the same time in all parts of the basin. The deposits of the Coya Machali Formation were later folded and thrust in the Miocene.

A suite of Quaternary volcanics radiometrically dated at 1.1 Ma (Arcos et al. (1988); Charrier et al. (1996)) lies discordantly on top of all the deformed Mesozoic and Tertiary units. These consist mainly of basalts and pyroclastic flows and belong to the Tinguiririca Volcanic Group.

The Mesozoic units in the study area are all tilted to the West with dip angles of about 50°. Although there is a major stratigraphic unconformity between the Baños del Flaco Formation and the BRCU, there is no significant angular unconformity between the units. Tilting must have occurred after deposition of the BRCU

and prior to deposition of the Coya Machali Formation, however, because there is an angular unconformity of 15 to 20° between the Baños del Flaco Formation and the overlying Coya Machali Formation. Another sharp angular unconformity separates Mesozoic and Tertiary units and the Quaternary volcanics, which lie almost horizontally on top of all the other units. Folding is only observed in the deposits of the Coya Machali Formation. The pre-Tertiary, deformation is documented by the steeply inclined strata and rarely observed thrusts, while no major folds could be observed at the investigated scale. The most prominent structure in the study area is the Falla el Fierro fault (see figure 4.2) that cuts the BRCU and the Baños del Flaco Formation. Although offset along this fault is not very large (in the range of meters or tens of meters) it can be traced in other localities to the North and South of the study area. Charrier et al. (2002) suggested that the Falla el Fierro thrust is a reactivated normal fault that formed during basin formation in the Late Eocene.

One of the most enigmatic units in the study area is a 3–4 m thick layer of white tuff found directly on top of the Baños del Flaco Formation on the South side of the valley (figures 4.2, 4.3). This tuff layer has been dated with Ar–Ar chronometry at 104 Ma (see Wyss et al. (1994); Charrier et al. (1996)). The age was interpreted as a formation age of the tuff and shows that the layer can neither belong to the Baños del Flaco Formation (Tithonian to Neocomian, see figure 4.3) nor the overlying Coya Machali Formation (Eocene to Miocene, see figure 4.3). Stratigraphically, the white tuff layer takes the same position as the BRCU between the Baños del Flaco Formation and the overlying Coya Machali Formation. Yet field evidence does not allow constraining the relative ages of the White Tuff and the BRCU.

### **4.3 Previous work**

Charrier et al. (1996) used a combination of mapping and analysis of structures, biostratigraphic and radiometric age data, petrographic, sedimentologic and paleomagnetic data to reinterpret the stratigraphic sequence in the area. They found several characteristics in the area that have not been described from other areas. The most important results of the study were:

1. The Baños del Flaco Formation is eroded in this area and only the oldest

(Tithonian) deposits are preserved.

2. The Colimapu Formation, that is found conformably overlying the Baños del Flaco Formation in other locations, is missing in the Rio Tinguiririca valley.
3. The BRCU, which has not hitherto been described in any other area, unconformably overlies the Baños del Flaco Formation but wedges out both to the north and south.
4. Above where the BRCU wedges out on the southern flank of the valley, a white tuff layer is found exposed directly on top of the Baños del Flaco Formation. It is unclear from field evidence, whether this tuff layer lies above or below the BRCU. An Ar–Ar age of 104 Ma was determined for this tuff (Wyss et al. 1994). No large-scale volcanic deposits of similar age are known from other locations in the Central Andes.
5. A new South American Land Mammal Association (SALMA) was found in the Coya Machali Formation (Wyss et al. 1990). This unit had previously been mapped as the mid Cretaceous Colimapu Formation. However, the new fossils found near the base of the unit showed it to be Tertiary.

Charrier et al. (1996) suggested 4 possible scenarios for the position of the BRCU and the White Tuff based on field evidence: The White Tuff is an intercalation within the Baños del Flaco Formation that was exposed when the overlying members were eroded in the Cretaceous. The White Tuff was deposited after local erosion on top of the Baños del Flaco Formation and before the deposition of the BRCU. This would imply an unconformity between the Baños del Flaco Formation and the White Tuff and another between the White Tuff and the BRCU. The White Tuff was deposited after the deposition and local erosion of the BRCU but before deposition of the Coya Machali Formation. This scenario would also imply two unconformities, one between the BRCU and the White Tuff and another between the White Tuff and the Coya Machali Formation. The White Tuff is the lowest part of the Coya Machali Formation.

Scenarios 1 and 4 were termed unlikely by the authors on account of the fairly exact age brackets given for the Baños del Flaco and Coya Machali Formations. Neither of these fits with the 104 Ma age determined for the White Tuff and it is unlikely that this deposit is a member of either the overlying or underlying

formation. Of the other two possibilities, scenario 2 was preferred to scenario 3 but could not be conclusively proven to be true based on the available field evidence.

Belmar (2000) studied the low-grade metamorphism in the area. He found an apparently continuous increase in metamorphic grade from diagenetic conditions in the west (Coya Machali Formation) to prehnite-pumpellyite facies in the east (Rio Damas Formation). These findings were in contrast to earlier models for low-grade metamorphism in the Central Andes (Aguirre et al. (1987, 1989); Levi (1970); Levi et al. (1982); Ofler et al. (1980); Vergara et al. (1993)), which predicted sharp breaks in metamorphic grade over major stratigraphic unconformities. Belmar (2000) originally proposed long-lasting regional burial metamorphism affecting Mesozoic and Tertiary units as a likely mechanism to produce the observed pattern in metamorphic grade. However, Charrier et al. (2002) presented evidence that the Tertiary Coya Machali Formation was deposited in an extensional basin or series of basins that developed during the mid to late Eocene and were inverted and deformed during the Miocene. The authors found evidence for an eastern scarp near the basal unconformity of the Coya Machali Formation in the Rio Tinguiririca valley. In view of these results a single burial metamorphic event appears unlikely. The onset and end of deposition in the basin and the following compressive phase did not take place at the same time all along the north-south extent of the basin or series of basins. In the Rio Tinguiririca valley, deposition apparently began in the late Eocene (at about 35 Ma) and is thought to have continued to the early Miocene (about 20 Ma). Compression then occurred and the Coya Machali Formation was folded and thrust. Charrier et al. (2002) dated this compressional phase at about 20 to 15 Ma.

## 4.4 Results

The methods used for fission track analysis are described in chapter 1. 31 samples were prepared for fission track analysis (tables 4.1 and 4.2). 19 samples yielded enough zircon and apatite for dating, in the remaining samples only one of the two minerals could be analysed. All stratigraphic units in the study area were sampled, including the Quaternary volcanic deposits. Samples were analysed with the external detector method (see Wagner and Van den Haute (1992)). Ages were calculated with the software Trackkey 4.1 by Dunkl (2002) and are given as central

ages (Galbraith and Laslett (1993)) with  $1-\sigma$  errors for all zircon samples and for several apatite samples (kw1–12, kw2–13, kw2–20, kw2–22, kw2–32, kw2–35). Ages shown in brackets and *italics* are based on fewer than 10 single grain ages. For the remaining apatite samples ages were calculated and are shown as pooled ages because single grain age dating was not possible (see section 1.4.1). Pooled ages are also given with  $1-\sigma$  errors. Radial plots in figs. 4.5, 4.7, 4.9, 4.11, 4.13, 4.15 show single grain ages with  $\sigma$  errors on the left vertical, relative errors of the single grain ages on the horizontal and age in Ma on the right part of the plot. The oldest and youngest single grain ages of each sample are indicated (right). The plots are arranged in stratigraphic order with the stratigraphically highest plot at the top. Grey bars or areas in the plots mark deposition ages of the units in question.

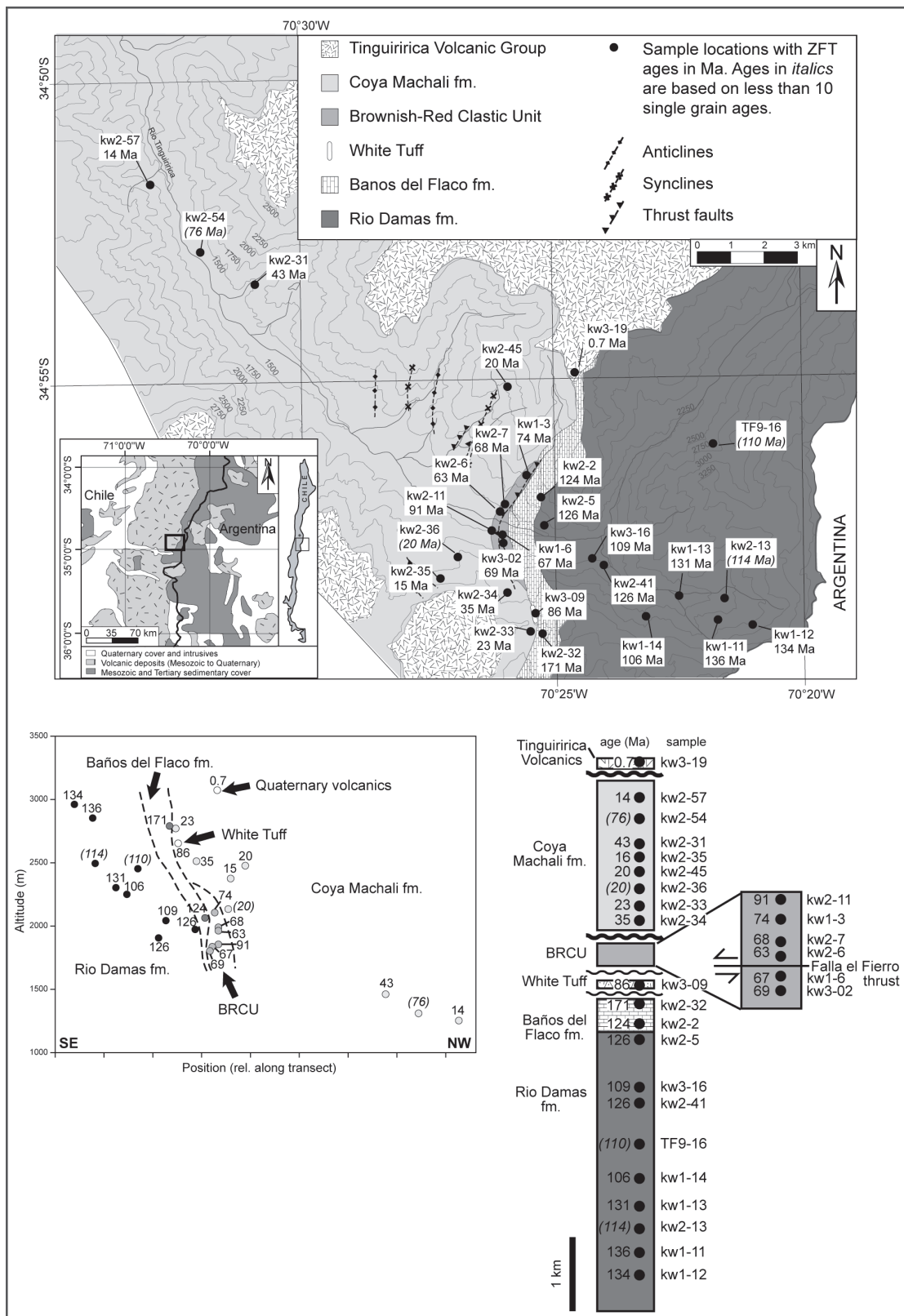
#### **4.4.1 Zircon fission track data**

27 zircon samples were prepared and irradiated for fission track analysis. Four of these samples yielded less than 10 single grain ages and the central ages for these samples are given in brackets in figures 4.4, 4.5, 4.13. Results are summarised in table 4.1. Figure 4.4 shows the distribution of zircon fission track central ages in the study area together with their position in the stratigraphic column and in a position altitude plot along a NW–SE transect (shown in Appendix A).



**Table 4.1:** Zircon fission track data of samples from all stratigraphic units in the study area: QV: Quaternary Volcanics (Tinguirrica Volcanic Group), CM: Coya Machali Formation, BRCU: Brownish-Red Clastic Unit, WT: White Tuff, BdF: Baños del Flaco Formation, RD: Rio Damas Formation.  $N_S$ ,  $N_I$  and  $N_D$  are numbers of tracks counted.

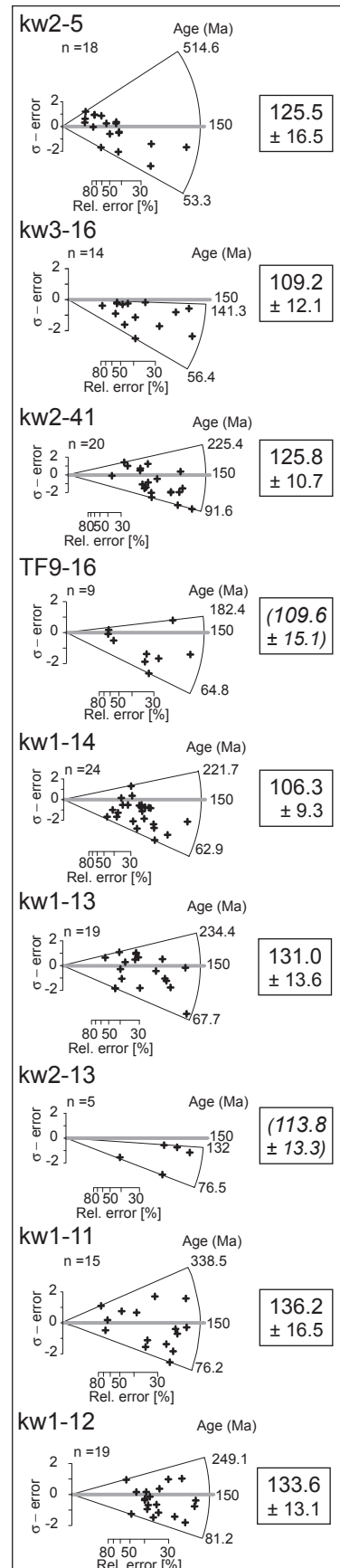
Sample number	Strat. unit	Latitude (S)	Longitude (W)	Altitude (m)	Grains	Spont. track density ( $\times 10^5 \text{ cm}^{-2}$ )	$(N_S)$	Ind. track density ( $\times 10^5 \text{ cm}^{-2}$ )	$(N_I)$	Std. track density ( $\times 10^5 \text{ cm}^{-2}$ )	$(N_D)$	$P(\chi^2)$ (%)	Central Age $\pm 1\sigma$ (Ma)	U (ppm)
kw3-19	QV	34° 54' 24.3"	70° 25' 00.0"	3070	20	1.59	(84)	48.677	(2572)	2.7759	(1366)	50.88	0.7 ± 0.1	806.84
kw2-31	CM	34° 53' 38.3"	70° 31' 11.7"	1458	19	95.043	(1912)	24.755	(498)	3.121	(1366)	<5	42.6 ± 10.5	353.58
kw2-33	CM	34° 59' 16.6"	70° 25' 37.1"	2767	37	20.887	(2014)	32.315	(3116)	4.9384	(2103)	<5	23.0 ± 1.9	262.66
kw2-34	CM	34° 58' 53.5"	70° 26' 09.1"	2509	16	33.968	(232)	25.476	(174)	3.7087	(1800)	97.39	35.4 ± 4.2	298.25
kw2-35	CM	34° 58' 33.1"	70° 27' 37.2"	2372	20	14.261	(371)	24.908	(648)	3.7124	(1800)	12.36	15.5 ± 1.5	311.43
kw2-36	CM	34° 58' 19.6"	70° 27' 22.0"	2131	7	31.375	(150)	42.042	(201)	3.705	(1800)	47.21	19.8 ± 2.5	444.88
kw2-45	CM	34° 55' 23.4"	70° 26' 13.0"	2474	20	23.655	(517)	31.525	(689)	3.6977	(1800)	<5	19.5 ± 1.9	369.74
kw2-54	CM	34° 52' 48.7"	70° 32' 29.5"	1307	5	124.704	(271)	34.512	(75)	3.0864	(1366)	<5	76.3 ± 17.1	473.76
kw2-57	CM	34° 51' 50.6"	70° 33' 13.1"	1250	21	24.621	(798)	38.475	(1247)	3.0519	(1366)	<5	14.2 ± 1.6	500.55
kw1-3	BRCU	34° 56' 53.4"	70° 25' 39.1"	2103	20	69.84	(1418)	32.014	(650)	4.9204	(2103)	<5	73.6 ± 7.0	282.00
kw1-6	BRCU	34° 57' 57.2"	70° 26' 05.4"	1834	12	54.742	(1244)	30.407	(691)	5.1187	(2103)	<5	66.5 ± 6.1	236.10
kw2-6	BRCU	34° 57' 15.4"	70° 26' 06.0"	1960	20	68.498	(1042)	29.056	(442)	3.7307	(1800)	52.53	62.8 ± 5.4	316.55
kw2-7	BRCU	34° 57' 10.3"	70° 25' 57.2"	1987	20	69.139	(777)	27.584	(310)	3.727	(1800)	<5	67.7 ± 10.4	298.34
kw2-11	BRCU	34° 57' 57.7"	70° 26' 17.6"	1852	23	64.122	(1704)	23.782	(632)	4.7761	(2103)	<5	90.5 ± 10.9	218.09
kw3-02	BRCU	34° 57' 44.4"	70° 26' 01.0"	1800	11	83.032	(995)	25.035	(300)	2.9829	(1366)	<5	68.7 ± 7.6	324.74
kw3-09	WT	34° 58' 52.7"	70° 25' 25.1"	2650	20	110.226	(1403)	26.476	(337)	2.9139	(1366)	65.00	86.4 ± 7.7	357.83
kw2-2	BdF	34° 57' 16.9"	70° 25' 51.3"	2061	14	122.103	(978)	34.583	(277)	4.7942	(2103)	<5	124.1 ± 13.8	288.76
kw2-32	BdF	34° 59' 16.8"	70° 25' 28.5"	2787	20	105.962	(1579)	16.106	(240)	3.716	(1800)	<5	170.5 ± 20.2	193.56
kw1-11	RD	34° 59' 13.9"	70° 22' 08.1"	2850	15	76.162	(785)	19.792	(204)	5.1006	(2103)	5.55	136.2 ± 16.5	153.99
kw1-12	RD	34° 59' 17.6"	70° 21' 49.0"	2958	19	78.809	(871)	20.449	(226)	4.8843	(2103)	75.88	133.6 ± 13.1	201.73
kw1-13	RD	34° 58' 30.4"	70° 22' 31.5"	2300	19	92.784	(1181)	25.533	(325)	5.0646	(2103)	<5	131.0 ± 13.6	215.14
kw1-14	RD	34° 58' 51.1"	70° 23' 11.5"	2247	24	49.119	(1470)	15.972	(478)	4.8663	(2103)	15.00	106.3 ± 9.3	134.45
kw2-5	RD	34° 57' 29.8"	70° 25' 31.7"	1970	18	88.435	(604)	19.327	(132)	3.7344	(1800)	20.44	125.5 ± 16.5	170.11
kw2-13	RD	34° 58' 49.2"	70° 22' 02.0"	2491	5	65.735	(551)	15.271	(128)	3.7197	(1800)	29.06	113.8 ± 13.3	250.18
kw2-41	RD	34° 58' 09.8"	70° 24' 10.2"	1903	20	87.526	(3690)	18.478	(779)	3.7013	(1800)	<5	125.8 ± 10.7	217.25
kw3-16	RD	34° 58' 01.6"	70° 24' 17.7"	2040	14	122.031	(788)	22.61	(146)	2.8449	(1366)	86.83	109.2 ± 12.1	293.49
TF9-16	RD	34° 56' 01.6"	70° 22' 03.9"	2450	9	51.038	(469)	12.079	(111)	3.7417	(1800)	30.09	109.6 ± 15.1	184.77



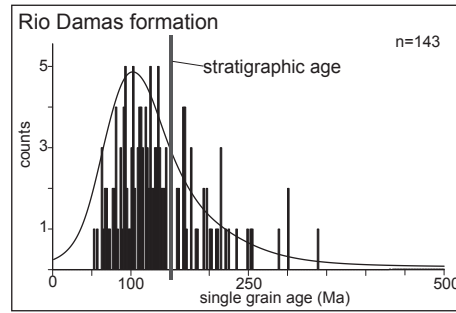
**Figure 4.4:** Central ages determined for zircon fission track samples from the Tinguiririca river valley, top: in map view, bottom: in an age vs. position plot along the transect shown in Appendix A and in a schematic stratigraphic column. Ages in brackets and *italics* are based on less than 10 single grain ages (see tab. 2.1).

## Rio Damas Formation

9 samples from the Rio Damas Formation were analysed (see table 4.1, figures 4.4, 4.5). They cover a range from close to the top of the unit to the lower part (the base is not exposed in the study area) and the difference in stratigraphic depth between the highest and lowest samples is about 3500 m. The relatively consistent central ages range between 106.3 and 136.2 Ma with no trend of increasing or decreasing age neither with stratigraphic depth nor with sample–elevation (table 4.1, figure 4.4). Radial plots of the individual samples are shown in figure 4.5 b. Central ages determined in the Rio Damas Formation are all significantly younger than the inferred stratigraphic age (Kimmeridgian, 156–150 Ma) of the unit. Single grain age spreads in the individual samples are all similar and grains preserving ages older than the stratigraphic age of the unit are still found in most samples (figure 4.5 b.). Figure 4.5 a. shows a histogram of all single grain ages of samples from the Rio Damas Formation. The maximum in the distribution is at about 100 Ma and thus clearly younger than the stratigraphic age. This, together with the fact that numerous grains older than the deposition age are still preserved, is indicative of partial annealing. The 100 Ma maximum is tentatively interpreted as roughly approximating the time of metamorphic overprint.



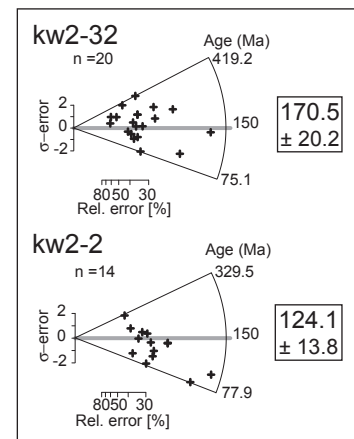
**Figure 4.5:** Radial plots of samples from the Rio Damas Fm.



**Figure 4.6:** Bar chart showing all ZFT single grain ages measured in samples from the Rio Damas Fm. The distribution shows a maximum at about 100 Ma, which is significantly younger than the stratigraphic age of the unit. Youngest single grain ages are at about 50 to 55 Ma.

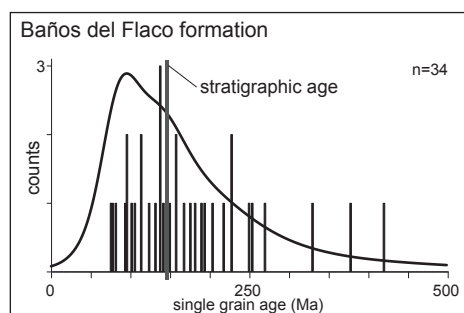
### Baños del Flaco Formation

Two samples from the Baños del Flaco Formation (kw2-2 and kw2-32) yielded central ages of 124.1 Ma and 170.5 Ma respectively (table 4.1, figures 4.4, 4.7). Kw 2-2 is from near the base of the unit on the North side of the valley and shows similar characteristics to samples from the Rio Damas Formation. The central age is younger than the stratigraphic age of the unit (Tithonian, 150–144) indicating at least partial annealing. The spread of single grain ages is also similar to those of samples from the Rio Damas Formation and grains with ages older than the stratigraphic age of the unit show that no total annealing of the sample occurred. Kw2-32 is from close to the topmost preserved part of the Baños del Flaco Formation in the vicinity or the unconformably overlying White Tuff. Although the difference in stratigraphic depth between these two samples is not very large (about 300 m), kw2-32 has a significantly older central age than any of the other samples from the Rio Damas or Baños del Flaco Formations. The central age (170.5 Ma) is much older than the stratigraphic age of the unit. However, the single grain age distribution of the sam-



**Figure 4.7:** Radial plots of two ZFT samples from the Baños del Flaco Fm. The horizontal grey bar marks the approximate deposition age of the unit. The samples are shown in stratigraphic order with the stratigraphically highest sample at the top.

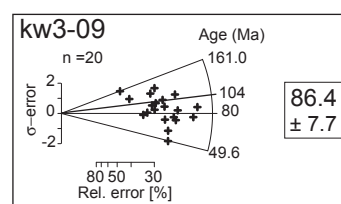
ple (figure 4.7 b.) shows that the sample also contains individual grains younger than the stratigraphic age, thus indicating that partial annealing occurred in this sample as well.



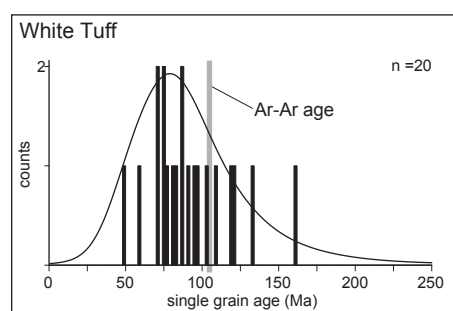
**Figure 4.8:** Bar chart showing all single grain ages measured in samples from the Baños del Flaco Fm.

## White Tuff

The White Tuff layer (kw3-09, see table 4.1), which lies directly on top of the erosional surface of the Baños del Flaco Formation, has a zircon fission track central age of  $86.4 \pm 7.7$  Ma. The sample passes the  $\chi^2$ -test and the age is interpreted as a cooling age. Figure 4.9 shows the single grain age distribution of the White Tuff.



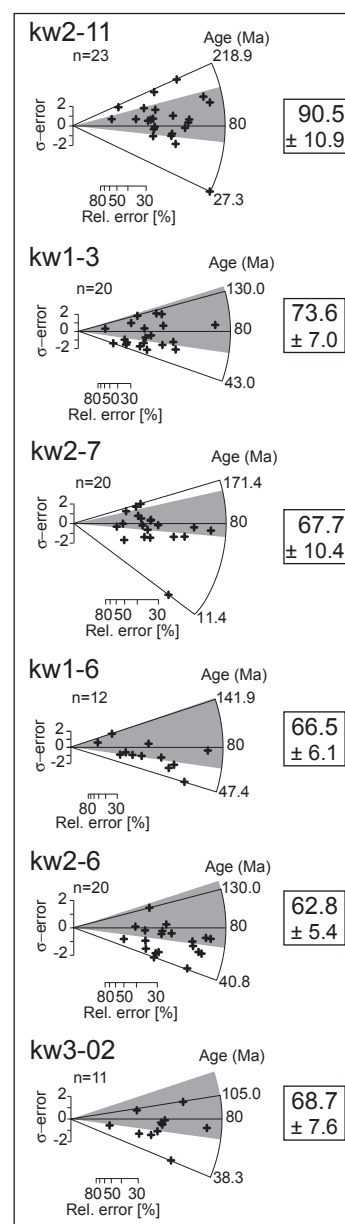
**Figure 4.9:** Radial plot of the ZFT sample from the White Tuff.



**Figure 4.10:** Bar chart showing the single grain ages measured in the sample from the White Tuff.

### Brownish–Red Clastic Unit

6 samples from the BRCU were analysed (table 4.1, figures 4.4, 4.11). 2 samples are from the footwall of the Falla el Fierro thrust (kw1–6 and kw3–02, see figure 4.4) and 4 from the hanging wall. The samples are all sediments containing volcanic material and some of the zircons from these samples are rounded indicating that they were reworked and transported before deposition. The 5 stratigraphically lower samples (figure 4.4) yielded central ages ranging between 62.8 and 73.6 Ma. An older age of 90.5 Ma was determined for the uppermost sample from the highest stratigraphic level, near the top of the unit. Because there is no independent indication that heating and annealing of fission tracks in zircon occurred after deposition, these ages are thought to represent detrital ages grains from the source areas. However, a histogram of the single grain ages from all six samples (see figure 4.11 a.) shows that most of the individual grains have late Cretaceous ages. The central ages are surprisingly similar and the sediments deposited in the BRCU appear to have come from a restricted source area where active volcanism occurred in the late Cretaceous.



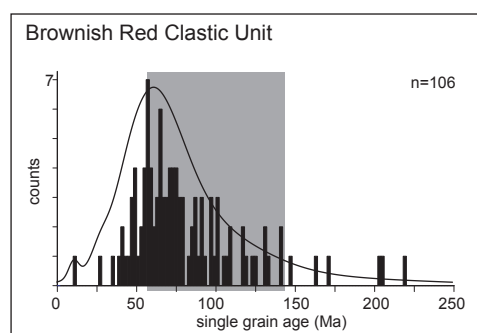


**Figure 4.12:** Bar chart showing all ZFT single grain ages measured in the 6 samples from the BRCU. The grey bar marks the supposed time-span in which the unit was deposited (Cretaceous). The maximum of the distribution is at about 60 to 70 Ma, in the late Cretaceous.

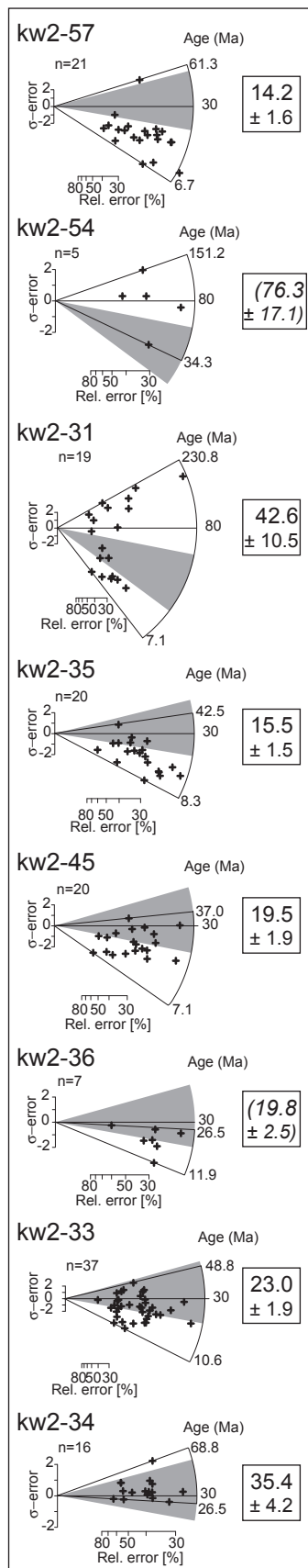


**Figure 4.13:** Radial plots of 8 ZFT samples from the Coya Machali Fm.

## Coya Machali Formation

8 samples from the Coya Machali Form were analysed (tab. 4.1, figs 4.4, 4.13). Central ages range from  $14.2 \pm 1.6$  Ma to  $76.3 \pm 17.1$  Ma. Fig. 4.14 shows a histogram of all single grain ages from the Coya Machali Fm. There is a pronounced peak at about 20 Ma but also a significant number of grains with ages much older than the stratigraphic age of the Coya Machali Fm are present. Fig. 4.13 shows radial plots of the individual samples from the Coya Machali Fm. Samples kw2–34 and kw2–33 are from the lower levels of the Coya Machali Fm and central ages of 35.4 and 23 Ma were determined for these two samples. Samples kw2–36 and kw2–45 have ages of 19.8 and 19.5 Ma respectively. All these ages fit with the period of active extension and sedimentation in the basin, from the Late Eocene to Early Miocene. Kw2–31 has a central age of 42.6 Ma and clearly contains at least two different grain populations (see figure 4.13). The age is therefore interpreted as a mixed age of detrital grains transported into the basin from outside and grains formed during volcanism associated with basin formation. Kw2–54 also contains detrital grains with ages much older than the deposition of the Coya Machali Fm (tab. 4.1, fig. 4.13). The remaining two samples, kw2–35 and kw2–57 both show ages that are younger than the generally accepted stratigraphic age of the Coya Machali Fm. Since there is no indication of substantial post-depositional heating, the samples possibly indicate that the stratigraphic range of the Coya Machali Fm has to be extended towards the middle Miocene.



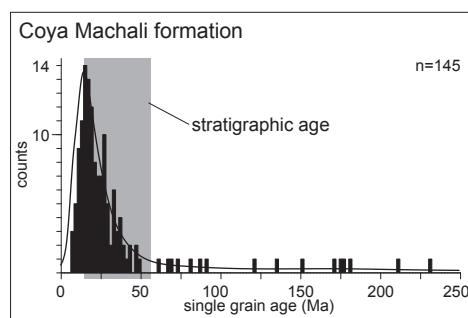


**Figure 4.14:** Bar chart showing all ZFT single grain ages measured in samples from the Coya Machali Fm. The grey bar marks the time-span of deposition of the unit (Eocene to early Miocene). There is a maximum in the distribution at about 20 Ma (early Miocene) but a number of grains show ages significantly older than the given deposition age of the unit.

### Tinguiririca Volcanic Group

One sample (kw3-19) from a tuff layer in the Quaternary volcanic rocks was dated to  $0.7 \pm 0.1$  Ma (table 4.1, figures 4.4, 4.15), well in agreement with other radiometric data (see Charrier et al. (1996)).

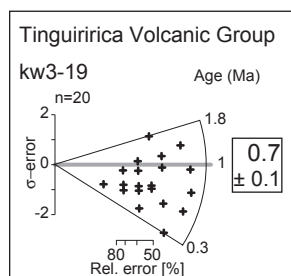


**Figure 4.15:** Radial plot of a ZFT sample from the Quaternary volcanics.

### 4.4.2 Apatite ages

23 apatite samples were analysed (see tab. 4.2, figure 4.16). However, single grain age dating could only be applied to 6 samples containing enough grains with sufficient spontaneous fission tracks. For each of these 6 samples at least 20 grains were analysed and the ages are given as central ages (tab. 4.2). For the remaining samples a modified population age method (see section 1.4.1, Wagner and Van den Haute (1992)) was applied: all grains with good surfaces were counted, including

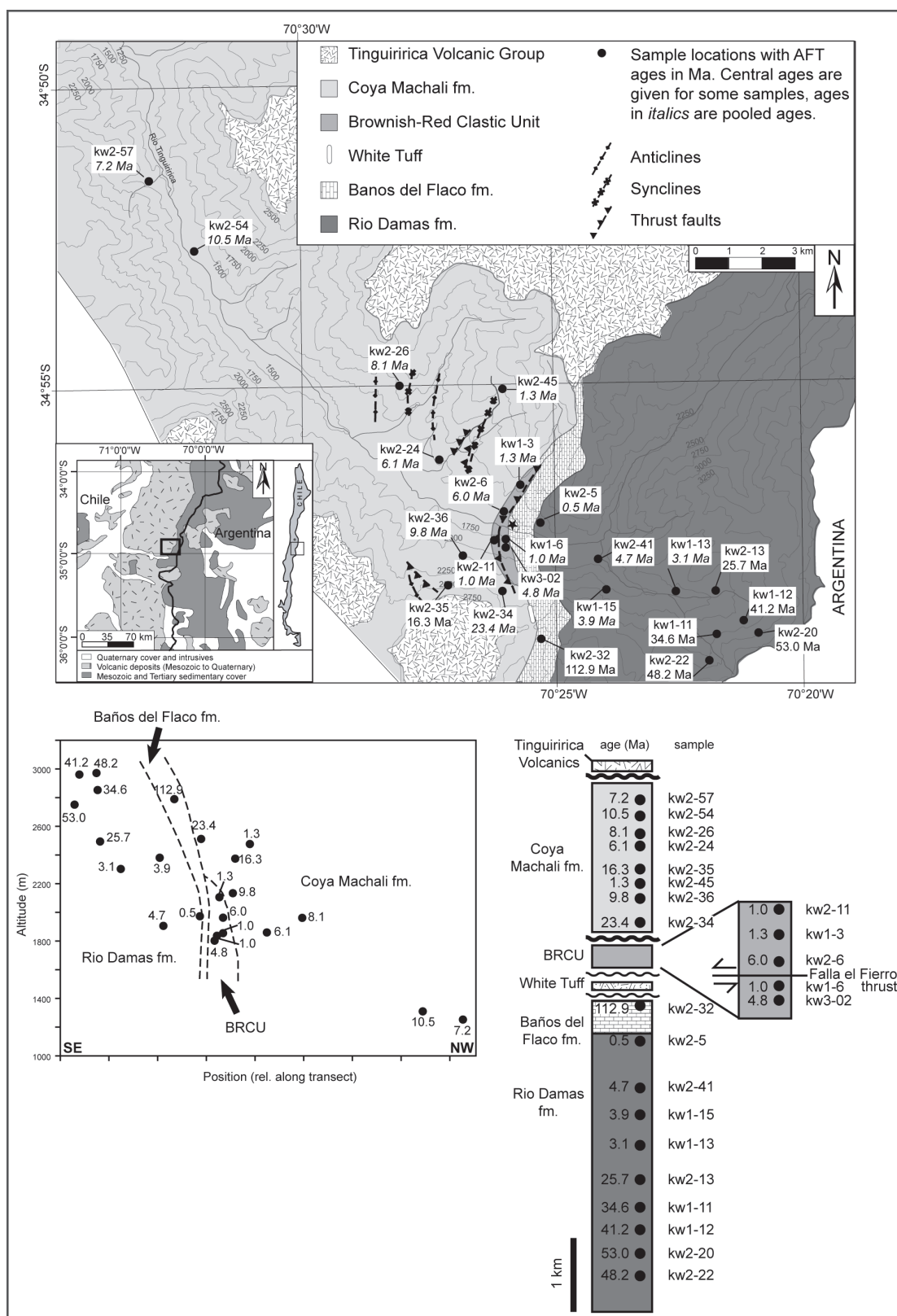


**Figure 4.16:** Apatite fission track data in the Tinguiririca river valley. Ages are given as central ages or pooled ages (see tab. 2.2). top: map view, bottom: position (relative position along the transect in Appendix A) vs. altitude plot and in a schematic stratigraphic column.

those grains with no spontaneous tracks. Pooled ages were then calculated for the total  $N_s/N_i$  ratio of all counted grains. The number of counted grains ranges from 19 to 60. Because of the lack of spontaneous tracks and the relatively low U content of most of these samples, the calculated ages have large relative errors (see table 4.2).

**Table 4.2:** Apatite fission track data: CM: Coya Machali Formation, BRCU: Brownish-Red Clastic Unit, BdF: Baños del Flaco Formation, RD: Rio Damas Formation.  $N_S$ ,  $N_I$  and  $N_D$  are numbers of tracks counted. Pooled ages are given for samples that contained too few spontaneous tracks for single grain age dating, central ages are given for samples where enough individual grains could be dated.

Sample number	Strat. unit	Latitude (S)	Longitude (W)	Altitude (m)	Grains	Spont. track den-sity ( $\times 10^5 \text{ cm}^{-2}$ )	$(N_S)$	Ind. track den-sity ( $\times 10^5 \text{ cm}^{-2}$ )	$(N_I)$	Std. track den-sity ( $\times 10^5 \text{ cm}^{-2}$ )	$(N_D)$	$F(\chi^2)$ (%)	Pooled Age (Ma)	Central Age $\pm 1\sigma$ (Ma)	U (ppm)	mean track length ( $\mu\text{m}$ )	std. dev. length ( $\mu\text{m}$ )
kw2-57	CM	34°51'50.6"	70°33'13.1"	1250	33	0.221	(12)	5.864	(318)	11.1907	(4148)	84.13	7.2 $\pm$ 2.1		6.30		
kw2-54	CM	34°52'48.7"	70°32'29.5"	1307	45	0.177	(16)	3.275	(296)	11.4417	(4148)	69.64	10.5 $\pm$ 2.7		3.86		
kw2-26	CM	34°55'08.5"	70°28'27.4"	1959	30	0.180	(8)	4.476	(199)	11.9437	(4148)	81.04	8.1 $\pm$ 3.0		4.98		
kw2-35	CM	34°58'33.1"	70°27'37.2"	2372	20	0.613	(77)	7.582	(952)	11.8396	(2159)	21.31	16.2 $\pm$ 2.0	<b>16.3<math>\pm</math>2.1</b>	7.95	13.8	1.7
kw2-36	CM	34°58'19.6"	70°27'22.0"	2131	40	0.169	(17)	3.587	(361)	12.2572	(2159)	84.08	9.8 $\pm$ 2.5		3.62		
kw2-24	CM	34°56'23.8"	70°26'55.1"	1857	40	0.119	(18)	4.193	(633)	12.6748	(2159)	55.45	6.1 $\pm$ 1.5		4.23		
kw2-11	BRCU	34°57'57.7"	70°26'17.6"	1852	40	0.033	(5)	3.898	(586)	7.2047	(3564)	53.87	1.0 $\pm$ 0.5		6.13		
kw2-45	CM	34°55'23.4"	70°26'13.0"	2474	40	0.032	(7)	4.905	(1068)	11.7005	(2159)	41.97	1.3 $\pm$ 0.5		5.15		
kw2-34	CM	34°58'53.5"	70°26'09.1"	2509	60	0.377	(79)	3.380	(709)	12.3964	(2159)	<5	23.4 $\pm$ 3.0		4.02		
kw2-6	BRCU	34°57'15.4"	70°26'06.0"	1960	60	0.098	(22)	3.721	(837)	13.3707	(2159)	<5	6.0 $\pm$ 1.3		3.80		
kw1-6	BRCU	34°57'57.2"	70°26'05.4"	1834	29	0.042	(6)	5.877	(847)	8.5586	(3564)	74.42	1.0 $\pm$ 0.4		8.48		
kw3-02	BRCU	34°57'44.4"	70°26'01.0"	1800	40	0.063	(13)	2.400	(494)	10.6887	(4148)	47.53	4.8 $\pm$ 1.4		2.96		
kw1-3	BRCU	34°56'53.4"	70°25'39.1"	2103	50	0.035	(5)	3.921	(562)	8.3651	(3564)	99.95	1.3 $\pm$ 0.6		6.18		
kw2-5	RD	34°57'29.8"	70°25'31.7"	1970	28	0.018	(2)	5.871	(654)	9.5256	(3564)	98.22	0.5 $\pm$ 0.4		7.72		
kw2-32	BdF	34°59'16.8"	70°25'28.5"	2787	52	4.726	(956)	8.820	(1784)	12.5356	(2159)	<5	112.9 $\pm$ 6.7	<b>112.9<math>\pm</math>7.6</b>	9.18		
kw2-41	RD	34°58'09.8"	70°24'10.2"	1903	39	0.105	(41)	4.559	(1779)	11.9788	(2159)	10.72	4.7 $\pm$ 0.8		4.79		
kw1-15	RD	34°58'43.7"	70°23'59.5"	2378	24	0.178	(11)	6.124	(378)	7.9783	(3564)	<5	3.9 $\pm$ 1.2		10.02		
kw1-13	RD	34°58'30.4"	70°22'31.5"	2300	18	0.120	(4)	5.207	(173)	7.7877	(3082)	46.05	3.1 $\pm$ 1.5		8.35		
kw1-11	RD	34°59'13.9"	70°22'08.1"	2850	12	1.974	(54)	10.124	(277)	10.4927	(3564)	93.66	34.6 $\pm$ 5.3	<b>34.6<math>\pm</math>5.3</b>	10.19		
kw2-13	RD	34°58'49.2"	70°22'02.0"	2491	24	0.975	(135)	8.394	(1162)	13.0923	(2159)	56.82	25.7 $\pm$ 2.6	<b>25.7<math>\pm</math>2.6</b>	7.03		
kw2-22	RD	34°59'43.0"	70°21'59.7"	2969	20	2.383	(524)	10.711	(2355)	12.8140	(2159)	52.07	48.2 $\pm$ 3.1	<b>48.2<math>\pm</math>3.1</b>	10.21	9.9	1.5
kw1-12	RD	34°59'17.6"	70°21'49.0"	2958	21	1.242	(71)	4.758	(272)	9.3322	(3564)	73.57	41.2 $\pm$ 5.7	<b>41.2<math>\pm</math>5.7</b>	6.56	11.5	1.9
kw2-20	RD	34°59'14.1"	70°21'36.7"	2748	19	2.501	(466)	10.316	(1922)	12.9531	(2159)	73.19	53.0 $\pm$ 3.6	<b>53.0<math>\pm</math>3.6</b>	9.67	9.5	2.0

## Samples analysed with the external detector method

Four samples from the Rio Damas Formation, one sample from the Baños del Flaco Formation and one sample from the Coya Machali Formation could be analysed with the external detector method (see tab. 4.2, figs 4.17, 4.19, 4.20).

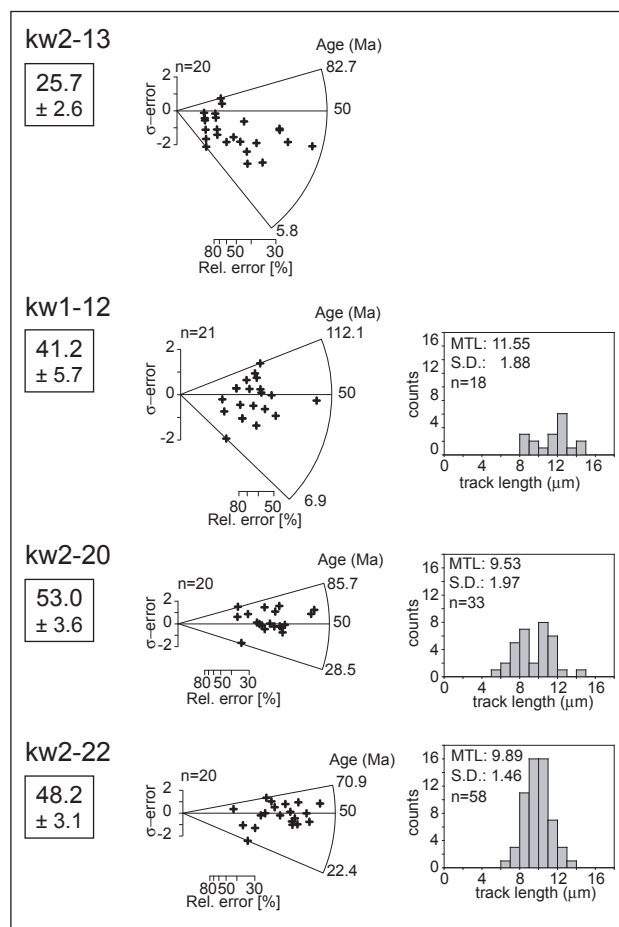


**Figure 4.17:** Radial plots of 4 AFT samples from the Rio Damas Fm. Ages are given as central ages in Ma with  $1-\sigma$  errors. The plots are in stratigraphic order with the stratigraphically highest sample at the top. Track length data was measured in three of the samples (see tab. 4.2) and track length distributions are plotted next to the radial plots. MTL: mean track length, S.D.: standard deviation of MTL, n: number of horizontal tracks measured. In all three samples, tracks  $>15\mu\text{m}$  were scarce or absent.

The four samples are from the lower part of the Rio Damas Formation. They yielded central ages between 25.7 and 53 Ma and all pass the  $\chi^2$ -test (tab. 4.2, figs 4.16, 4.5, 4.7, 4.13). Radial plots of the samples are shown in figs 4.5, 4.7, 4.13. Track length distributions of confined horizontal tracks were measured in three

samples (kw1–12, kw2–20 and kw2–22, see figure 4.18) and thermal modelling of temperature–time–paths was carried out using the software AFTSolve (Ketcham et al. (2000)). Figure 4.18 shows a model run and track length distribution of sample kw2–22. Interestingly, in all three samples long fission tracks ( $>15 \mu\text{m}$ ) are completely missing. Mean track lengths are between 9 and 10  $\mu\text{m}$ . Modelling of temperature time paths (figure 4.18) shows rapid cooling of the samples in the late Cretaceous. The samples cooled below the apatite PAZ in the Early Tertiary. After a slight T–increase, possibly due to burial, the samples were heated in very recent times to temperatures within the apatite PAZ. Reheating is immediately followed by rapid cooling to surface temperatures. Based on the modelling results, the Eocene central ages of the samples are interpreted to be meaningless and the samples underwent a two–stage cooling history with late Cretaceous cooling followed by slight Tertiary reheating and a final late Tertiary/Quaternary heating pulse.

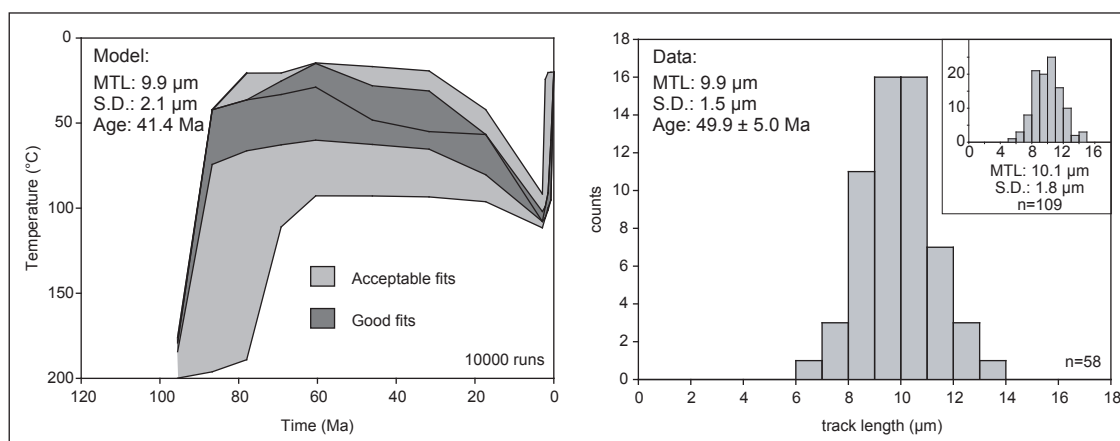


**Figure 4.18:** left: Temperature–time path modelled for sample kw2–22 with the software AFTSolve (Ketcham et al. (2000)). Constraints were set as follows: Temperature within the zircon PAZ at 95 Ma ( $>180^\circ\text{C}$ ), temperature less than  $80^\circ\text{C}$  at 60 Ma (cooling of the sample), temperature between  $25^\circ\text{C}$  and  $120^\circ\text{C}$  at 3 Ma. 10000 model runs were calculated using a Monte Carlo modelling scheme and the apatite annealing model of Laslett et al. (1987) (Durango apatite). The light grey area shows acceptable solutions, the dark grey area marks good fits, the black line is the best fit found in this run. right: Track lengths measured in sample kw2–22. There are no tracks longer than  $15 \mu\text{m}$ . MTL: mean track length, S.D.: standard deviation of MTL, n: number of horizontal tracks measured. inset: Track lengths measured in three samples (kw1–12, kw2–20, kw2–22) from the lower Rio Damas Formation.

Sample kw2–32 from the Baños del Flaco Formation, just below the eroded surface of the unit, yielded a central age of 112.9 Ma. The sample fails the  $\chi^2$ -test

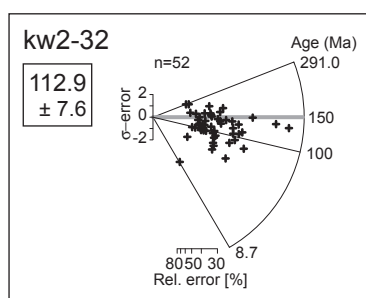


**Figure 4.19:** Radial plot of an AFT sample from the Baños del Flaco Fm. The age is given as a central ages in Ma with a  $1\text{-}\sigma$  error.

and shows a very large spread in single grain ages (see figure 4.7). No track length measurements were possible in this sample. However, a single very young grain could possibly indicate that this sample also underwent late reheating.

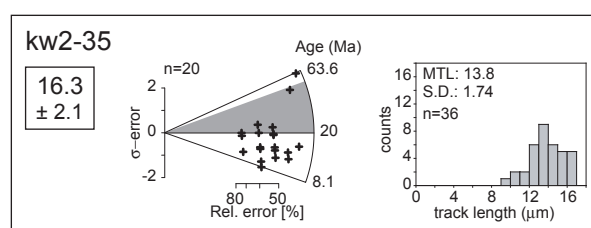


**Figure 4.20:** Radial plot of an AFT sample from the Coya Machali Fm. The age is given as a central ages in Ma with a  $1\text{-}\sigma$  error. The track length distribution was measured and is plotted beside the radial plot. MTL: mean track length, S.D.: standard deviation of MTL, n: number of horizontal tracks measured.

Sample kw2-35 from the Coya Machali Formation (tab. 4.2, fig. 4.13) has a central age of 16.3 Ma. Fig. 4.21 shows a confined track length-histogram for this sample (right). In contrast to the samples from the Rio Damas Formation, long tracks are present. Modelling of this sample with AFTSolve (fig. 4.21) shows cooling of the sample in the middle Miocene and, almost immediately, reheating to temperatures within the apatite PAZ. Slow cooling occurred during the late Miocene. Final cooling below the apatite PAZ could have been between about 7 and 3 Ma ago. Following the interpretation of the zircon fission track data, the rapid cooling is probably related to syn-sedimentary volcanic activity in the source area of the sediments. Detrital grains were then rapidly deposited in the Coya Machali Formation. Because there are no independent constraints on cooling or heating events for this sample, the results from modelling can only be considered

as one possible solution.

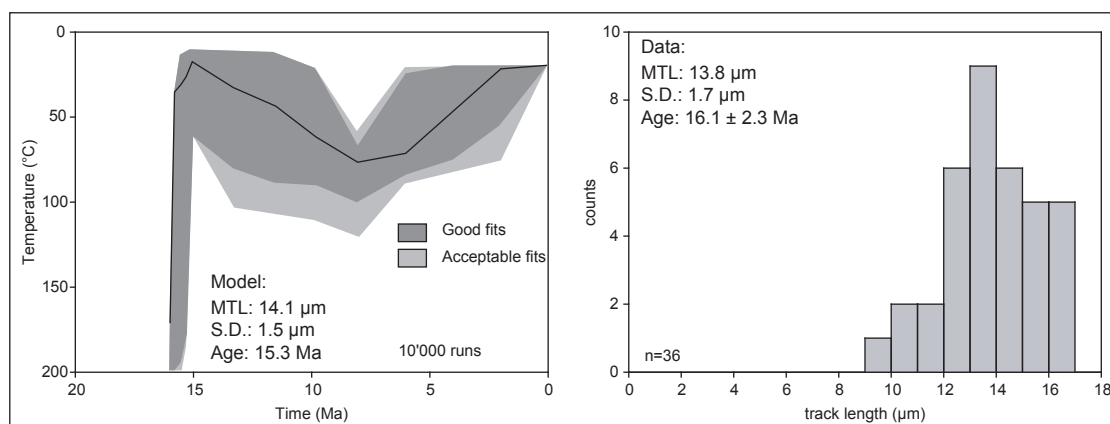


**Figure 4.21:** left: Temperature time path modelled for sample kw2–35 with the software AFT-Solve (Ketcham et al. (2000)). Constraints were set as follows: Temperature within the zircon PAZ at 17 Ma ( $>180^{\circ}\text{C}$ ), temperature less than  $60^{\circ}\text{C}$  at 15 Ma (cooling of the sample), temperatures between 20 and  $120^{\circ}\text{C}$  at 8 Ma. 10000 model runs were calculated using a Monte Carlo modelling scheme and the apatite annealing model of Laslett et al. (1987) (Durango apatite). The light grey area shows acceptable solutions, the dark grey area marks good fits, the black line is the best fit found in this run. right: Track lengths measured in sample kw2–35. MTL: mean track length, S.D.: standard deviation of MTL, n: number of horizontal tracks measured.

### Apatite samples counted with the modified population method

17 apatite samples contained a large number of grains with no spontaneous tracks (see table 4.2). All grains with suitable surfaces were counted and pooled ages were calculated for the samples. 1 sigma errors on the ages calculated by this method are larger than on ages determined by single grain age dating.

In the central part of the study area, near the village of Termas del Flaco and the hot springs and near the Quaternary volcanics very young ages ( $<2$  Ma) were determined in apatites from all the stratigraphic units. With increasing distance from this area, apatite ages increase to Eocene to Cretaceous ages. This pattern most likely evidences the decreasing effect of a local heat-source due to hydrothermal activity that occurred in the Quaternary and affected apatite crystals to different degrees depending on their distance from the heat-source. Since the degree of thermal overprint cannot be constrained for the individual samples, no information about possible earlier events in the area can be gained from the samples.



### 4.4.3 Paleostress analysis

#### Methods

Kinematic axes (principal shortening and extension directions) were derived from mesoscale structures in order to analyse the regional tectonic history. For this purpose fault–slip sets (orientation of fault plane, sense and direction of movement) were analysed. The direction of movement being given by a lineation (mechanical striation or slicko–fibre orientation), sense of movement was determined mainly by slicko–fibre growth direction or offset of marker horizons. Inhomogeneous fault set data were separated into homogenous subsets based on field observations, and supported by analysis of kinematic compatibility using principal axes of incremental strain (Marret and Allmendinger (1990)). Paleostress was assessed with the right dihedron method described by Angelier and Mechler (1977). This simple graphical method is applicable to newly formed fractures, as well as to the reactivation of pre–fractured media, allowing the evaluation of the coherence of the data and reflecting the bulk finite strain state (Pfiffner and Burkhard (1987)). Eigenvectors and eigenvalues (Bingham (1964)) have been used to determine mean axes of compression and extension. For the calculation of kinematic axes and the visualisation of the fault sets we used the program TectonicsFP (Franz Reiter and Peter Acs 1996–2000).

#### Results

An overview of the data is given in table 4.3 and the deformation axes are plotted in figure 4.22. Two different senses of movement could be determined: An older phase of SW–NE compression with some evidence of associated strike–slip. This compressive regime is evidenced by brittle thrust faults, i.e. the Falla el Fierro thrust (see figure 4.2). A later phase of NW–SE extension with very minor strike–slip movements is evidenced by a series of small–scale brittle normal faults. The relative timing of the two phases is deduced from field evidence, i.e. outcrops where two different striations were found on the same fault plane. The older compressive phase is thought to represent the inversion of the Eocene basin and folding and faulting of the Coya Machali Formation. Brittle thrust faults and fold axis planes strike more or less perpendicular to the calculated sigma 1 direction (see figure 4.22). The extensive phase occurred after compression and evidence in

the form of brittle normal faults can be seen in all stratigraphic units in the area except the Quaternary volcanics. The timing of the extension is therefore thought to be late Miocene but no definite age constraints have been found.

**Table 4.3:** Mean axes of compression and extension calculated for 11 outcrops in the study area (see fig. 4.22). At least 2 phases of brittle deformation probably occurred in the study area: 1. a phase of compression with main compressive axes oriented ENE-WSW, 2. a phase of extension with main extensive axes oriented NW-SE.

No.	Stratigraphic unit	Lithology	$\sigma_1$ : Strike/Dip	$\sigma_2$ : Strike/Dip	$\sigma_3$ : Strike/Dip	Datasets	Rating	Latitude (S)	Longitude (W)
1	base of the Coya Machali fm.	intrusive	085/24	180/12	295/62	21	2	34°56'55.9"	70°26'07.9"
2	contact between the BRCU and the Baos del Flaco fm.	conglomerate	264/04	354/06	139/82	4	1	34°56'48.9"	70°25'31.5"
3a	contact between Baos del Flaco fm and Rio Damas fm	conglomerate	240/15	342/38	132/48	7	2	34°57'22.3"	70°25'28.0"
3b	contact between Baos del Flaco fm and Rio Damas fm	conglomerate	052/18	172/57	313/26	3	1	34°57'22.3"	70°25'28.0"
4	contact between Baos del Flaco fm and Rio Damas fm	conglomerate	054/9	512/53	151/36	7	2	34°57'49.3"	70°25'22.6"
5	lower Coya Machali fm	conglomerate	046/22	292/46	153/36	6	2	34°58'37.3"	70°26'04.9"
6	Coya Machali fm	volcanite	046/11	197/78	315/06	2	2	34°55'28.8"	70°26'23.1"
7	lower Rio Damas fm	conglomerate	047/42	179/37	291/27	10	2	34°59'12.2"	70°22'03.9"
8	lower Rio Damas fm	conglomerate	008/58	232/25	133/20	4	1	34°58'31.6"	70°22'02.0"
9	lower Rio Damas fm	conglomerate	063/28	241/62	333/01	13	2	34°58'42.2"	70°21'46.2"
10	lower Rio Damas fm	conglomerate	042/66	217/24	308/02	9	2	34°58'47.8"	70°21'06.9"
11	Coya Machali fm	volcanite	199/03	004/87	109/01	11	1	34°56'18.1"	70°26'02.0"

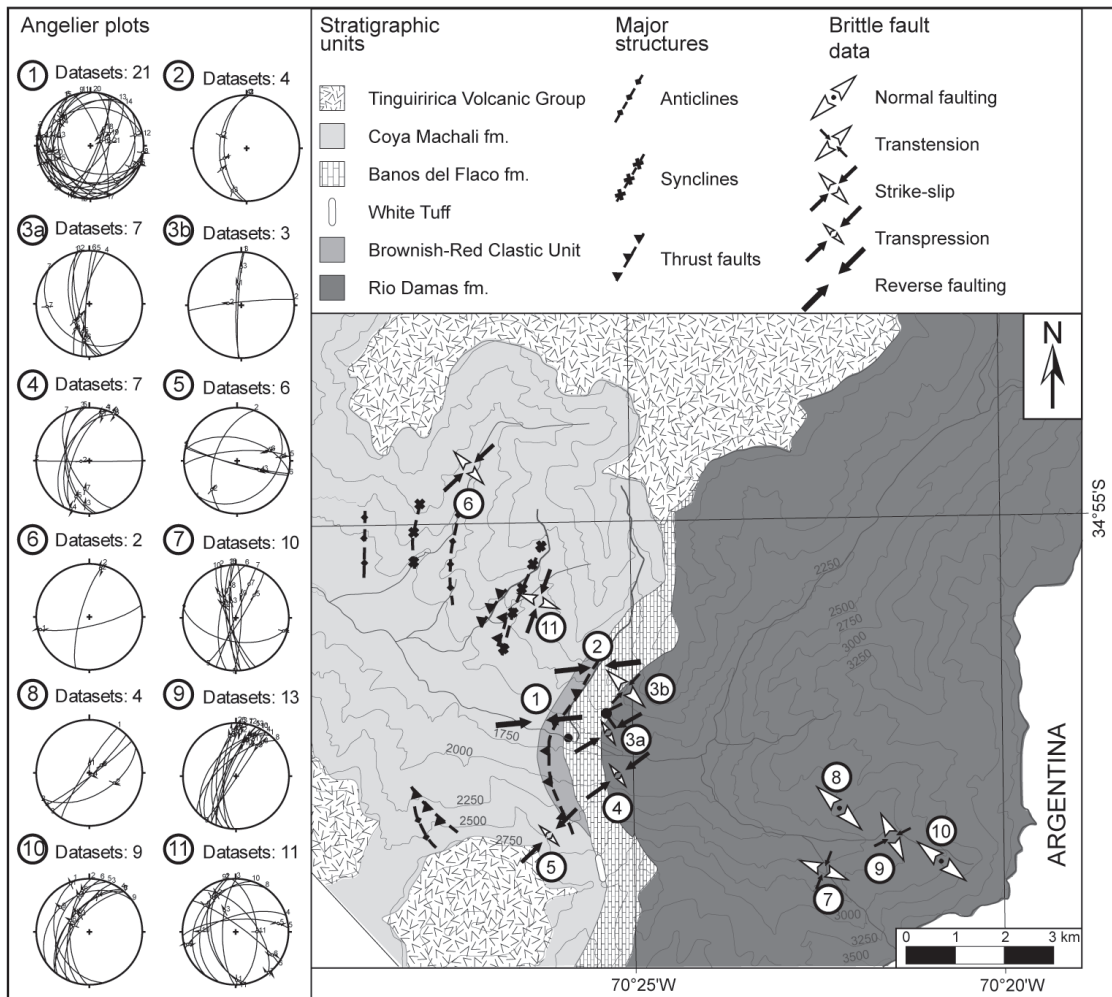


**Figure 4.22:** Brittle deformation at various localities in the study area calculated from analysis of striations measured on brittle fault planes. The calculated  $\sigma$ -1, 2 and 3 directions are given in tab. 4.3. At least two different phases can be distinguished: 1. a phase of ENEWSW compression with associated strike-slip activity, 2. a phase of NWSE extension.

## 4.5 Discussion

### 4.5.1 Age of the White Tuff

The two ages acquired for the White Tuff layer with different methods differ significantly. The Ar–Ar age determined by Wyss et al. (1994) is  $104 \pm 0.5$  Ma while the ZFT cooling age from this study is  $86.4 \pm 7.7$  Ma. This difference has an influence on interpretation of the situation during heating in the Rio Damas and Baños del Flaco Formations during the Cretaceous. If the formation age of 104

Ma is accurate, then erosion of the Baños del Flaco Formation had already taken place and the tuff was deposited more or less at the time of maximum heating in the lower units as discussed in chapters 2, 3. This would mean that temperatures within the zircon PAZ were reached at only 300 to 400 m below the surface. The Baños del Flaco Formation is only about 350 m thick in the study area and samples from the base of the Baños del Flaco Formation and from the top of the Rio Damas Formation all show evidence of partial annealing. The sample from the top of the Baños del Flaco Formation cooled somewhat earlier and has an AFT age of  $112.9 \pm 7.6$  Ma. If the ZFT cooling age of 86 Ma is accurate and cooling in the thin tuff layer can be assumed to more or less correspond to the time of deposition, then erosion of the Baños del Flaco Formation could have continued until after 90 Ma and cooling in the Rio Damas and Baños del Flaco Formations could have taken place during erosion and exhumation. However, burial alone cannot have been the trigger for heating during the mid Cretaceous. Even if the Baños del Flaco Formation was originally 2000 m thick and sediments of the Colimapu Formation had also been deposited in the area, assuming high geothermal gradients of  $30^\circ\text{C}/\text{km}$ , the top of the zircon PAZ would have been at least 6 km deep in the lower part of the Rio Damas Formation. Additional heating from an unknown source must have occurred in order to cause partial annealing of fission tracks in zircon at the base of the Baños del Flaco Formation and even, to a minor extent, near the present-day top of this unit.

#### 4.5.2 Age of the BRCU

Charrier et al. (1996) suggested several different scenarios for the relative positions of the White Tuff and the BRCU and for associated stratigraphic unconformities. In their preferred model, the White Tuff is older than the BRCU and there are stratigraphic unconformities between the Baños del Flaco Formation and the White Tuff, the White Tuff and the BRCU and between the BRCU and the Coya Machali Formation. Our data support this hypothesis. Zircon fission track ages of samples from the BRCU are consistently late Cretaceous and, with one exception from the top of the unit, younger than the cooling age determined for the White Tuff layer. The samples from the BRCU are all sediments and therefore the ZFT ages cannot be interpreted as in situ cooling ages but, instead, represent detrital ages from the source areas of the sediments. The sediments in the BRCU are

mainly reworked volcanic deposits and continental sediments and the zircon grains found in these rocks can be assumed to have formed during volcanic activity and to have later been eroded and redeposited in the BRCU. Because the BRCU is known from non-avian dinosaur bones found therein to be Cretaceous and the ZFT ages are mainly late Cretaceous, erosion and renewed deposition of the sediments must have occurred fairly soon after initial deposition of the volcanic material. Since most of the zircon grains are not much rounded, transport cannot have been very far.

### 4.5.3 Tilting of the Mesozoic units

The mechanism that led to tilting of the Mesozoic units is not known. Possibly, compression led to thrusting along a steep fault when the basin was inverted. However, time constraints can be given for the tilting. The BRCU lies on top of the Baños del Flaco Formation with no apparent angular unconformity and tilting cannot have taken place until after deposition of the BRCU. The fission track data, as shown above, imply a late Cretaceous age for the BRCU. Early Eocene ages preserved in partially annealed apatite fission track samples from the lower part of the Rio Damas Formation indicate exhumation of these samples to depths above the apatite PAZ during the early Tertiary. Track length measurements and modeling of temperature-time paths for these samples suggest rapid cooling through the apatite PAZ. The samples were taken at stratigraphic levels about 3500 to 3700 m below uppermost preserved part of the Baños del Flaco Formation and thus were certainly within or even below the apatite PAZ as long as the units were still in a horizontal position. The samples were affected by a late heating event in the central part of the study area and partial annealing occurred. This can be implied from the complete absence of long tracks in the samples. Thus, the ages derived for these samples have to be treated as minimum ages – the absolute effect of the annealing cannot be quantified without more detailed information on the chemical composition of the apatites. Thermal modelling of track length data on samples from the lower Rio Damas Formation shows cooling of the samples in the Late Cretaceous to Early Tertiary (figure 4.18). This was most likely related to tilting and erosion. For an assumed geothermal gradient of 30 °C/km the lower part of the Rio Damas Formation must have been exhumed to less than 2 km below the surface.

#### 4.5.4 Deposition of the Coya Machali Formation and inversion of the extensional basin

The Coya Machali Formation was deposited unconformably on to the tilted and eroded Mesozoic strata. According to Charrier et al. (2002) this occurred in an extensional intra-arc basin setting during the late Eocene to early Miocene. Deposition was followed by compression and inversion of the basin in the early to mid Miocene. The ZFT age data confirm their model. The samples from the lower part of the Coya Machali Formation have late Eocene to early Miocene ages (35 to 20 Ma) and decrease toward higher stratigraphic levels. These ages are thought to represent either in situ cooling ages in volcanic deposits or similar to the BRCU grains that were formed during volcanic activity in or near the basin and then reworked. Further to the west two samples containing detrital zircon grains with significantly older ages were found. These samples come from higher levels in the Coya Machali Formation and mark a transition from mainly pyroclastic flows and lavas in the lower part of the unit to fluvial and lacustrine deposits with volcanic intercalations (see Charrier et al. (1996)). According to Charrier et al. (2002) deposition of the Coya Machali Formation ended at about 20 Ma. The same authors report a single Ar–Ar age of 16.1 Ma measured in the Las Leñas river area to the North of the Rio Tinguiririca valley. They attributed this to syntectonic sedimentation during compression and basin inversion. However, two samples from the Coya Machali Formation have ages of 16 and 14 Ma respectively and one of the samples containing detrital grains also contains a population of younger grains with an age of 16 Ma. From their stratigraphic positions (see figure 4.4) it appears unlikely that these samples represent syntectonic deposits during basin inversion. On the other hand, the deposits of the Coya Machali Formation are only about 2000 m thick and there is no evidence for exceptionally high temperatures in this unit that would account for partial annealing of fission tracks in zircon. Local effects such as contact metamorphism near intrusions may have had an influence on individual samples but, nonetheless, there appears to be some indication that sedimentation continued somewhat longer in this area than previously thought.

### **4.5.5 Extensional phase after basin inversion**

Evidence from paleostress analysis and the presence of small-scale brittle normal faults indicate an extensional phase sometime after compression and inversion of the basin. No evidence was found for the timing and duration of this phase. The extension direction derived from fault plane analysis is oriented NW–SE and fits well with the observed strike of the brittle normal faults, which is NE–SW.

### **4.5.6 Late heating near Termas del Flaco**

The somewhat peculiar pattern of apatite fission track ages (see figure 4.16) points to a local heat-source, which led to almost complete annealing of fission tracks in apatite. From the available apatite fission track data the area of intense thermal overprint can be extended along the Falla el Fierro fault and further eastward along the valley bottom (figure 4.23). Possibly hydrothermal activity along active fault zones such as the Falla el Fierro thrust generated temperatures sufficient to cause this annealing of fission tracks. The hot springs at Termas del Flaco show that some geothermal activity is ongoing even at present. The effect of the heating event decreases with increasing distance from the heat-source and samples in the middle and lower part of the Rio Damas Formation were only partly reset. Samples from fairly high elevations on the south side of the valley seem more or less unaffected. It is difficult to judge without track length analysis and modeling of temperature time paths how much each individual sample was affected.

## **4.6 Model for the evolution of the study area from the mid Jurassic to the present**

Based on the data presented here and on earlier work by Charrier et al. (1996) and Charrier et al. (2002) a model for the development of the study area from the mid Jurassic to the present is proposed. The individual phases are summarised below and illustrated in figures 4.24, 4.25.



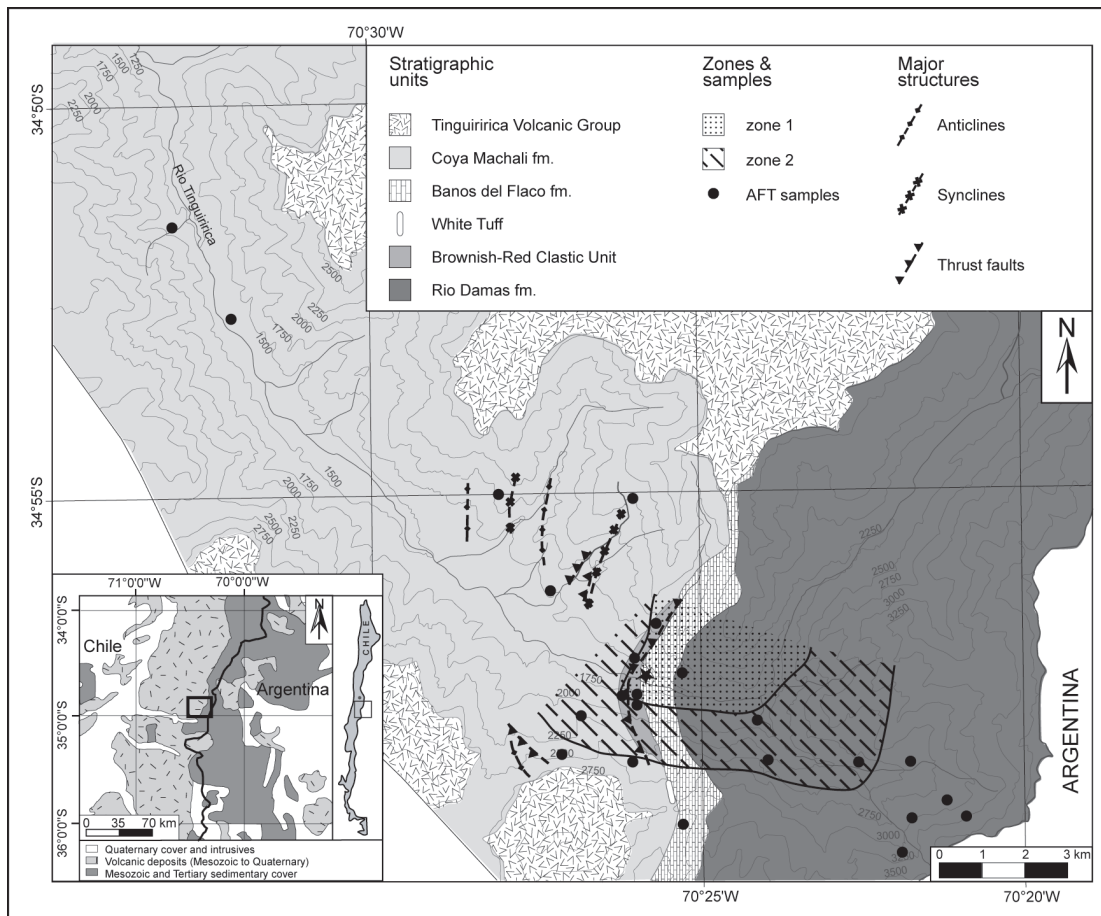


**Figure 4.23:** Zones of thermal overprint of AFT samples during Quaternary heating. In zone 1, fission tracks in apatite were almost completely annealed, in zone 2 fission tracks were substantially annealed. Thermal overprinting also occurred outside these zones as evidenced by thermal modelling (see fig. 2.20 but to a lesser extent).

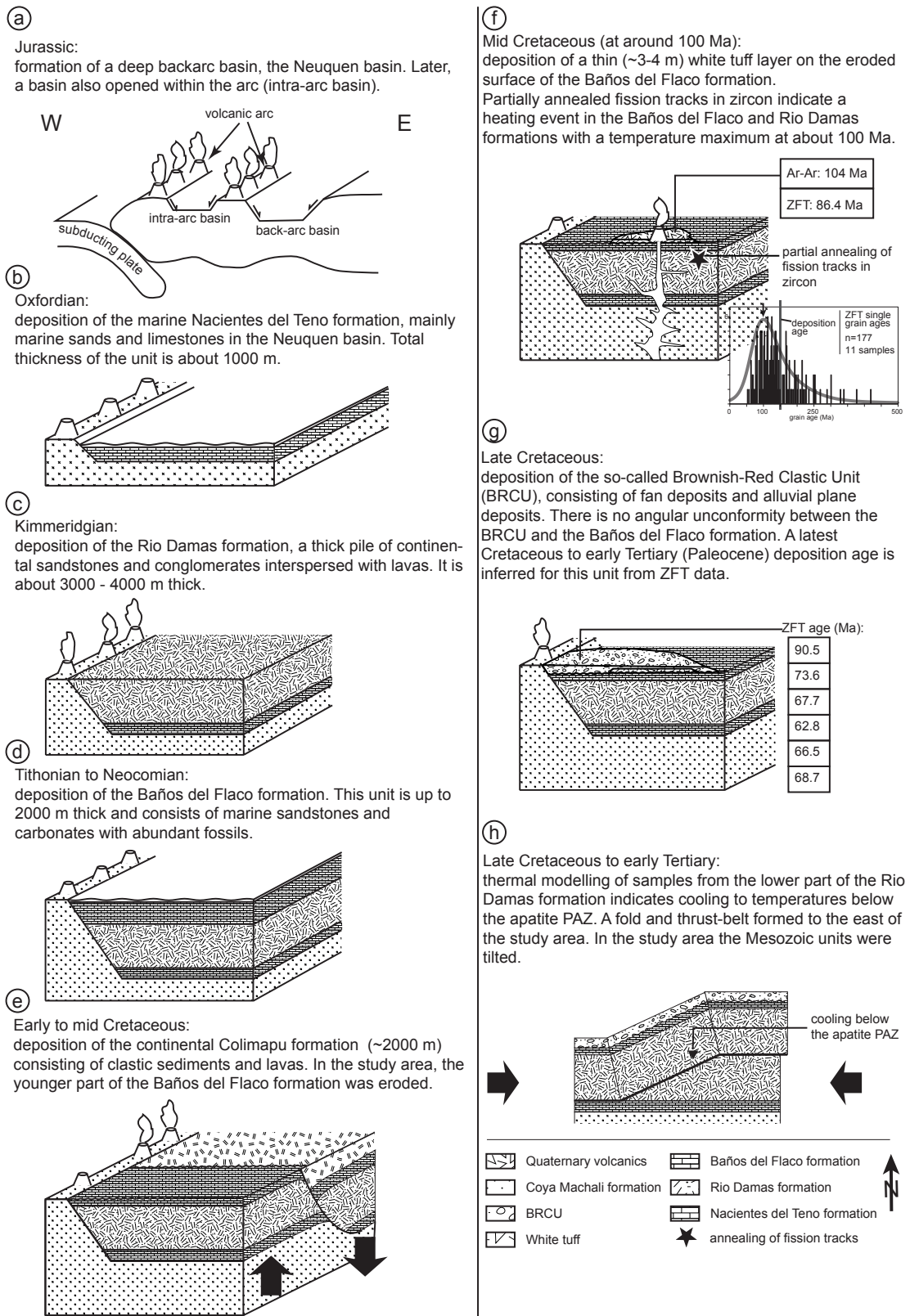
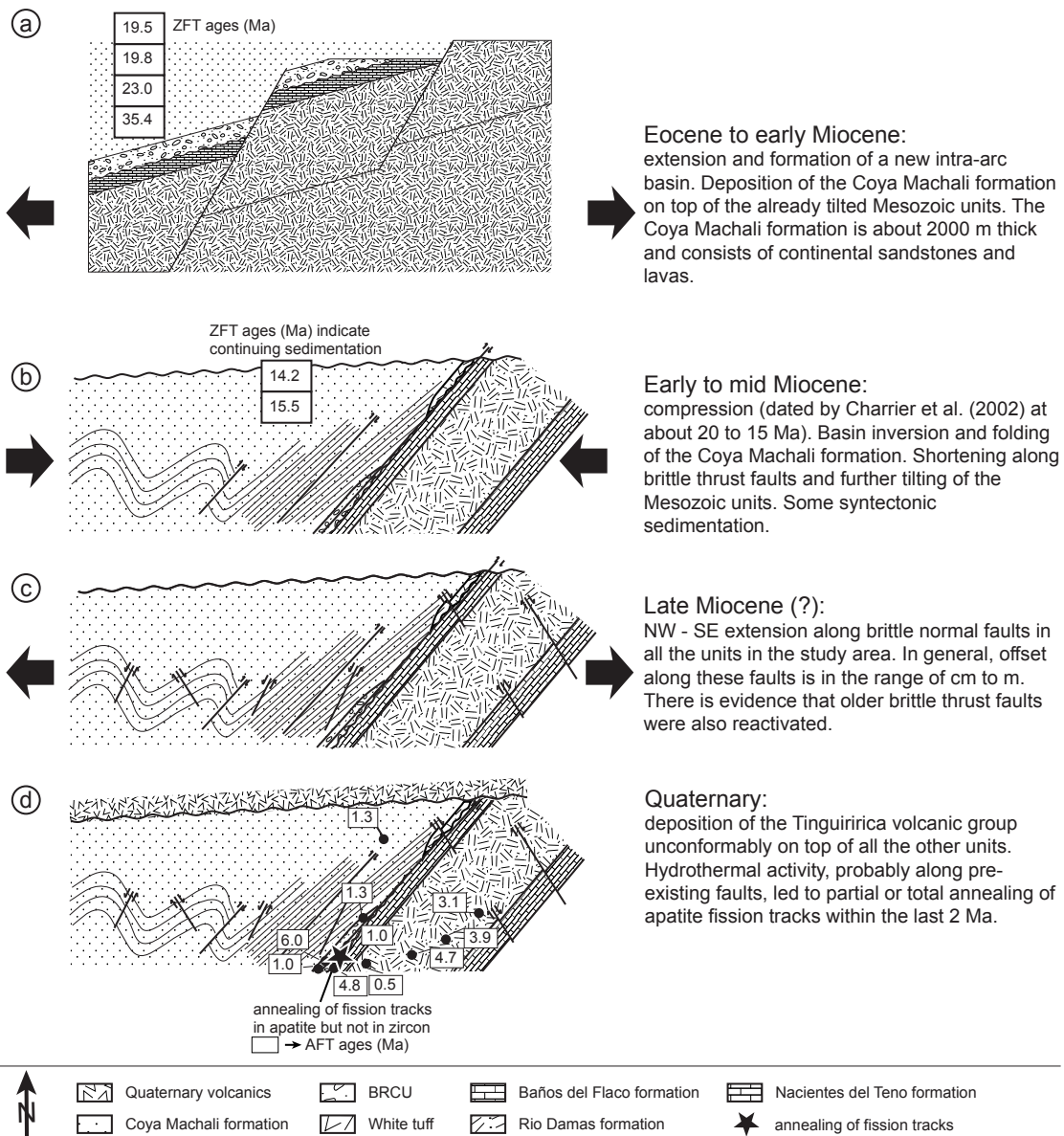


**Figure 4.24:** Jurassic to late Cretaceous evolution of the study area. Detailed discussion of the individual points in the text.



**Eocene to early Miocene:**  
 extension and formation of a new intra-arc basin. Deposition of the Coya Machali formation on top of the already tilted Mesozoic units. The Coya Machali formation is about 2000 m thick and consists of continental sandstones and lavas.

**Early to mid Miocene:**  
 compression (dated by Charrier et al. (2002) at about 20 to 15 Ma). Basin inversion and folding of the Coya Machali formation. Shortening along brittle thrust faults and further tilting of the Mesozoic units. Some syntectonic sedimentation.

**Late Miocene (?):**  
 NW - SE extension along brittle normal faults in all the units in the study area. In general, offset along these faults is in the range of cm to m. There is evidence that older brittle thrust faults were also reactivated.

**Quaternary:**  
 deposition of the Tinguiririca volcanic group unconformably on top of all the other units. Hydrothermal activity, probably along pre-existing faults, led to partial or total annealing of apatite fission tracks within the last 2 Ma.

**Figure 4.25:** Early Tertiary to present development of the study area. Detailed discussion of the individual points in the text.

### 4.6.1 Mid to late Jurassic

In the mid to late Jurassic a backarc basin, Neuquen backarc basin, was formed and filled with sediment (Charrier et al. (1996), Charrier et al. (2002), Mpodozis and Ramos (1989)) (fig. 4.24 a.). During the Oxfordian the basin was flooded and a sequence of marine carbonates and sands was deposited. The Nacientes del Teno Formation is about 1000 m thick and is capped by a thick gypsum upper member indicating changing conditions in the basin. This unit is not exposed in the study area but further to the East in Argentina (fig. 4.24 b.). The Rio Damas Formation lies conformably above the Nacientes del Teno Formation and consists mainly of continental sandstones, conglomerates and lavas. The deposits are thought to be Kimmeridgian. No biostratigraphically significant fossils have been found in this unit and the age is based on the well constrained ages of the bracketing units (fig. 4.24 c.). In the Thitonian to Neocomian the basin was again flooded and a thick sequence of marine carbonates and sands was deposited the Baños del Flaco Formation. This unit is up to 2000 m thick and contains several ammonite species that allow biostratigraphical dating of the formation. The deposits represent 2 transgression regression cycles (fig. 4.24 d.).

### 4.6.2 Early to mid Cretaceous

To the North of the study area, the mid Cretaceous Colimapu Formation lies conformably on top of the Baños del Flaco Formation. It consists of continental sandstones and lavas and is about 2000 3000 m thick. In the study area, however, the Colimapu Formation is not present and the upper part of the Baños del Flaco Formation has been eroded leaving only the Tithonian deposits. Presumably, local uplift in the basin must have led to this change in facies but there is no evidence in the study area to explain this local phenomenon such as a large pluton or a salt dome or similar (fig. 4.24 e.). In the mid Cretaceous a white tuff layer was deposited on top of the eroded surface of the Baños del Flaco Formation. At the time of deposition, erosion of the Baños del Flaco Formation had already taken place. At more or less the same time, heating to temperatures within the zircon PAZ occurred in the Rio Damas and Baños del Flaco Formations. Temperatures were too high to be accounted for by burial alone but the cause of heating is unknown (fig. 4.24 f.).

### 4.6.3 Late Cretaceous

Late Cretaceous ZFT ages in sediments from the BRCU indicate a late Cretaceous age for the unit. It lies unconformably on top of the Baños del Flaco Formation but without any apparent angular unconformity and it is thought, therefore, that tilting of the older units had not begun at that time. The BRCU consists of fan and alluvial plane deposits and was probably deposited near a retrograding basin margin (Charrier et al. (1996)). The high content of volcanoclastic material in the deposits suggests a predominantly volcanic source for the sediments (fig. 4.24 g.).

### 4.6.4 Late Cretaceous to early Tertiary

Apatite fission track samples from the lower part of the Rio Damas Formation have early Eocene cooling ages. These samples have since been partially annealed and the original central ages were probably slightly older. The samples are from a stratigraphic depth of about 3500 to 3700 m below the uppermost preserved part of the Baños del Flaco Formation and therefore, even at fairly low geothermal gradients, must have been within the apatite PAZ as long as the units were in a horizontal position. Cooling of these samples below the PAZ of apatite during the early Tertiary (probably Paleocene to early Eocene) implies that tilting and exhumation of the samples to depths above the apatite PAZ occurred during that time (fig. 4.24 h.).

### 4.6.5 Eocene to early Miocene

The Coya Machali Formation was deposited during the late Eocene to early Miocene in an extensional intra-arc basin (Charrier et al. (2002)). Deposition in the study area began at about 35 Ma. ZFT age data indicate that sedimentation may have continued somewhat longer than hitherto thought ages of 14 to 16 Ma have been determined for samples from the middle part of the Coya Machali Formation (fig. 4.25 a.). Basin inversion is thought by Charrier et al. (2002) to have occurred during the early to mid Miocene and to have taken place in pulses. According to the same authors, compressional deformation caused formation of new brittle normal faults and folding of the Coya Machali Formation. Paleostress analysis in the Termas del Flaco area confirms a phase of SW-NE to W-E compression. Fault axis planes and thrust fault traces in the Coya Machali Formation strike more or

less perpendicular to the compression axis calculated from the paleostress data (fig. 4.25 b.). Compression was followed by a further extensional phase, evidenced by numerous newly-formed small-scale brittle normal faults and probably reactivation of some pre-existing faults. The former affect all the Mesozoic and Tertiary units in the area. The relative timing of this extensive phase is implied from field evidence (i.e. superposition of two lineaments on the same fault plane) and from the fact that normal faults can be found even to offset young intrusives in the Coya Machali Formation. Offset along these brittle normal faults is generally on the scale of cm to meters and the extension axis can be inferred from paleostress analysis to have been NW–SE and is more or less perpendicular to the strike of the newly formed normal faults (fig. 4.25 c.).

#### **4.6.6 Quaternary**

In the Quaternary the basalts and tuffs of the Tinguiririca volcanic group were deposited unconformably on top of the folded and tilted older units. The volcanic deposits have been dated at 1.1 Ma (Arcos et al. (1988); Charrier et al. (1996)) and a zircon fission track cooling age of 0.7 Ma was determined for a tuff from this group. Most likely in the Quaternary, a local heat-source led to substantial annealing of fission tracks in apatite near the heat-source (fig. 4.25 d.). The pattern of apatite ages is very irregular in the study area and directly reflects this thermal overprint. Track lengths measured in apatites show that the samples from the lower part of the Rio Damas Formation in the southeastern part of the section were affected slightly by this heating and shortening of the fission tracks occurred at a very late stage.

### **4.7 Conclusions**

Tectonic development in the Rio Tinguiririca valley is characterised by several features not known from other areas. The mid Cretaceous Colimapu Formation and the late Miocene Farellones Formation are completely missing in the area and the Baños del Flaco Formation has been largely eroded; only the Tithonian deposits of this unit are preserved (see figure 4.3). A mid Cretaceous tuff layer (White Tuff) and a sequence of late Cretaceous fan and alluvial plane deposits, the Brownish–Red Clastic Unit, lie unconformably on top of the Baños del Flaco

Formation but with no angular unconformity. Comparable deposits of this age have not yet been described in any other location in the Central Andes. Fission track dating on zircons and apatites from the Rio Tinguiririca show the following:

1. Heating to temperatures of at least 180 °C occurred in the Rio Damas and Baños del Flaco Formations during the mid Cretaceous. The cause of this heating is unknown but burial alone – assuming normal geothermal gradients – cannot have been the only factor.
2. The White Tuff is older than the BRCU. The cooling age for the tuff determined in this study is significantly younger than the Ar–Ar age published by Wyss et al. (1994). This difference in age has an influence on the interpretation of the relative timing of heating in the Jurassic units and erosion of the Baños del Flaco Formation.
3. Tilting of the Mesozoic units began in the late Cretaceous (after deposition of the BRCU) or early Tertiary (Palaeocene). By the early Eocene samples in the lower part of the Rio Damas Formation had already cooled to temperatures below the apatite PAZ and, therefore were probably at a depth of less than 2000 m.
4. Zircon fission track data from the Coya Machali Formation indicate that sedimentation may have continued for longer than hitherto assumed. The youngest ages determined for samples in this unit (14 to 16 Ma) are considerably younger than 20 Ma, which is given as the approximate end of deposition by Charrier et al. (2002).
5. A local heating event occurred in the Quaternary and caused almost complete annealing of samples near the heat source. Most of the samples in the study area appear to have been affected to a greater or lesser extent by this heating event. The cause of heating is unknown but hydrothermal activity, possibly along brittle fault zones, is suggested as a possible mechanism and is also directly evidenced by the hot springs at Termas del Flaco.

Evidence for a phase of extension sometime in the mid to late Miocene was found. Extension appears to have been NW–SE and this orientation, calculated from paleostress analysis, is more or less perpendicular to the observed strike of brittle normal faults that affected all the Mesozoic and Tertiary units in the study area.

Uncertainties remain as to the mechanisms leading to heating in the Rio Damas and Baños del Flaco Formations both during the Cretaceous and during the Quaternary. The age of the White Tuff layer is a key point in interpreting the relative timing of heating in the Jurassic units and erosion of the Baños del Flaco Formation but the cooling age determined in this study differs from an Ar–Ar age published by Wyss et al. (1994) and no conclusive evidence exists as to which age is more accurate.



# Chapter 5

## Conclusions

Zircon and apatite fission track dating has helped to gain insights into the style and timing of metamorphism in the area, to resolve the stratigraphic positions and relations of the White Tuff layer and the Brownish–Red Clastic unit and to better constrain the timing of several events in the tectonic development of the area.

### 5.1 Metamorphism

The model suggested by Belmar (2000) of a single long-lasting burial metamorphism in the study area must be abandoned based on the fission track data from this study. Two distinct cycles of heating and alteration of the rocks can be distinguished in the study area. In the middle Cretaceous, heating occurred in the Rio Damas and Baños del Flaco Formations to temperatures between about 200 and 300 °C. This is evidenced by partial annealing of fission tracks in zircon and by occurrences of metamorphic minerals and mineral assemblages indicating prehnite–pumpellyite to pumpellyite–epidote facies conditions. The heating was not caused by burial of the units but, instead, was possibly connected to a period of active volcanism and/or magmatism in the area that lasted from about 104 Ma to 86 Ma. Thermal modelling of apatite samples from the lower part of the Rio Damas Formation indicates that cooling of the units occurred in the Late Cretaceous to Early Tertiary and was followed by a period of very minor thermal activity in Eocene to Miocene times. An extensional basin was opened in the Late Eocene and filled with about 1500 m of volcanic and sedimentary deposits (Coya Machali Formation). Within this basin, very low-grade burial metamorphism may

have occurred. However, the pattern of apatite fission track data in samples from the Coya Machali Formation is very irregular. Thermal modelling on an apatite sample from the Coya Machali Formation indicates rapid cooling prior to deposition and then slow heating of the sample to temperatures within the apatite PAZ during the middle to Late Miocene and subsequent cooling. The irregular pattern of apatite fission track ages in the Coya Machali Formation is thought to be caused by a series of pulses of hydrothermal activity in the basin that caused local thermal overprinting of the rocks at different times. This hypothesis is supported by the observation of secondary minerals, such as zeolites, in the samples that typically indicate hydrothermal activity. In the Late Tertiary or Quaternary, a local heat-source led to thermal overprinting of the rocks in parts of the study area. The heat-source was probably located close to the hot springs of Termas del Flaco and the Falla el Fierro fault zone. The degree of thermal overprinting decreases with increasing distance from the heat-source. Hydrothermal activity is the most likely cause of heating of the rocks. The Quaternary heat-source was located almost exactly at the transition between the Mesozoic and Tertiary deposits in the study area. The two sets of rocks with two separate thermal histories were both overprinted by the same event. The difference in metamorphic grade between the older rocks (prehnite-pumpellyite facies) and the younger deposits (zeolite facies) was probably considerably blurred by this late heating and isolated occurrences of zeolite minerals in the rocks of the Rio Damas Formation can probably also be attributed to this event.

The results of this study do not support the models of Levi (1970); Levi et al. (1989). In those studies, burial metamorphism was thought to be the main mechanism of alteration at low grades in the rocks of the Central Andes. In the Rio Tinguiririca valley, burial metamorphism played only a subordinate role and alteration was mainly caused by pulses of hydrothermal activity in the basins. Indications for hydrothermal activity during the middle to Late Cretaceous, the Tertiary and possibly the Quaternary are found in the study area.

## 5.2 Stratigraphy

The fission track data support the scenario favoured by Charrier et al. (1996) for the setting and relative positions of the White Tuff and the BRCU. Additionally

to the Ar–Ar age of 104 Ma for the White Tuff (Wyss et al. (1994)) a ZFT cooling age of 86.4 Ma was determined. In general, a middle Cretaceous age for the White Tuff was thereby confirmed. ZFT age data from the BRCU are mostly significantly younger than both ages determined for the White Tuff and the BRCU can thus be shown to have been deposited after the White Tuff. The difference between the Ar–Ar age of 104 Ma and the ZFT cooling age of 86 Ma for the White Tuff may, if both ages are accurate, indicate a period of active volcanism during the middle Cretaceous. Although the age of the BRCU cannot be exactly determined based on the detrital ZFT central ages, deposition can nonetheless be constrained to the Late Cretaceous as proposed by Charrier et al. (1996). A Maastrichtian age is proposed for this unit.

### 5.3 Tectonic evolution of the area

Tectonic evolution in the Rio Tinguiririca valley is characterised by several features not known from other areas. The mid Cretaceous Colimapu Formation and the late Miocene Farellones Formation are completely missing in the area and the Baños del Flaco Formation has been largely eroded; only the Tithonian deposits of this unit are preserved. A mid Cretaceous tuff layer (White Tuff) and a sequence of late Cretaceous fan and alluvial plane deposits, the Brownish–Red Clastic Unit, lie unconformably on top of the Baños del Flaco Formation but with no angular unconformity. Comparable deposits of this age have not been described in other localities in the Central Andes. Fission track dating on zircons and apatites from the Rio Tinguiririca shows the following:

1. Heating to temperatures of at least 180°C occurred in the Rio Damas and Baños del Flaco Formations during the mid Cretaceous. The cause of this heating is thought to be hydrothermal activity, possibly associated with active volcanism and/or magmatism.
2. The White Tuff was deposited in the middle Cretaceous and bears witness to volcanic activity at that time.
3. The BRCU was deposited in the Late Cretaceous (probably Maastrichtian).
4. Tilting of the Mesozoic units began in the late Cretaceous (after deposition of the BRCU) or early Tertiary. Thermal modelling on apatite samples

from the lower Rio Damas Formation indicates rapid cooling during the Late Cretaceous to Early Tertiary, which is interpreted to be associated with tilting and erosion of the Mesozoic units.

5. Zircon fission track data from the Coya Machali Formation indicate that sedimentation may have continued for longer than hitherto assumed. The youngest ages determined for samples in this unit (14 to 16 Ma) are considerably younger than 20 Ma, which is given as the approximate end of deposition by Charrier et al. (2002). Sedimentation in the Tertiary extensional basin may thus have continued to the middle Miocene.
6. A local heat-source in the Latest Tertiary or Quaternary caused substantial annealing of fission tracks in apatite in parts of the study area. The cause of heating is unknown but hydrothermal activity, possibly along brittle fault zones, is suggested as a possible mechanism and is also directly evidenced by the hot springs at Termas del Flaco.

There is evidence that extension occurred during the middle to Late Miocene. Extension appears to have been NW–SE and this orientation, calculated from paleostress analysis, is more or less perpendicular to the observed strike of brittle normal faults that affected all the Mesozoic and Tertiary units in the study area.

Based on earlier work by Charrier et al. (1996) and Charrier et al. (2002) and the results of this study, the tectonic development of the area can be described as follows (see figures 4.24, 4.25): Mesozoic units in the study area represent deposits of the Neuquén backarc basin. In the Early to middle Cretaceous a period of local uplift and erosion occurred in the basin and the deposits of the Baños del Flaco Formation were eroded. Elsewhere, the Baños del Flaco Formation is completely preserved. Heating took place in the Rio Damas and Baños del Flaco Formations during the Cretaceous and was either at its peak or just past it when the White Tuff was deposited unconformably on top of the Baños del Flaco Formation. Again, this seems to be a local occurrence since no volcanic deposits of similar ages are known from other locations in the Central Andes. During the late Cretaceous, the BRCU was deposited on top of the Baños del Flaco Formation. The fact that there is no angular unconformity between the Baños del Flaco Formation and the BRCU shows that tilting of the Mesozoic units cannot have begun until the early Tertiary. Late Cretaceous to Early Tertiary cooling of samples in the lower

part of the Rio Damas Formation is indicated by thermal modelling of apatite samples and is interpreted to show tilting and erosion of the Mesozoic units. The angular unconformity between the Coya Machali Formation and the older units as well as the setting of the Coya Machali Formation, which was not deposited directly on top of the other units but in an extensional basin to the west of the Neuquen backarc basin, indicate that some tilting of the Mesozoic units must have taken place before onset of deposition of the Coya Machali Formation in the late Eocene (at about 35 Ma). ZFT from the Coya Machali Formation indicate that deposition in the Termas del Flaco area continued for somewhat longer than originally thought. Ages range from 35 to 14 Ma. According to Charrier et al. (2002), deposition in the basin ended at about 20 Ma and basin inversion and associated deformation lasted from about 20 to 15 Ma. Based on the ZFT ages, continuation of sedimentation until the middle Miocene (about 14 Ma) is proposed. Inversion of the basin took place during west-east to SW-NE oriented compression. Shortening was accommodated through thrusting along brittle faults and folding of the Coya Machali Formation. Fold axis planes and fault planes strike NW-SE or north-south and fit the direction of compression calculated from paleostress analysis (NE-SW). Basin inversion was followed by a period of gentle extension. A series of small-scale normal faults was formed in all the Tertiary and Mesozoic units in the area. Offset along these faults is minor and is on the scale of centimeters to several meters. In the Quaternary, the young volcanic rocks of the Tinguiririca Volcanic Group were deposited unconformably on top of the Mesozoic and Tertiary units. At more or less the same time, local heating near the village of Termas del Flaco and along the Falla el Fierro thrust fault led to substantial annealing of fission tracks in apatite in parts of the study area.



# Bibliography

- L. Aguirre, B. Levi, and J. O. Nyström. The link between metamorphism, volcanism and geotectonic setting during the evolution of the andes. In Cliff R. A. & Yardley B. W. D. Daly J. S., editor, *Evolution of metamorphic belts*, pages 223–232. Geological Society Special Publication 43, 1989.
- L. Aguirre, B. Levi, and R. Offer. Unconformities as mineralogical breaks in the burial metamorphism of the andes. *Contributions in Mineralogy and Petrology*, 66:361–366, 1987.
- J. Angelier and P. Mechler. Sur une méthode graphique de recherche des contraintes principales généralement utilisable en tectonique et en sismologie: la méthode des dièdres droits. *Bulletin de la Société Géologique de France*, VII(19): 1309–1318, 1977.
- J. R. Arcos, R. Charrier, and F. Munizaga. Volcanitas cuaternarias en la hoyita superior del río Tinguiririca (34°40'S, 70° 21' W): Características geológicas, antecedentes geoquímicos y geocronológicos. *5th Congreso Geológico, Santiago*, 3 (1-2):1245–1260, 1988.
- M. Belmar. *Low-grade metamorphism in Central Chile at 35° South*. PhD thesis, University of Basel, 2000.
- L. Bettison and P. Schiffman. Compositional and structural variations of phyllosilicates from the Point Sal ophiolite, California. *American Mineralogist*, 73:62–76, 1988.
- R.E. Bevens, D. Robinson, L. Aguirre, and M. Vergara. Episodic burial metamorphism in the andes - a viable model? *Geology*, 31(8):705–708, 2003.

- C. Bingham. *Distributions on a sphere and the projective plane*. PhD thesis, Yale University, New Haven, 1964.
- M.T. Brandon. Decomposition of fission-track grain-age distributions. *American Journal of Science*, page 535 ff., 1992.
- M.T. Brandon. Probability density plot for fission-track grain-age samples. *Radiation Measurements*, 26(5):663–676, 1996.
- R. Charrier, O. Baeza, S. Elgueta, J. J. Flynn, P. Gans, S. M. Kay, N. Munoz, A. R. Wyss, and E. Zurita. Evidence for cenozoic extensional basin development and tectonic inversion south of the flat-slab segment, southern central andes, chile (33[deg]-36[deg]s.l.). *Journal of South American Earth Sciences*, 15(1):117–139, 2002.
- R. Charrier, A. R. Wyss, J. J. Flynn, C.C. Swisher III, M. A. Norell, F. Zapatta, M. C. McKenna, and M. J. Novacek. New evidence for late mesozoic-early cenozoic evolution of the chilean andes in the upper tinguiririca valley (35[deg]s), central chile. *Journal of South American Earth Sciences*, 9(5-6):393–422, 1996.
- I. R. Duddy, P. F. Green, and G. M. Laslett. Thermal annealing of fission tracks in apatite 3. variable temperature behaviour. *Chemical Geology (Isotope Geoscience Section)*, 73:25–38, 1988.
- I. Dunkl. Trackkey: a windows program for calculation and graphical presentation of fission track data. *Computers & Geosciences*, 28(1):3–12, 2002.
- R. L. Fleischer and G. R. Hart. Fission track dating: techniques and problems. In W. W. Bishop, J. A. Miller, and S. Cole, editors, *Calibration of hominid evolution*, pages 135–170. Scottish Academic Press, Edinburgh, 1972.
- R. L. Fleischer, P. B. Price, and R. M. Walker. *Nuclear tracks in solids: principles and applications*. University of California Press, Berkeley, 1975.
- R. F. Galbraith. The radial plot: graphical assessment of spread in ages. *Nuclear Tracks and Radiation Measurement*, 17:207–214, 1990.
- R. F. Galbraith and G. M. Laslett. Statistical models for mixed fission track ages. *Nuclear Tracks and Radiation Measurement*, 21:459–470, 1993.



- K. Gallagher, R. W. Brown, and C. Johnson. Fission track analysis and its application to geological problems. *Annual Rev. Earth Planet. Sci.*, 26:519–572, 1998.
- A. J. W. Gleadow. Fission track dating methods: What are the real alternatives? *Nuclear Tracks*, 5:3–14, 1981.
- A. J. W. Gleadow, A. J. Hurford, and R. D. Quaife. Fission track dating of zircon: improved etching techniques. *Earth and Planetary Science Letters*, 33:273–276, 1976.
- G. Gottardi and E. Galli. *Natural Zeolites*. Springer Verlag, Berlin, 1st edition, 1985.
- P.F. Green, I. R. Duddy, A. J. W. Gleadow, P. R. Tingate, and G. M. Laslett. Thermal annealing of fission tracks in apatite 1. a qualitative description. *Chemical Geology (Isotope Geoscience Section)*, 59:237–253, 1986.
- P.F. Green, I. R. Duddy, G. M. Laslett, K. A. Hegarty, A. J. W. Gleadow, and J. F. Lovering. Thermal annealing of fission tracks in apatite 4. quantitative modelling techniques and extension to geological timescales. *Chemical Geology (Isotope Geoscience Section)*, 79:155–182, 1989.
- A. J. Hurford. Standardization of fission track dating calibration: Recommendation by the fission track working group of the i.u.g.s. subcommission on geochronology. *Chemical Geology (Isotope Geoscience Section)*, 80:171–178, 1990.
- A. J. Hurford and P. F. Green. A users guide to fission track dating calibration. *Earth and Planetary Science Letters*, 59:343–354, 1982.
- A. J. Hurford and P. F. Green. The zeta age calibration for fission track dating. *Isotope Geoscience*, 1:285–317, 1983.
- A. J. Hurford and K. Hammerschmidt. The  $^{40}\text{Ar}$ - $^{39}\text{Ar}$  and  $\text{k-Ar}$  dating of the bishop and fish canyon tuffs: calibration ages for fission track dating standards. *Chemical Geology (Isotope Geoscience Section)*, 58:23–32, 1985.
- R. A. Ketcham, R. A. Donelick, and M. B. Donelick. Aftsolve: A program for multi-kinetic modeling of apatite fission-track data. *Geological Materials Research*, 2(1):1 ff., 2000.

- H. Kristmannsdottir and J. Tomasson. Zeolite zones in geothermal areas in iceland. In L. B. Sand and F. A. Mumpton, editors, *Natural Zeolites: Occurrence, Properties, Use*, pages 277–284. Pergamon Press, Oxford, 1978.
- G. M. Laslett, P. F. Green, I. R. Duddy, and A. J. W. Gleadow. Thermal annealing of fission tracks in apatite 2. a quantitative analysis. *Chemical Geology (Isotope Geoscience Section)*, 65:1–13, 1987.
- B. Levi. Burial metamorphic episodes in the andean geosyncline, central chile. *Geol. Rundschau*, 59:994–1013, 1970.
- B. Levi, L. Aguirre, and J. O. Nyström. Metamorphic gradients in burial metamorphosed vesicular lavas: Comparison of basalt and spilite in cretaceous basic flows from central chile. *Contrib. Mineral. Petrol.*, 80:49–58, 1982.
- B. Levi, L. Aguirre, J. O. Nyström, H. Padilla, and M. Vergara. Low-grade regional metamorphism in the mesozoic-cenozoic volcanic sequences of the central andes. *Journal of metamorphic Geology*, 7:487–495, 1989.
- R. Marret and R. W. Allmendinger. Kinematic analysis of fault slip-data. *Journal of Structural Geology*, 12:973–986, 1990.
- F. W. Mc Dowell and R. P. Keizer. Timing of mid. tertiary volcanism in the sierra madre occidental between durango city and mazatlan, mexico. *Geological Society of America Bulletin*, 88:1479–1487, 1977.
- F. W. Mc Dowell, W. C. McIntosh, and K. A. Farley. A precise  $^{40}\text{Ar}$ – $^{39}\text{Ar}$  reference age for the durango apatite (u-th) and fission-track dating standard. *Chemical Geology*, 214:249–263, 2005.
- C. Mpodozis and V. A. Ramos. The andes of chile and argentina. In J. A. Reine-mund G. E. Ericksen, M. T. Pinochet, editor, *Geology of the Andes and its relation to hydrocarbon and mineral resources*, volume 11 of *Earth Science Series*, pages 59–90. Circum-Pacific Council for Energy and Mineral Resources, Houston, Texas, 1989.
- I. E. Odom. Glauconite and celadonite minerals. In S. W. Bailey, editor, *Reviews in Mineralogy, vol. 13: Mica*, pages 545–572. Mineralogical Society of America, 1984.

- 
- R. Offler, L. Aguirre, B. Levi, and S. Child. Burial metamorphism in rocks of the western andes of peru. *Lithos*, 13:31–42, 1980.
- O. A. Pfiffner and M. Burkhard. Determination of paleo-stress axes orientations from fault, twin and earthquake data. *Annales Tectonicae*, 1:48–57, 1987.
- S. Potel, S. Th. Schmidt, and C. de Capitani. Composition of pumpellyite, epidote and chlorite from new caledonia - how important are metamorphic grade and whole-rock composition? *Schweizerische Mineralogische und Petrographische Mitteilungen*, 82:229–252, 2002.
- P. B. Price and R. M. Walker. Chemical etching of charged particle tracks in solids. *Journal of applied physics*, 33:3400–3406, 1962.
- M. K. Rahn, M. T. Brandon, G. E. Batt, and J. I. Garver. A zero-damage model for fission-track annealing in zircon. *American Mineralogist*, 89:473–484, 2004.
- V. A. Ramos. The tectonics of the central andes; 30° to 33° s latitude. *Geological Society of America*, Special Paper 218:31–54, 1988.
- M. D. Schmitz and S. A. Bowring. U-pb zircon and titanite systematics of the fish canyon tuff: an assessment of high-precision u-pb geochronology and its application to young volcanic rocks. *Geochimica et Cosmochimica Acta*, 65(15): 2571–2587, 2001.
- M. Steinmann, D. Hungerbuhler, D. Seward, and W. Winkler. Neogene tectonic evolution and exhumation of the southern ecuadorian andes: a combined stratigraphy and fission-track approach. *Tectonophysics*, 307(3-4):255–276, 1999.
- T. Tagami, A. Carter, and A. J. Hurford. Natural long-term annealing of the zircon fission track system in vienna basin deep borehole samples; constraints upon the partial annealing zone and closure temperature. *Chemical Geology*, 130:147–157, 1996.
- T. Tagami, R. F. Galbraith, R. Yamada, and G. M. Laslett. Revised annealing kinetics of fission tracks in zircon and geological implications. In P. Van den Haute and F. De Corte, editors, *Advances in Fission - Track Geochronology*, pages 99–112. Kluwer Academic Publishers, 1998.

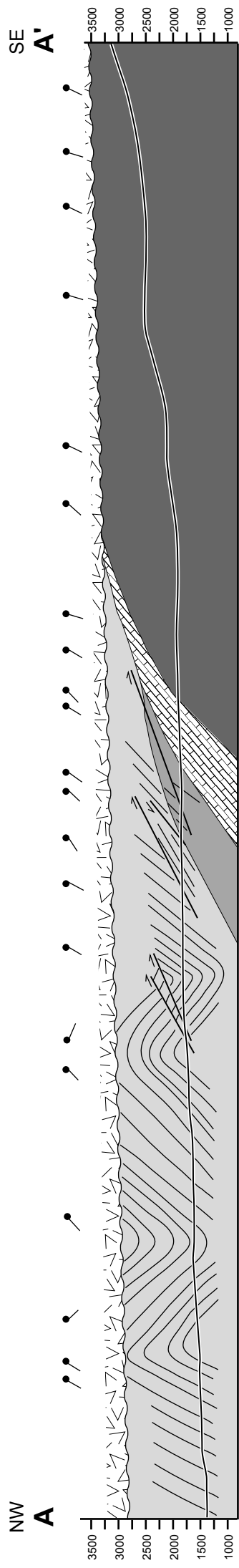
- T. Tagami and C. Shimada. Natural long-term annealing of the zircon fission track system around a granitic pluton. *Journal of Geophysical Research*, 101 (B4):8245–8255, 1996.
- Z. Timar-Geng, B. Fuegenschuh, U. Schaltegger, and A. Wetzel. The impact of the jurassic hydrothermal activity on zircon fission track data from the southern upper rhine graben area. *Schweizerische Mineralogische und Petrographische Mitteilungen*, 84(3):257–269, 2004.
- M. Vergara, B. Levi, J. O. Nyström, E. Fonesca, and C. Roeschmann. Variation in lower-cretaceous secondary mineral assemblages and thermal gradients across the andes of central chile (30–35° s). *Revista Geologica de Chile*, 21:295–302, 1994.
- M. Vergara, B. Levi, and R. Villarroel. Geothermal-type alteration in a burial metamorphosed volcanic pile, central chile. *Journal of metamorphic Geology*, 11:449–454, 1993.
- G.A. Wagner and P. Van den Haute. *Fission-Track Dating*. Enke, P.O.Box 10 12 54, D-7000 Stuttgart 10, 1 edition, 1992.
- A. R. Wyss, J. J. Flynn, M. A. Norell, C. C. III Swisher, M. J. Novacek, M. C. McKenna, and R. Charrier. Paleogene mammals from the andes of central chile: A preliminary taxonomic, biostratigraphic, and geochronologic assessment. *American Museum Novitates*, (10):31 pp., 1994.
- A. R. Wyss, M. A. Norell, J. J. Flynn, M. J. Novacek, R. Charrier, M. C. McKenna, D. Frassinetti, P. Salinas, and J Meng. A new early tertiary mammal fauna from central chile: implications for stratigraphy and tectonics. *Journal of Vertebrate Paleontology*, 10(4):518–522, 1990.
- F. Zapatta Nicolis. *Nuevos antecedentes estratigraficos y estructura del area de Termas del Flaco, valle del Rio Tinguiririca, VI Region, Chile*. PhD thesis, Departamento de Geologia, Universidad de Santiago, Chile, 1995.

# Appendix A

## Map and schematic crosssection

A geological map of the study area and a schematic crosssection can be found on the next pages.

Data appendices (electron microprobe analyses, XRD diffractograms, paleostress data, zeta calibration) are on the enclosed CD.




	Tinguiririca Volcanic Group
	Coya Machali fm.
	Brownish-Red Clastic Unit
	Banos del Flaco fm.
	Rio Damas fm.
	measured dip angles


23°


70°30'W

# Geological map of Termas del Flaco


34°50'S

 Tinguiririca Volcanic Group  
Quaternary

 Banos del Flaco fm.  
Tithonian


 Coya Machali fm.  
Eocene - Miocene

 Rio Damas fm.  
Kimmeridgian

 Brownish-Red Clastic Unit  
Cretaceous

 White Tuff  
Cretaceous

 Anticlines

 Synclines

 Thrust faults



1 km



34°55'S

A

Falla El Pterro

Termas del Flaco

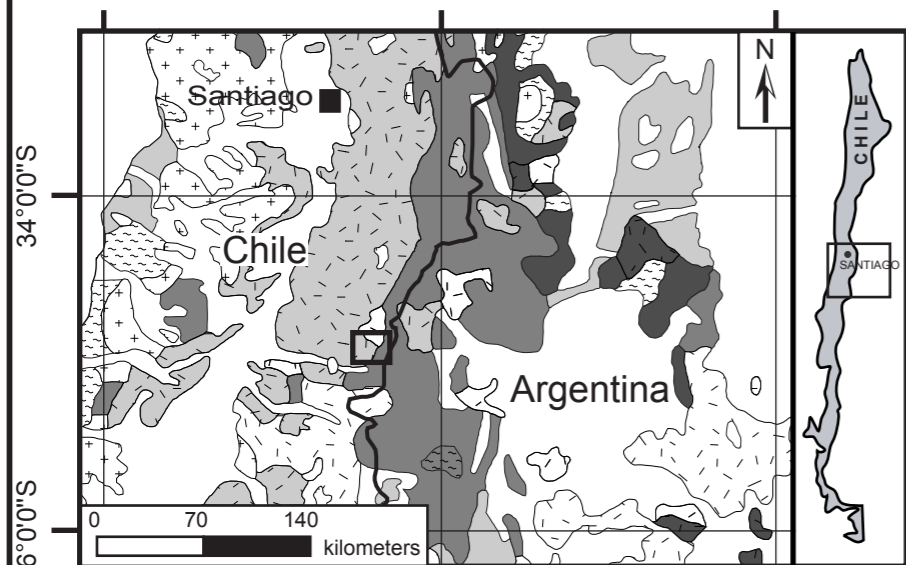
White Tuff

ARGENTINA

72°0'0"W

70°0'0"W

68°0'0"W



34°0'0"S

36°0'0"S

70°25'W

70°20'W

# Curriculum vitae

## Katherine Waite

### Personalien

Geboren: 16. September 1975 in London  
Aufgewachsen: Gempfen (SO)  
Heimatland: Vereinigtes Königreich

---

### Ausbildung

1991 – 1995: Gymnasium in **Münchenstein (BL)**, Abschluss mit Matura Typus C

1995 - 2000: Studium in Erdwissenschaften an der **Universität Basel**

Diplomarbeit: abgeschlossen im Sommer 2000

Titel: „*Mineralogical and gemmological analysis of corundum from Tunduru and Songea, southern Tanzania*“

Thema: Genaue mineralogische und gemmologische Beschreibung der Sapphire aus Tunduru und Songea, Erstellung einer Datenbank mit den verschiedenen Analysen

Betreuer: Prof. H. Hänni, Uni Basel und SSEF

2000 - 2005: Doktorarbeit am Departement Geowissenschaften der Universität Basel

Titel: „*Low-grade metamorphism and fission track analysis in the Main Cordillera of the Andes – Central Chile, 35° South*“

Betreuer: Prof. M. Frey (ursprünglich Hauptbetreuer des Projekts)  
Prof. S. Schmid (übernahm als Hauptgesuchsteller/Fakultätsverantwortlicher)  
PD Dr. S. Th. Schmidt (Betreuung für Metamorphose)  
PD Dr. B. Fügenschuh (Betreuung der Fission Track Analysen)

---